



EML 4905 Senior Design Project Organization

A B.S. THESIS
PREPARED IN PARTIAL FULFILLMENT OF THE
REQUIREMENT FOR THE DEGREE OF
BACHELOR OF SCIENCE
IN
MECHANICAL ENGINEERING

F-1U PREDATOR:

SAE BRAZIL 2012 AERODESIGN COMPETITION

Jorge Larrarte
Alex Rosales
Miguel Verdia

Advisor: Professor Dr. Andrés Tremante

November 21, 2012

This report is written in partial fulfillment of the requirements in EML 4511. The contents represent the opinion of the authors and not the Department of Mechanical and Materials Engineering.

Ethics Statement and Signatures

The work submitted in this B.S. thesis is solely prepared by a team consisting of Jorge Larrarte, Alex Rosales, and Miguel Verdia and it is original. Excerpts from others' work have been clearly identified, their work acknowledged within the text and listed in the list of references. All of the engineering drawings, computer programs, formulations, design work, prototype development and testing reported in this document are also original and prepared by the same team of students.

Jorge Larrarte

Team Member

Alex Rosales

Team Member

Miguel Verdia

Team Member

Dr. Andrés Tremante

Faculty Advisor

Dr. Sabri Tosunoglu

Faculty Advisor

Table of Contents

Ethics Statement and Signatures	i
List of Tables	vii
List of Figures	ix
Abstract.....	1
1. Introduction	3
1.1. Problem Statement.....	3
1.2. Motivation.....	4
1.3. Literature Survey.....	5
1.3.1. History of Aviation	5
1.3.2. Unmanned Aerial Vehicles.....	8
1.3.3. Remote Controlled Airplanes.....	10
1.3.4. Present Technologies.....	10
1.3.5. Future of the Discipline.....	13
2. Project Formulation	15
2.1. Major Components	15
2.1.1. Airfoil.....	15
2.1.2. Wings and Tail Configuration.....	16
2.1.3. Fuselage	18
2.1.4. Power Plant.....	19

3.	Design Alternatives	20
3.1.	Airfoil Selection	20
3.2.	Vertical Wing Location Considerations	20
3.3.	High Wing.....	21
3.3.1.	Mid Wing.....	22
3.3.2.	Low Wing.....	23
3.4.	Tail Wing Considerations	24
3.5.	Landing Gear Considerations	25
3.6.	Proposed Design	26
4.	Analytical Analysis.....	31
4.1.	Inverse Design Method	34
4.1.1	Background Theory of the Inverse Calculation Method	35
4.2.	Optimization	37
4.2.1.	Gradient Methods.....	37
4.2.2.	Non Gradient Methods	39
4.2.3.	Hybrid Methods	42
4.2.4.	Zhukovsky to NACA.....	45
4.2.5.	Conjugate Gradient	47
4.2.6.	Hybrid Method.....	51
4.2.7.	Conclusion of Optimization.....	57

5. Airfoil Selection	59
5.1 Wing Theory.....	59
5.2 Wing Loading	60
5.3 Stall Considerations.....	60
Thick Airfoil ($tc > 14\%$)	60
Moderate Airfoil ($6\% < tc < 14\%$).....	61
Thin Airfoil ($tc < 6\%$).....	61
Taper Ratio.....	62
5.4 Wing Incidence and Dihedral angles.....	63
5.5 Take-Off Properties Calculations	64
5.6 Selection Process	68
5.7 Computational Fluid Dynamics Simulation	74
5.7.1 Introduction to CFD.....	74
5.7.2 Simulation Set up	75
5.7.3 Simulation Results.....	76
5.8 Static Thrust Force Calculation	81
6. Structural Analysis.....	86
6.1 Static analysis.....	86
6.2 Wing Loading Test.....	89
7 Airplane Construction	90

7.1 Overview	90
7.2 Body	91
7.3 Ribs.....	92
7.3.1 Front Rib.....	92
7.3.2 Middle Rib	94
7.3.3 Secondary Middle Rib	95
7.3.4 Back Rib.....	97
7.4 Mount	99
7.5 Backbone or Aluminum Tube.....	100
7.6 Plate	101
7.7 Connectors	102
7.7.1 "L" Connector.....	102
7.7.2 Butterfly Connector	103
7.8 Fuselage	104
7.8.1 Cowl.....	104
7.8.2 Body Fuselage	107
7.9 Tail and Wings Construction	109
7.10 Monokote.....	114
7.11 Electronic Components.....	114
8 Design Considerations.....	117

8.1 Assembly and Disassembly	117
8.2 Maintenance of the system	120
8.3 Environmental Impact.....	121
9 Project Management	123
9.1 Organization of Work and Timeline	123
9.2 Project Breakdown.....	123
9.3 Research and Development Cost.....	124
9.4 Project Expenses Cost	126
9.5 Commercialization	127
10 Conclusion.....	128
11 References	130
12 Appendix	131
12.1 Appendix A: FIU CNC METAL CUTTING SERVICES	131
12.2 Appendix B: FLORIDA HOTWIRE TECHNICIANS.....	132
12.3Appendix C: WESTON HOBBY STORE: HOUSE OF POWER.....	133
12.4 Appendix D: TECHNICAL DRAWINGS	134

List of Tables

Table 1 - Advantages and Disadvantages of High Wing Configuration.....	21
Table 2 - Advantages and Disadvantages of the Mid Wing Configuration	22
Table 3 -Advantages and Disadvantages of the Low Wing Configuration	23
Table 4 - Advantages Compilation	25
Table 5 - Case 2 Parameters.....	45
Table 6 - Case 1 Parameters.....	51
Table 7 - Case 1 Results.....	52
Table 8 - Case 1 algorithm sequence	53
Table 9 - Case 2 Parameters.....	55
Table 10 - Case 2 Results.....	55
Table 11 - Case 2 Algorithm Sequence	56
Table 12 - Wing Area.....	70
Table 13 - Air Properties	70
Table 14 - Desired Weight of Aircraft	70
Table 15 - Take-off Calculations results	71
Table 16 - Calculations of the airfoil	72
Table 17 - Optimized results and selection of airfoil	73
Table 18- Initial parameters to consider in the flow simulation.....	75
Table 19 - SCFS Simulation Results	76
Table 20 - 13X4 1st Pitch Propeller results	81
Table 21 - 13X4 Wide Pitch Propeller results.....	82
Table 22 - 14X7 Propeller results	83

Table 23 - Break Down of Responsibilities by Task and Team Member 124

Table 24 – Material and Accessories Expenses..... 126

Table 25 - Engine Specifications and Cost..... 127

List of Figures

Figure 1 - Caley's Glider Design [3]	5
Figure 2 - Image of Wright Brothers during their first flight [3]	6
Figure 3 - Image of a Predator Drone [4]	9
Figure 4 - Front Wing of a Formula 1 Car used to create Down force	11
Figure 5 - Example of Inverse Design of an Airfoil	12
Figure 6 - Example of Optimization Software	13
Figure 7 - Airplane Structure	15
Figure 8 - Structural Scheme of an Airplane Wing	17
Figure 9 - Empennage Configuration Types	18
Figure 10 - Types of Fuselage	19
Figure 11 - Examples of Airfoils Designs [1]	20
Figure 12 - High Wing Configuration Example [1]	21
Figure 13 - Mid Wing Configuration Example [1]	22
Figure 14 - Low Wing Configuration Example [1]	23
Figure 15 - Tail Wings Examples Configurations [1]	24
Figure 16 - Landing Gear Configurations [1]	25
Figure 17 - High Wing Configuration Selection for the Final Prototype	27
Figure 18 - High Wing Configuration Selection for the Final Prototype 2	27
Figure 19 - Structure of the Airplane	27
Figure 20 - Landing Gear Configuration Selection for the Final Prototype	28
Figure 21 - Tail Wing Configuration for the Final Prototype	29
Figure 22 - Aircraft Conceptual Design Concept	31

Figure 23 - Propeller Configuration of the Airplane	32
Figure 24 - Propeller Selection Table & Formula	32
Figure 25 - Lift Coefficient Graph & Formula	33
Figure 26 - Takeoff Distance Formulation.....	33
Figure 27 Examples of unimodal and multimodal single design variable functions.....	38
Figure 28 - Example of Differential Evolution Structure and Sequence	41
Figure 29 Particle Swarm Sequence and Structure.....	42
Figure 30 - Evolution of Airfoil	44
Figure 31 - Case 1 Local Error.....	44
Figure 32 - Case 1 Total Error.....	45
Figure 33 - Case 2 Guess, Target and Final Airfoil.....	46
Figure 34 - Case 2 Evolution of Airfoil.....	46
Figure 35 - Case 2 Local Error.....	46
Figure 36 - Case 2 Total Error.....	47
Figure 37 - Convergence path of Conjugate gradient Method.....	48
Figure 38 - Value of variable X convergence vs. iterations	49
Figure 39 - Value of Y variable vs. iterations.....	50
Figure 40 - Max error vs. iterations	50
Figure 41 - Objective function convergence vs. iterations	51
Figure 42 - Screenshot of Case 1.....	51
Figure 43 - Case 1 Convergence History	52
Figure 44 - Case 1 Overall Function Evaluation Convergence	53
Figure 45 - Path Convergence	53
Figure 46 - Screenshot of	54

Figure 47 - Case 2 Convergence History	55
Figure 48 - Case 2 Overall Function Evaluation Convergence	55
Figure 49 - Path Convergence.....	56
Figure 50 - Pareto Front Analysis	58
Figure 51 - Airfoil Thickness List.....	60
Figure 52 – Span/Mesh vs. Span location plot.....	62
Figure 53 - Incidence Angle Picture	63
Figure 54 - Antonov 225.....	63
Figure 55 - XFOIL 6.96 Interface.....	69
Figure 56 - SolidWorks Calculation screen of the CFD Simulation.....	74
Figure 57 - CAD model of wing and its computational domain	76
Figure 58 - Pressure distribution on the top surface	77
Figure 59 - Pressure distribution on the bottom surface	77
Figure 60 - Cut Plot of Pressure	78
Figure 61 - Flow trajectories of the pressure on the top surface	78
Figure 62 - Flow trajectories of the pressure on the bottom surface.....	79
Figure 63 - Flow Trajectories of the Velocity	79
Figure 64 - Cut plot of the velocity.....	80
Figure 65 - Flow trajectories of the Vorticity	80
Figure 66 - Thrust Force vs. RPM	83
Figure 67 - Test Bench 1.....	84
Figure 68 - Test Bench 2.....	85
Figure 69 - Flight Mechanics	86
Figure 70 - Conceptual Structural Design with Forces.....	87

Figure 71 - Displacement in X	88
Figure 72 - Displacement in Z.....	88
Figure 73 - Von Misses stress.....	88
Figure 74 - Wing Load Testing Process	89
Figure 75 - Body Design Inspiration	91
Figure 76 - Front Rib Design and Features.....	93
Figure 77 - Parts Attached to the Front Rib	93
Figure 78 - Front Rib Servos	93
Figure 79 - Middle Rib Design and Features	94
Figure 80 - Wing and Ribs connection	95
Figure 81 - Secondary Rib Design and Features.....	96
Figure 82 - Secondary rib location and configuration.....	96
Figure 83 - Back Rib Design and Features	97
Figure 84 - Back Rib with rear landing gear, arms suspension and shock absorbers	98
Figure 85 - Suspension Arm design and Features.....	98
Figure 86 - Plastic Engine Mount	99
Figure 87 - Aluminum Engine Mount.....	100
Figure 88 - Backbone or Main Tube Design and Specifications	100
Figure 89 - Bending process of the Aluminum Tube or Backbone	101
Figure 90 - Plate design and Dimensions	102
Figure 91 - L shape Aluminum connectors Design.....	103
Figure 92 - Butterfly connection	104
Figure 93 - First Two steps of the manufacturing process of the Cowl	105
Figure 94 - Steps 3 and 4 of the manufacturing process of the Cowl.....	106

Figure 95 - Final steps of the Cowl manufacturing process.....	106
Figure 96 - Fuselage Foam Design.....	107
Figure 97 - CNC Foam Cutting of the Body Fuselage	108
Figure 98 - Fuselage Assembly	109
Figure 99 - CNC Wing manufacturing process	110
Figure 100 - Main Wing Cutting process.....	110
Figure 101 - Holes Diameters and locations in the Main Wing	111
Figure 102 - Balsa wood reinforcement profiles.....	111
Figure 103 - Tail Wings Elevators construction.....	112
Figure 104 - Tail Wings Assembly	112
Figure 105 - Ailerons Design	113
Figure 106 - Flaps Design	113
Figure 107 - Futaba Servos.....	114
Figure 108 - 6 Channel Receiver	115
Figure 109 - Splitter Cable.....	115
Figure 110 - Transmitter and Battery.....	116
Figure 111 - Servos and Channels Diagram	116
Figure 112 - Screenshot of the exploded view	117
Figure 113 - Tube Support from SolidWorks	118
Figure 114 - Tube Support Prototype	118
Figure 115 - Connection of the plates to the ribs using L-shape support.....	119
Figure 116 - Structure of the airplane and its main components.....	120
Figure 117 - Servo controller of the front wheel	121
Figure 118 - Timeline Representation.....	123

Figure 119 - Project Task Division 125

Abstract

One of the greatest challenges in modern science is multifaceted aerodynamic design. This is due to the nature of the discipline and the complexity of the calculations required. In the last 20 years, the discipline of CFD (computational fluid dynamics) has made great strides in trying to accurately predict fluid behavior around a specific shape. The team composed of Alex Rosales, Jorge Larrarte, and Miguel Verdia will develop an aerodynamic shape not only with the help of inverse design techniques, but also taking advantage of design optimization techniques. The shape developed will be used in an aircraft to compete in an aerodynamic competition.

The SAE Brazil Aero Design 2012 is an international competition held by the Society of Automotive Engineers. The aim of this event is to challenge student teams from different academic institutes with the goal of achieving a handcrafted aircraft with the particular capability of being able to fly with the maximum payload possible. Attending this competition will prepare the team members for the challenges of working in challenging situations with high incentives.

The research and design phase of this project will involve the modeling of airfoil shapes and wing geometries using computational fluid dynamics (CFD), with frictionless models integrated in the simulation in order to better account for the fluid forces and aerodynamic analysis of the lift coefficient and its changes with varying angle of attack.

Some of the phases for this project comprise of:

- Design of an airfoil cross section in several of Dr. Dulikravich's software codes in order to create and predict the theoretical values of the C_L (lift coefficient).
- CFD simulation of wing geometries accounting for turbulence and vortex generation
- Wing structurally analyzed in Solidworks and ANSYS for load failure.

Once these research or studies have been performed, the design team will focus on the fuselage creation. This stage will consist of landing gear selection and design, engine components location selection, electrical mechanism integration, and most importantly load compartment design. The design team expects that this careful task oriented approach to aerodynamic design will serve to guide future competitors from FIU College of Engineering in this type of event.

1. Introduction

1.1. Problem Statement

The purpose of this design project was to successfully compete in the SAE Brazil Aero Design competition by designing an aircraft that would be able to gain first prize due to its flying load capacity. A secondary goal was to be able to do this while complying with all the rules and regulations established by SAE. Focusing on the aerodynamic design part of the design process has shown the benefits of optimization techniques.

A main obstacle in aerodynamic design applications has been the fact that the most used method to achieve aerodynamic shapes is inverse design. Inverse design methods consist of selecting a particular lift or pressure signature with the help of a CFD software. At this point, calculations are then made in order to predict a specific shape that will create the preconceived selection. This type of method has been recurrently used in the last 20 to 30 years in the design of aircrafts and wing blades. The problem with this type of approach is that it has required a predetermined pressure goals that might negatively affect an array of secondary effects such as a rapid loss of pressure with a slight angle of attacks. Using optimization methods, which depend more upon results and behaviors than input pressure distributions, have very recently began to prove to be more efficient at obtaining ideal aerodynamic shapes that later will become wings, rotor blades, etc.

1.2. Motivation

The Senior Design team feels very passionate about the opportunity to be able to represent FIU and compete in the SAE Brazil Aero Design competition. This society gives future engineers the chance to display their abilities against each other. These are abilities that students have accumulated through the completion of a bachelor of engineering and abilities that the members of our team have obtained through several of the courses taught in this university. Motivation is necessary in order to build an aircraft from the ground up and to completely design every aspect of it. Motivation is something that must already reside in anyone that chooses the mechanical engineering field as a career. Additional motivation was gained from the fact that all of the members of this design team are very passionate about the field of fluid dynamics and aerospace in general, therefore this type of project was second nature to the team. Another important aspect of this challenge was the material selection process combined with the stress analysis study required for an aircraft design. This creative endeavor has taken our group through load analysis problems not typical for everyday common applications. Also, the time it has taken to make selections corresponding to materials, specific densities, and allowed factors of safety have been more important than in most other projects due to the fact that weight is such an important aspect of the competition and aero shape design in general.

1.3. Literature Survey

1.3.1. History of Aviation

Aviation has always been a dream throughout human history. Since the beginning, birds were the source of admiration and inspiration for the human mind; flying was something one aspired to obtain. In the fifth century, the kite was developed, and was widely held as not a real advance, but it still proved the possibility of flight for a species different from birds. It was not until the nineteenth century when George Caley, an English aeronautical engineer, who was able to carry people from different places using kites and gliders. He also designed a helicopter-shaped device powered by a propeller that was situated on the horizontal axis.

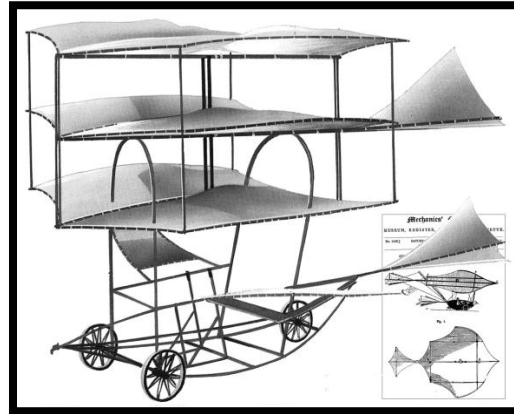


Figure 1 - Cayley's Glider Design [3]

Since Cayley, the history of aviation entered into a stage of progress and promise, an era where many researchers developed studies and inventions in order to design something that would finally allow for human flight.

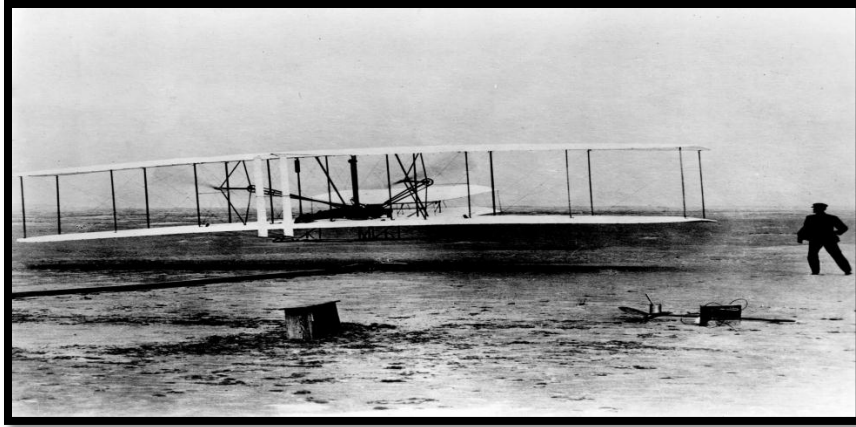


Figure 2 - Image of Wright Brothers during their first flight [3]

December 17, 1903, was a key date for modern aviation history. On that day, Oliver and Wilbur Wright managed to rise about 260 meters from the ground in a motor-powered aircraft, which was heavier than air for a period of 59 seconds. From that day, the Wright brothers are considered to be the pioneers of aviation around the world. After this important achievement, aeronautical sciences began a rapid advance, making it difficult to believe everything that was accomplished considering that its history had initiated in the fifth century.

During World War I, airplanes and aircrafts lighter than air were used as weapons. The designers built special models for reconnaissance and attack. As a consequence, more pilots were trained and more planes were built in the four year conflict than in the thirteen years since the first flight. After the war, the progress in airplanes and engines design increased considerably. Two-winged aircraft, with engines and propellers placed at the rear were soon replaced by aircraft with engines located at the front. Much of the military surplus was sold to the airmen that trained with it; they

used it to do any activity that would produce income. These activities included passenger transport, aerial photography, flight instructions, and air racing or aerobatic shows.

One of the largest international aircraft companies that operated at the beginning of the World War II was Pan America World Airways. Along with its subsidiaries and affiliates it served a network of 82,000 miles on routes that reached 47 countries around the world. The demands of war accelerated the development of aircraft and significant progress was achieved in attack such as bombing, dog fighting, as well as air transportation of troops, tanks, and heavy equipment. Thus, for the first time in history, aviation became a decisive factor in the development of the war. Also, the fabrication of small airplanes was rapidly increased. In 1941, American military aircrafts were operated on all fronts. The aviation industry employed 450,000 people compared to the 190,000 it had prior to the war. That year, 3,375,000 passengers were carried by the 18 American airlines, one million more than in 1940. The payload and mail increased by about 30 percent.

Towards the end of the war, air battles grew in intensity and duration, and aircraft production peaked. Experience in the manufacturing of military aircraft during the war was used in the construction of civilian aircraft around the end of the hostilities. Airlines arranged for larger and faster aircrafts with advances such as pressurized cabins. Airports, weather forecasting, and navigational aids were improved in order to be more efficient and reliable in order to meet public demand for the air transportation

of passengers and cargo. This expansion grew to unidentified levels due to the sudden prosperity of the postwar period.

The experiments in the field of aerodynamics, design of new metals, new power plants, and electronic advances brought the development of high-speed turbojet airplanes that were designed for transoceanic flights, supersonic flight, aircraft rockets, and experimental aircraft for short takeoff and vertical takeoff used for rockets.

1.3.2. Unmanned Aerial Vehicles

The history of unmanned aerial vehicles is related to war. It started in the American Civil War with a basic concept of launching balloons with explosive devices to explode on the enemy side. The Japanese tried the same method during World War II, but proved to be inefficient for the objective. In 1960, the United States began to design the famous “drones”, which are unmanned vehicles used for reconnaissance and combat roles.

The first time that drones were used was in the Vietnam War. Those drones were called “Fire bees” and they were assigned to the task of reconnaissance. The initial technology carried by these drones was simple daylight cameras. Later improvements such as communication devices and thermal sensors with night vision cameras were added. Israel has been at the forefront of the study and development of the UAV technology. Some examples that are extensively used by the US Air Force are the Hunter and Pioneer drones, which are directly derived from Israeli technology. One of the most popular drones used by the United States is the Predator, which is loaded with high class

missiles and can stay in the air for almost forty hours. This fact has repeatedly demonstrated that the drone was developed for long-range purposes.



Figure 3 - Image of a Predator Drone [4]

UAV's are not only used for military purposes, they also have a lot of other commercial and security applications such as in the agricultural industry, mineral exploration, border and coastal surveillance, air and ground traffic control, etc. Also, some competitions have been established for students interested in the aerospace field, allowing them to research and develop a specified type of remote controlled aircraft, which has the ability to travel a specified distance and carry a specified weight. For the future, constant development and research will allow drones to be smaller, affordable, and more precise. For now, all of the work is focused on the military field.

1.3.3. Remote Controlled Airplanes

Air modeling is considered a sport where the objective is to model an aircraft heavier than air on a scale smaller than a regular aircraft, which can fly at a certain height and carry a certain load. This sport is directly related to aerospace and mechanical engineering, for its high engineering concept design and testing. It has many categories, but the most popular one is radio controlled airplanes. The sport has grown throughout the years, which can be seen by the increasing number of competitions for students and hobbyists.

The first radio controls were designed with vacuum tubes and had a few buttons which made the plane head to a specific position. The transmitter used radio waves, which were received by the receiver device inside the plane. This receiver transformed and sent the electrical impulses to electromechanical devices which allowed the person to control the airplane, but its big size and the multiple failures resulted in many complications for the users at that time.

These days, any radio control has an internal microprocessor and regular software, which allows the user to program and record different parameters for different models, making the flight easier and safer.

1.3.4. Present Technologies

The aerodynamic design of aircraft and aerodynamic structures is currently being heavily influenced by inverse design methods. Desired behaviors are predetermined as

an ideal in a particular area or shape to be designed. Airfoils are a great example of this technology. Many of the concepts being currently used applicable to inverse design maintain a certain common logic. They have the common ability to converge to a specific shape, but vary in the amount of computer time required to do so, which is referred to as iterations. Some of these concepts are currently being used to achieve shapes that are used in turbo machinery and propeller designs in general. The automotive industry uses them to identify some of the aerodynamic shapes employed by sports cars. The auto performance industry heavily relies on these methods to create front wings and spoilers which are responsible for creating the crucial down force. This exemplifies the typical situation where inverse design techniques have become essential to performance. This down force could be calculated, in the case of the racing industry, by the maximum turning radius and velocity. Given this parameter, determining what the wing airfoil should look like becomes a simple problem with the use of inverse design.



Figure 4 - Front Wing of a Formula 1 Car used to create Down force

Another great advantage of inverse design techniques is their ability to very rapidly converge to a shape with the desired capabilities. This was and is still of great importance to design companies due to the high cost that long computer times could represent. These are some of the reasons that inverse design methods play a crucial role in today's technology field. The future of the discipline will be shaped by the strengths and weaknesses of the current technology. One main drawback that hinders inverse design methods is the necessity for a given derived behavior of the shape to be created.

In the case of airfoil design, an experienced aerodynamicist might conclude after extensive research that airfoil shapes with a high coefficient of lift would be superior to those without. He would then determine an expected lift coefficient behavior to be used in the inverse design of a new airfoil. This can be seen in Figure 5.

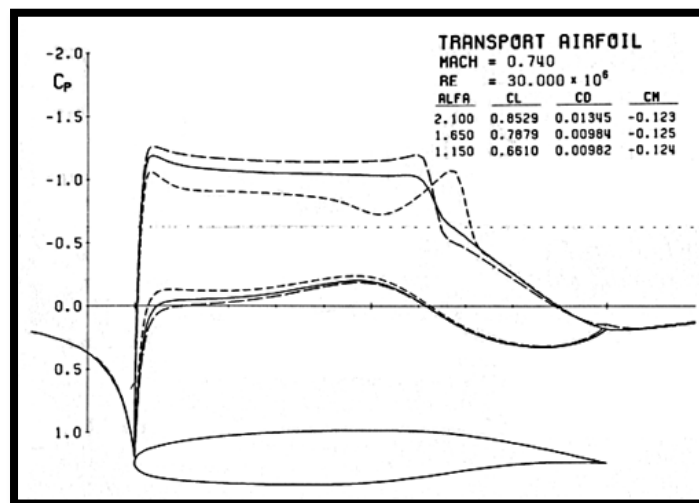


Figure 5 - Example of Inverse Design of an Airfoil

The bottom portion of the image represents an airfoil, and the lines emanating from this shape represent the performance of the lift coefficient in this case. This lift

coefficient has several lines, which represent initial, current, and any changes in the lift coefficient as it reaches or converges to the previously determined target, also included. The one inherent flaw or limitation of such a process depends upon the abilities of the previously mentioned aerodynamicist. However, no matter the skill it should be understood that the final design could not possibly be truly ideal given the great amount of variables.

1.3.5. Future of the Discipline

Great innovations were produced during the years from the use of inverse design methods, but understanding its shortcomings also helps to understand the path that the discipline must take in order to improve. Optimization is in all regards another tool in CFD and aero shape design in general, but it holds a definite advantage over its predecessors. Optimization mainly consists of leaving certain parameters fixed. This could be volume, length, or surface area in the case of a wing. The program will then iterate all possible solutions in order to create a three dimensional representation of the parameters left unfixed.

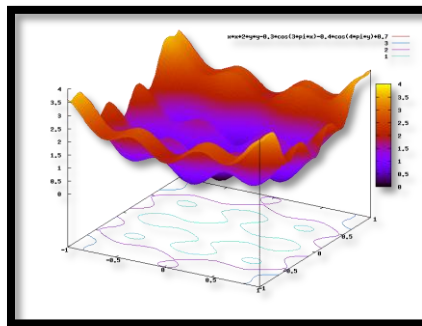


Figure 6 - Example of Optimization Software

As shown in Figure 6, the CFD optimization technique will display all of an option's signature behaviors in this type of a graphical display. Superimposing other parameters of the design will allow the designer to be able to select the best design conditions regardless of any preconceived notions. Some optimization methods also allow the user to specify the sensitivity of the design manufacturing tolerances.

Optimization techniques represent the next step in the evolution of the aerospace discipline. These methods will create the path for newer and better turbines and also fluid displacing machinery. Optimization methods are not subject to the aerospace industry alone. They could also play a crucial role in all design disciplines including chemistry, computer science, new materials, etc.

2. Project Formulation

2.1. Major Components

The SAE Brazil competition has specified all the restraints each team should meet in order to be able to compete. Those restraints have been divided between the major components of the aircraft and flight requirements. The major components of the remote aircraft are wings, airfoil, tail configuration, fuselage, landing gear, material, engine, radio control, servos, and battery.

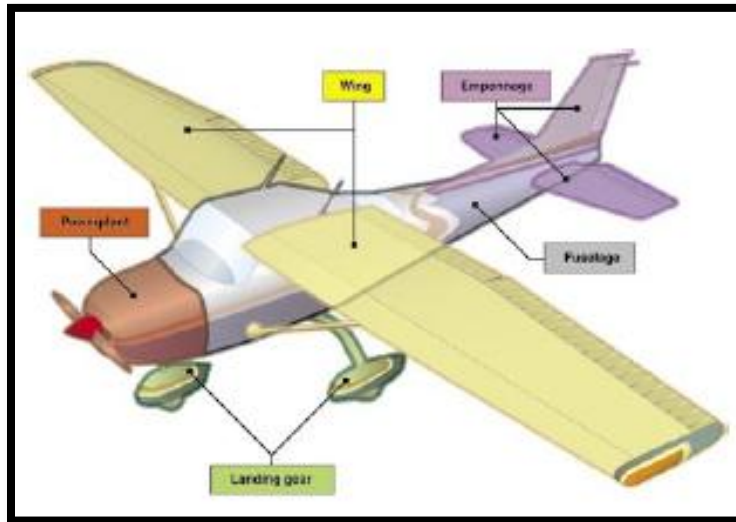


Figure 7 - Airplane Structure

2.1.1. Airfoil

The airfoil is one of the most important components to be studied at the design stage of any aircraft. Its importance is due to the fact that the cross-section of the wing is what makes it possible that an aircraft can move through the air by producing an

aerodynamic force called “Lift Force”, which is perpendicular to the direction of the airplane's motion.

There are different types of airfoils for different types of airplanes and their specifications. For this project, the McNair Fellowship program allowed one of the team members to research, design, and test a unique type of airfoil that would satisfy the lifting requirements of the competition. This research was conducted by Miguel Verdia during the summer of 2012 as a part of his McNair Fellowship investigation. The specifications of this particular airfoil are described in the Analytical Analysis of this thesis report.

2.1.2. Wings and Tail Configuration

The wings of any aircraft are a structure composed of airfoils attached to each of the side of the fuselage which support the airplane during flight. The position of the wings along the fuselage varies depending of the airplanes needs, which could be attached to the middle, top, or to the lower body of the fuselage. Also, the number of wings are subjective to the design's concept, but a single set of wings are the most common amongst the industry.

Wings have three main structural parts which are the ribs, spars, and stringers. At the rear of the airplane wings are two different control surfaces called ailerons and flaps. Ailerons create aerodynamic forces to make the airplane roll, while the flaps move down at the same time as the airplane in order to increment the lifting force of the wing during takeoff and landing.

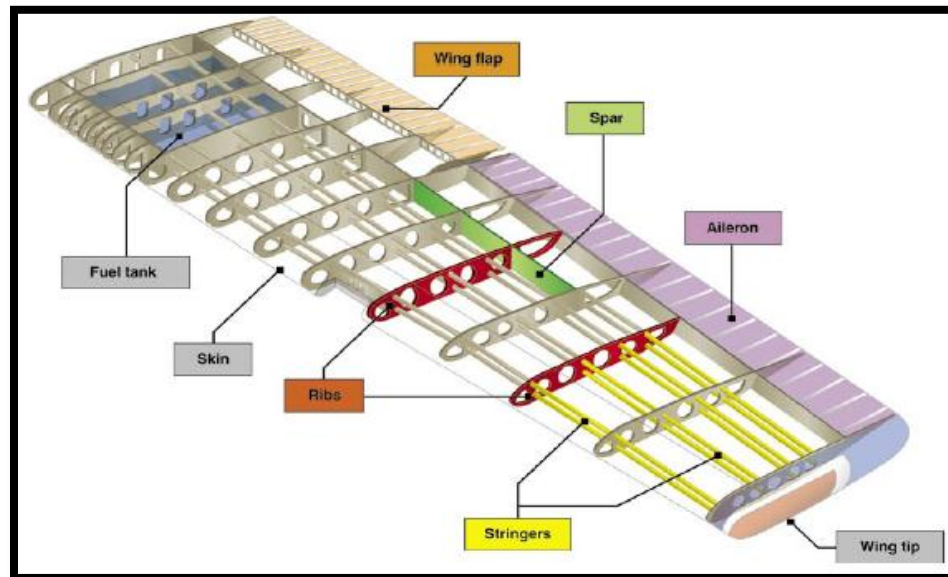


Figure 8 - Structural Scheme of an Airplane Wing

The wing tail configuration or empennage gives the airplane a way to control its rolling movement as well as a way to manage the direction of its flight. It is composed of vertical and horizontal stabilizer surfaces, along with a rudder, and an elevator which allows the plane to move its nose right or left; and trim tabs which are designed to reduce the control pressure. Other empennages use a stabilator, which increases the aerodynamic load at the tail and causes the nose of the airplane to move up.

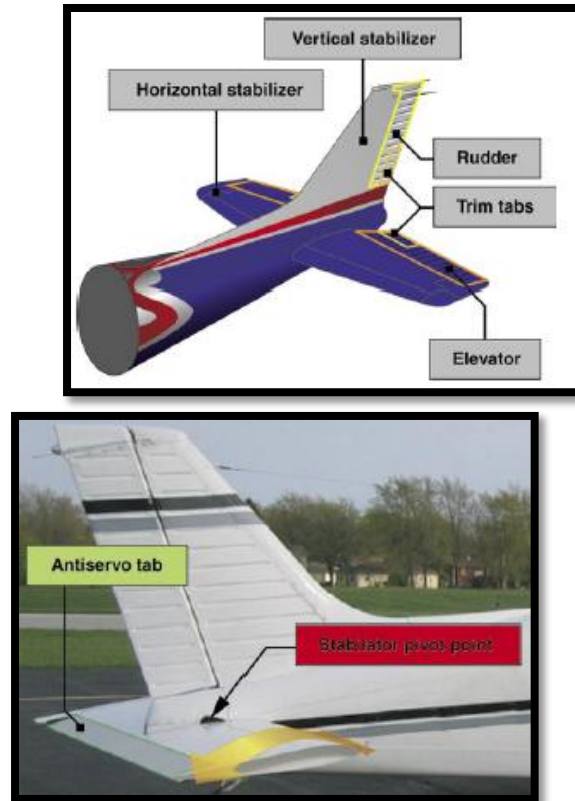


Figure 9 - Empennage Configuration Types

2.1.3. Fuselage

The fuselage is the main body of any aircraft and is designed for carrying objectives in addition to it being the structural connection for the wings and tail assembly. For this project it will have a space designed to carry the weight required to compete, which will be approximately 24 pounds. There are different types of fuselage, but the most popular are the monocoque, single shell structure; and the semimonocoque, which half of the single shell structure.

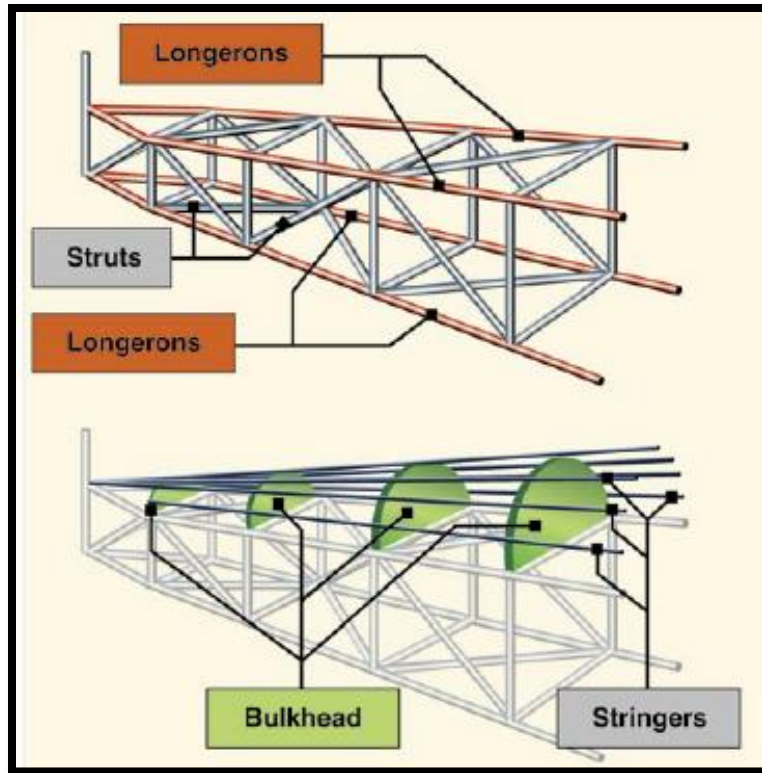


Figure 10 - Types of Fuselage

2.1.4. Power Plant

The power plant is the assembly of the engine and propeller, whose primary function is to generate through the engine, the required power necessary to produce the thrust force that will make the airplane fly. For the competition, the engine is one of the restrictions where the team has to choose among three types that are similar in all the specifications, changing only the weight and the propeller size. The cost analysis and specifications of the three types of engines are shown in the project breakdown section of this report.

3. Design Alternatives

3.1. Airfoil Selection

One important part of this design process has been the research and selection of an ideal airfoil. In other similar competitions, teams have selected airfoils from hundreds of different choices like NACA or *Zhukovsky*. These selections follow a historical perspective, consider aircraft velocity, and mission profile. Once an airfoil is selected, it must be analyzed in order to verify that the lift coefficient, drag coefficient and optimal angle of attack all work with the original design.

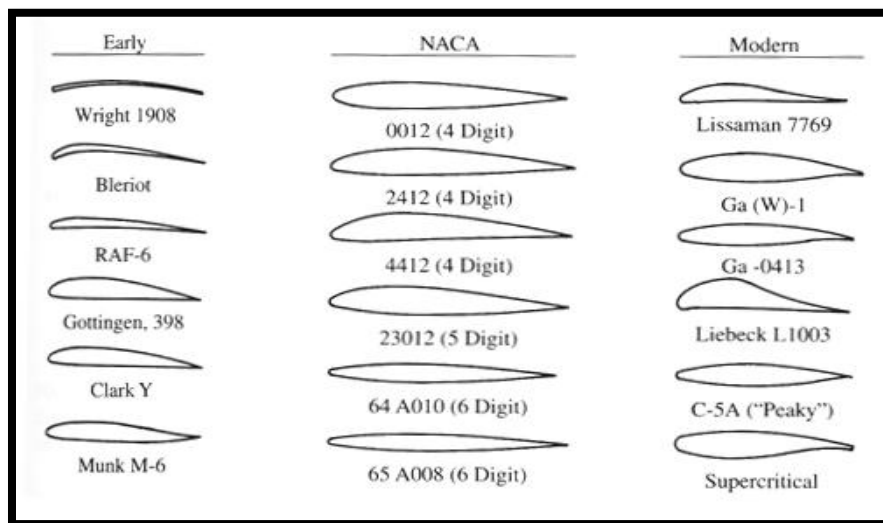


Figure 11 - Examples of Airfoils Designs [1]

3.2. Vertical Wing Location Considerations

Historically, wing position with respect to the fuselage has been as the figures show below. Each different selection offers a variety of distinct advantages and disadvantages. Some of the relationships that exist between wing position selection and advantages will be explored.

3.3. High Wing

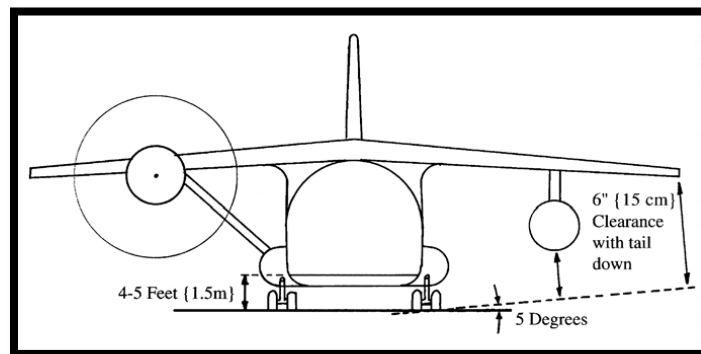


Figure 12 - High Wing Configuration Example [1]

Table 1 - Advantages and Disadvantages of High Wing Configuration

Advantages	Disadvantages
<ul style="list-style-type: none"> ➤ Allows placing the fuselage closer to the ground. ➤ Easy the cargo loading/unloading. ➤ Engines have sufficient ground clearance. ➤ Wingtips are not likely strike the ground. ➤ For low speed aircraft external struts can be used. They reduce the wing's weight, but they increase the drag. ➤ Simplifies connection to the fuselage 	<ul style="list-style-type: none"> ➤ Increases the weight of fuselage. ➤ Strengthened to support landing gear loads. ➤ Flattened at the bottom (for simplified loading/unloading) – weight is increased ➤ Cylindrical top requires fairing with the wings.

3.3.1. Mid Wing

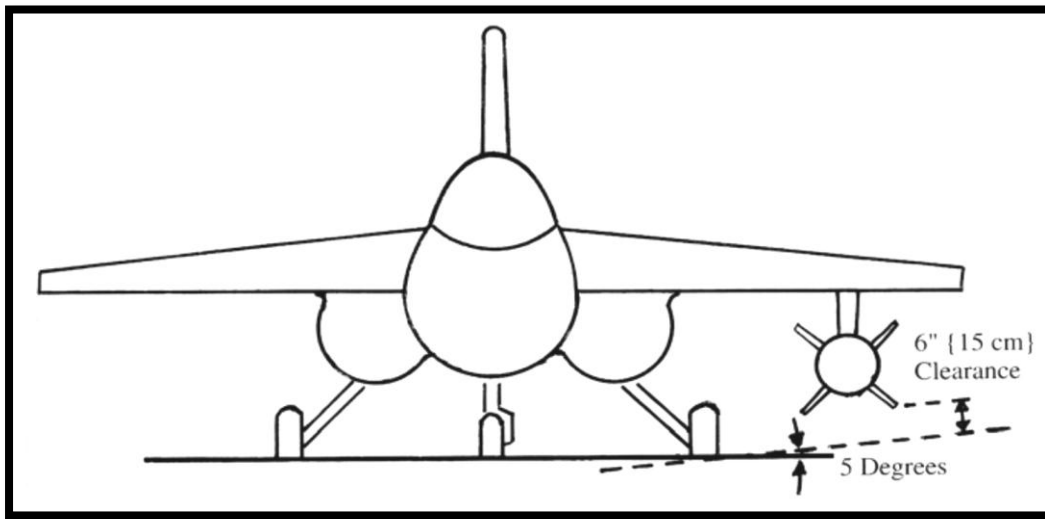


Figure 13 - Mid Wing Configuration Example [1]

Table 2 - Advantages and Disadvantages of the Mid Wing Configuration

Advantages	Disadvantages
<ul style="list-style-type: none">➤ Very good arrangement for aerobatic airplanes.➤ Does not restrict rear visibility.	<ul style="list-style-type: none">➤ Structural carrythrough presents the major problem➤ Requires carrythrough box or use of ring frames built into the fuselage.

3.3.2. Low Wing

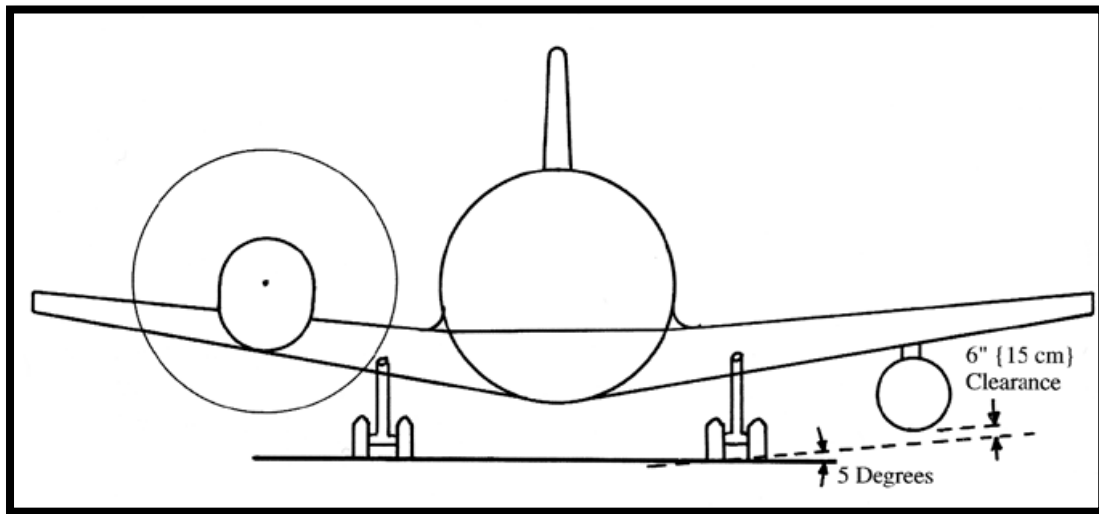


Figure 14 - Low Wing Configuration Example [1]

Table 3 -Advantages and Disadvantages of the Low Wing Configuration

Advantages	Disadvantages
<ul style="list-style-type: none"> ➤ Major advantage – landing gear storage. ➤ To provide engine clearance the fuselage has to be placed farther off the ground than a high wing aircraft. ➤ Provides greater fuselage clearance. ➤ Provides an added lift when close to the ground. 	<ul style="list-style-type: none"> ➤ Low wing arrangement requires special ground equipment for loading/unloading. ➤ Dihedral angle is determined from clearance requirements. ➤ Propeller engines are mounted above the wing – increases interference and fuel consumption. ➤ Added lift creates floating effect when landing.

3.4. Tail Wing Considerations

Tail wing selections, as shown in Figure 15, usually depend on previous mid wing selection, due to the fact that aerobatic interferences might be present. Another important factor to consider in tail selection is storage capability. It is easy to appreciate how the H-tail is a derived version of the conventional option.

Due to the competition restrictions for the regular class, weight is a primary factor to consider. Therefore the V-tail and Conventional will be tried initially for their ease of construction and low volume.

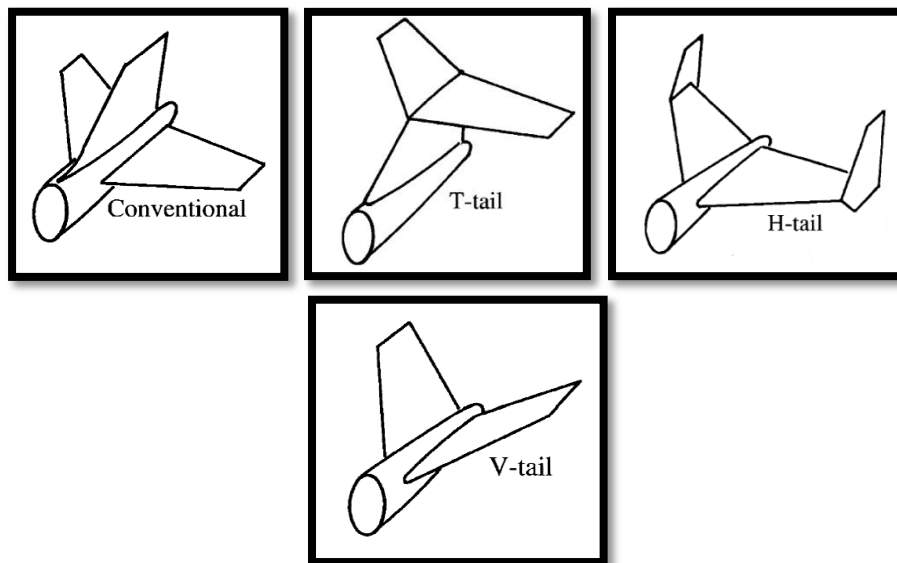


Figure 15 - Tail Wings Examples Configurations [1]

3.5. Landing Gear Considerations

For simple aircraft, two types of landing gears are the norm. These two types can be seen in Figure 16. They offer simple construction but they differ in the style of landing approach. Conventional small planes usually and historically rely on the conventional landing gear. This refers to the taildragger configuration shown in the figure below. It would seem logical for the team to prefer this due to its ease of construction, however, this design has proven problematic in this type of competition. In past events, aircrafts with this configuration have fallen victim to ground loops, and have also become hard to control when attempting takeoff.

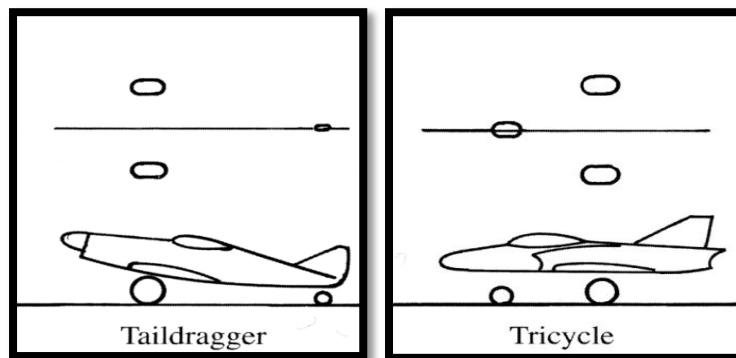


Figure 16 - Landing Gear Configurations [1]

Table 4 - Advantages Compilation

Advantages	High Wing	Mid Wing	Low Wing
Ground Clearance	XX	X	
Ground Lift effect			X
Simple connection to Fuselage	XX		X
Construction	XX		X
Low weight in Design	XX		X

3.6. Proposed Design

The proposed design was selected after careful consideration of all the alternatives mentioned before. Considering the size and mission objective of the proposed design, it was decided that the fuselage will be structurally defined by a light metal rod, or certain type of plastic that would be able to handle the necessary forces. The body design called for a backbone at the top which would support ribs at the bottom part of the structure. The main idea was to build an aircraft that would be able to fly without any of the skin surrounding the fuselage. This skin would have been added later as molded Styrofoam pieces that would have been able to be attached to this structural skeleton. This idea differed from previous designs in that it did not use wood plates in order to create a panel that would support the aircraft. By doing away with these, it was believed that the aircraft would gain a great weight advantage over its predecessors.



Figure 17 - High Wing Configuration Selection for the Final Prototype

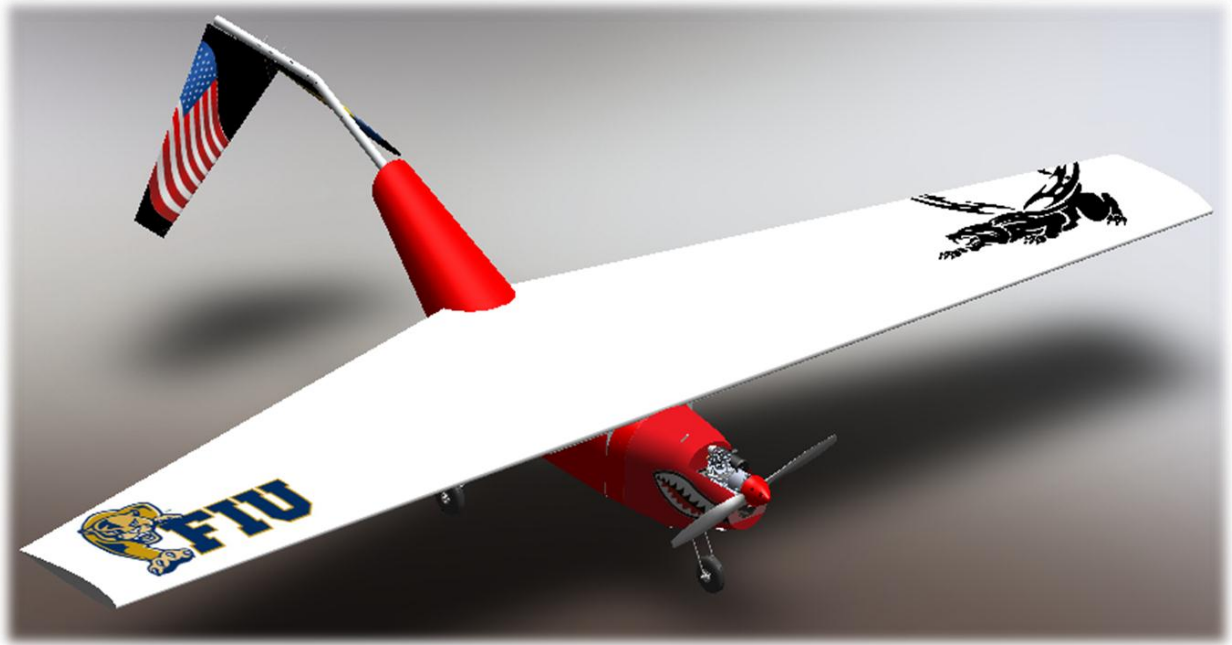


Figure 18 - High Wing Configuration Selection for the Final Prototype 2

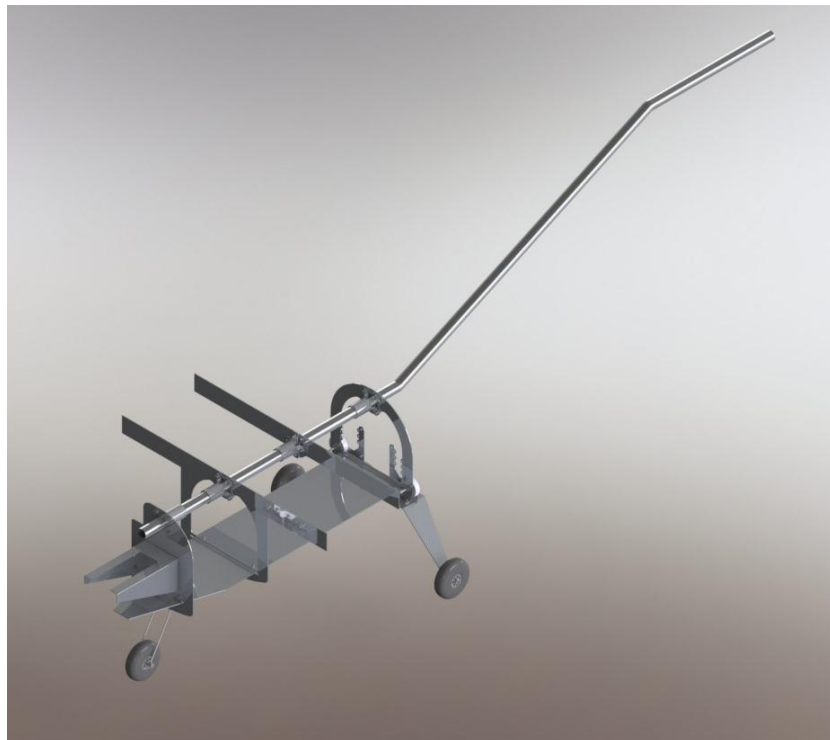


Figure 19 - Structure of the Airplane

The selection of wing location compared to the fuselage was also a bit intricate. It was the team's opinion that for pure flight reasons a low wing would add certain advantages that would benefit the purpose of the competition. Mid wing would also have offered great benefits, but it was decided against this type of configuration due to the problems it would have created in the manufacturing and loading. The choice became a high wing configuration since it allowed for the greatest benefits of construction ease and wing edge clearance in the event of instability. Even though the low wing choice was very attractive, it was agreed that the concern over wing tip low clearance and the added material needed to join the two wings together was too much of a disadvantage. Having looked back at other models in these competitions, it became evident that high wing design had been the preferred choice.

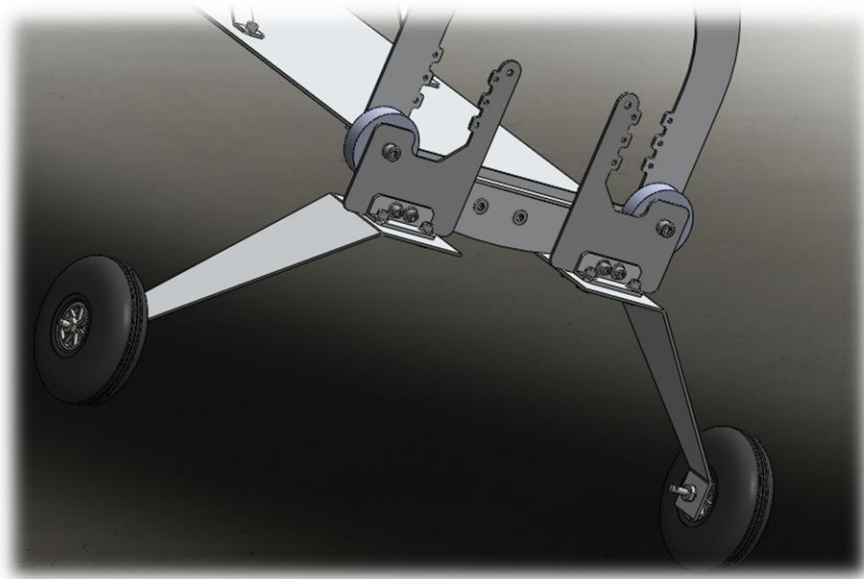


Figure 20 - Landing Gear Configuration Selection for the Final Prototype

For the landing gear it was determined that a tricycle configuration was necessary due to the fact that a tail dragger has been proven unreliable in this type of competition. Another reason that tricycle was chosen is that once the aircraft is loaded to capacity, about 40 lbs., there would have been a very pronounced critical structural point right after the first wheel. Therefore, a three wheel set-up became ideal. One thing that needed to be accounted for is that the center of gravity of the plane would need to be maintained between these two sets of wheels.

In order to facilitate these conditions, the aircraft center of gravity would have to be designed at exactly the same location as the middle of the cargo bay. This would have ensured that our center of gravity would not have changed throughout the competition.

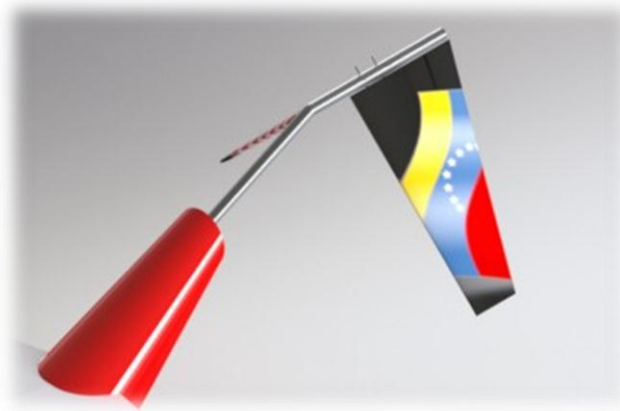


Figure 21 - Tail Wing Configuration for the Final Prototype

For the tail design the team leaned toward an inverted Y arrangement. The team felt that such a choice is something that was not usually tried in conventional aircrafts, but due to the low velocities the model would experience it was thought that the

disadvantages of such a choice would not have been significantly observed, and would have added stability to the airplane.

4. Analytical Analysis

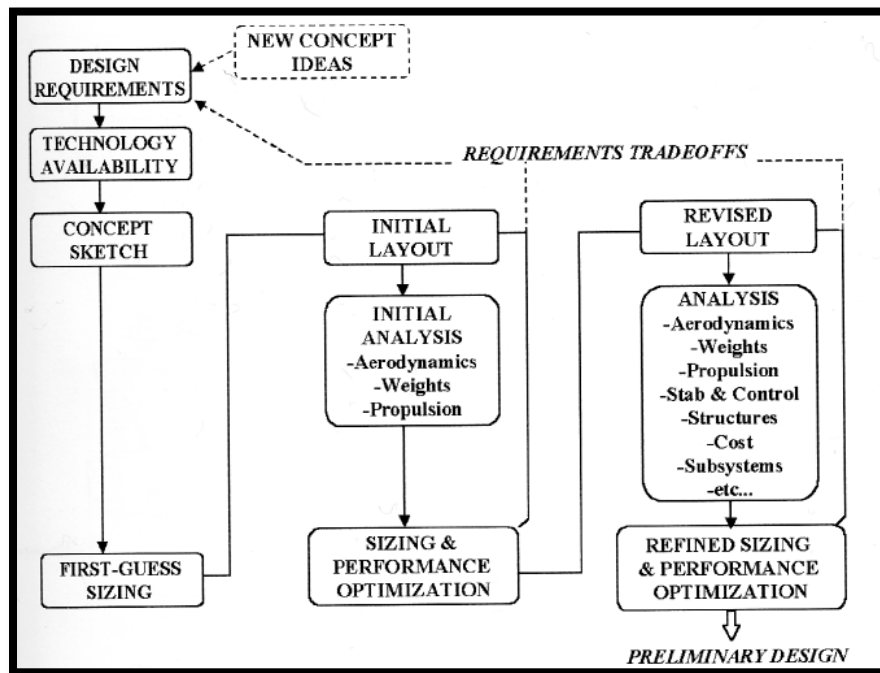


Figure 22 - Aircraft Conceptual Design Concept

Aircraft design of any kind is a constant process of revision. Like the diagram in Figure 20 shows, new proposed ideas start the process of conceptual design. After this process is started the sequential order of the process ensures that the concept is realistic enough to endure preliminary calculations of performance. To create an example, weight calculation is done prior to deciding upon the power plant. This creates a situation where one must decide on a propulsion strong enough to work with the initial guess, but subsequently such a propulsion device must now be part of that initial estimated weight guess. This process creates the need for several iteration techniques as this is a delicate and peculiar type of design process since most changes affect the weight of the aircraft, and weight is of a extreme importance in aerodynamic design.

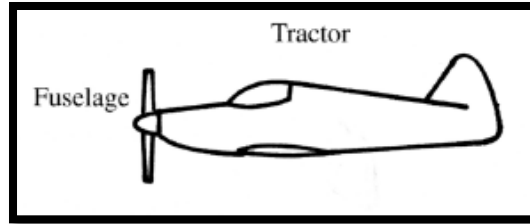


Figure 23 - Propeller Configuration of the Airplane

Propeller selection is the one of the main challenges for the team in order to select the best and appropriate propeller for the airplane. Generally speaking, the higher propeller diameter, a higher efficiency can be obtained. There are important considerations in this process, due to the fact, that many propellers shapes can give different vantages to the airplane. Some of them, offer high velocity during the flight, and other ones can provide more thrust power during the takeoff. The team used formula displayed in Figure 21 to determine the best propeller.

	British units	Metric units	$D = K_p \sqrt[4]{Power}$
No. blades	K_p	K_p	
2	1.7	0.56	
3	1.6	0.52	
4 +	1.5	0.49	
Power units	hp	kW	
Diameter units	ft	m	

Figure 24 - Propeller Selection Table & Formula

The maximum lift coefficient of the wing will usually determine the wing area, this strongly affects the aircraft takeoff weight to perform the design mission of the airplane. The following graph represents how important is to have a good airfoil design, in order to find the best lift coefficient in the airplane.

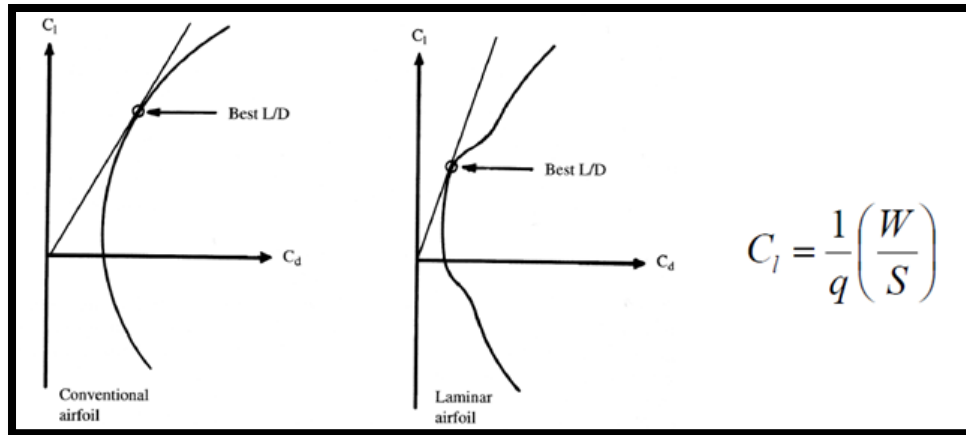


Figure 25 - Lift Coefficient Graph & Formula

One of the hardest specifications to design around is minimum takeoff distance. Due to this fact, the team used historical data perspective in order to have been able to design or predict a preliminary takeoff distance. Historical perspective design parameters are shown in Figure 24.

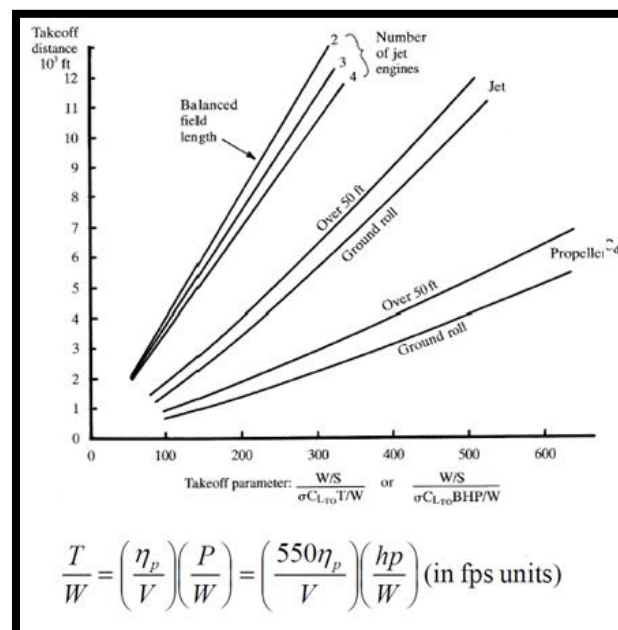


Figure 26 - Takeoff Distance Formulation

4.1. Inverse Design Method

Design of aerodynamic components has historically been composed of two kinds of categories: inverse design and shape optimization. Inverse design method requires the user to know specific parameters of the final configuration in order to use them as a goal for the final shape computation. Optimization in the other hand simply tries to find global properties of a preliminary design and from this point inch closer to an "optimal" solution to what the inverse design uses as a goal. It is important to note that although inverse design solutions require very little iteration, compared to optimization, they do require an intuitive knowledge of what the specified parameters would do as the aerodynamic shape changes flying conditions.

Final designs come from specified constrains given by the designer. This process will be shown in the inverse design data portion of the report. Surface pressure distribution will serve as the parameter that any initial shape would try to conform. The particular pressure distribution consideration is most likely a derived signature of an already successful design, or more simply the informed idea of an experienced aerodynamic designer. These improvements come about in the constant race to create a better design, but most importantly, in the likely chance that certain behaviors like flow separation might be minimized or prevented all together.

4.1.1 Background Theory of the Inverse Calculation Method

Stream function method will substitute the two-dimensional airfoil's potential flow by a vortex sheet aligned at the surface of the airfoil. For this condition to be satisfied there must be absolutely no flow through the surface of the two-dimensional airfoil shape. Total stream function must remain constant along the surface, therefore for a closed surface airfoil; the velocity distribution is equal to the vortex distribution as seen in equation (1).

$$\psi_s = U_0(y\cos\alpha - x\sin\alpha) + \frac{1}{2\pi} \oint s\gamma(s) \ln\left(\frac{r}{c}\right) ds \quad (1)$$

- ψ_s = stream function along airfoil surface
- U_0 = free stream velocity
- α = angle of attack
- (x,y) = coordinate of point on airfoil surface
- $\gamma(s)$ = vorticity distribution along airfoil surface
- r = distance from vortex density contribution on point (x,y)
- s = curvilinear coordinate along airfoil surface

The integral equation could be solved by dividing the vortex sheet into bounded elements of varying density values. This is done generally in the case of boundary element approach. The integral in equation (1) is solved by dividing the airfoil surface

into straight line boundary elements, or panels, with linearly varying vortex strength.

Therefore, the stream function equation for boundary element nodes becomes

$$\psi_s = U_0(y_i \cos\alpha - x_i \sin\alpha) - \sum_{j=1}^n (K_{ij}\gamma_j + K_{ij+1}\gamma_{j+1}) \quad (2)$$

Where n is the number of boundary elements, γ_j and γ_{j+1} are vortex strengths at node j and j+1 and K_{ij} and K_{ij+1} . From equation (2), the expression for the y coordinate of any panel node y_i on the airfoil surface can be written as

$$y_i = [\Psi_s - \sum_{j=1}^n (K_{ij}\gamma_j + K_{ij+1}\gamma_{j+1})] / (U_0 \cos\alpha) + x_i \tan\alpha \quad (3)$$

If vortex strength γ_j at the nodes are prescribed and x_i locations of panel endpoints defined, knowing that Ψ_s will be constant along the airfoil surface we can iteratively solve for the y locations y_i of all panels which define the airfoil. This method will then produce an airfoil shape that satisfies pressure distribution input, which would be equivalent to vortex distribution as previously explained. The pictures below show examples of the process explained.

4.2. Optimization

4.2.1. Gradient Methods

Optimization is the process of maximizing or minimizing a given function in order to find optimum levels for the active variables. The purpose of the optimization is to find an optimum value for the objective function, or the cost function as is sometimes called. This function is simply a combination of the variables found in the problem in such a way that it describes with its magnitude the value of the system it represents. A common example of this could be a function that describes the negative or beneficial parameters of a wing. In such type of problem we could suppose that three main ingredients come together to describe an optimum wing geometry. These three factors that could be considered are lift, friction and moment, creating a summation formula such that, as it gets larger, it becomes more ideal would entail maximization, contrary using the reciprocal of said summation would instead indicate minimization. The main point is that it is relatively easy to set up the search direction as one to minimize or maximize, but a quantitatively realistic summation might sometimes prove hard to conjure.

$$U = U(\mathbf{X}) \quad \mathbf{X} = \{X_1, X_2, \dots, X_N\}$$

Another parameter used in optimization is constrained. The way one might set up the objective formula could lead for the numerical solution where, one of the parameters being described falls in a range that it's not physically logical. In the previous example wing cross sectional area could in a numerical analysis solution become represented as a

negative number. This should be avoided, for this reason constraints are built so the process could only develop possible optimum values. Another reason constraints or inequalities are used is for single objective optimizations where the optimum solution leads to a undesirable characteristic. It is however important to know where this could lead in situations where the number of variables becomes too large to visualize.

Objective functions have another possible particularity; they may be unimodal or multimodal. Unimodal functions are the ones where only one maximum or minimum exists inside the range being analyzed. Contrary to that, multimodal functions have two or more maximums or minimums in the range of analysis. This classification does not indicate that the function needs to be continuous during such range, just that the indicated extreme point or points exist.

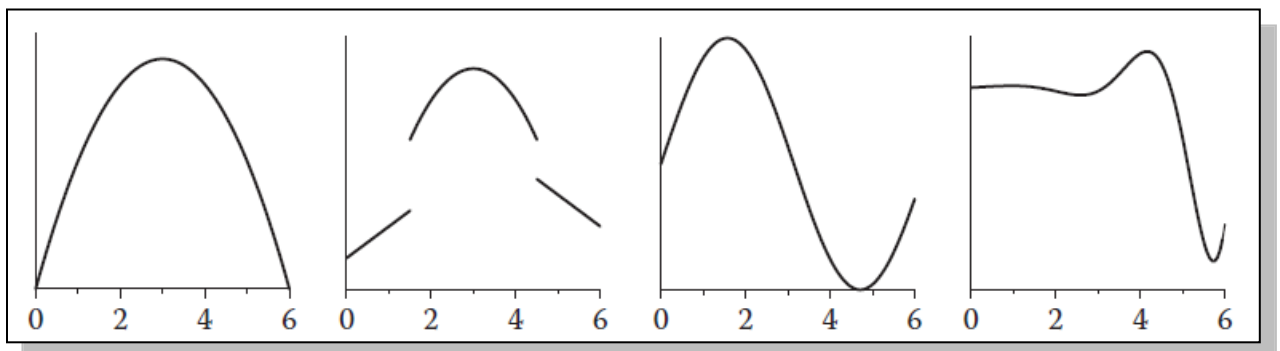


Figure 27 Examples of unimodal and multimodal single design variable functions

Gradient based methods are said to be deterministic since they rely in the functions gradient in order to find a possible extreme value. The major drawback of these methods is that their reliance in local gradient makes them unable to locate an extreme point that is uphill of the initial guess. These methods work like a fluid in a mountainous terrain, they will always a lower point, but they could not climb out no matter the magnitude of a nearby global minimum. In general these methods are used to zero in function valleys once the vicinity of the global minimum has being established. The basic equation of gradient methods is as follows:

$$\mathbf{X}^{k+1} = \mathbf{X}^k + \alpha^k \mathbf{d}^k$$

Where:

- \mathbf{X} is the vector of design variables
- α is the search step size
- \mathbf{d} is the direction of descent
- k is the iteration counter

4.2.2. Non Gradient Methods

- **Differential Evolution**

This method is very similar to the generic algorithm and most of the non-gradient based methods, it also an evolutionary method which works just like Darwin's theory of surviving of the fittest where the strongest individual will survive and take its

genes to the future generation by combining its chromosomes with those of a mate in a process called crossover. This specific algorithm works by placing individual collections of variables, which will be called individuals next to predators. These predators will seek out the weakest individual closest to them in order to allow for evolution to take place. Some weak individuals that are not nearby will survive in order to allow such individual to pass certain traits that are not beneficial at the moment. This type of set up will prevent the algorithm from decaying into a local minimum. Mutation will also affect the parameters of the individuals with the chance of producing an improved individual. After several trials the D.E. method will demonstrate that the choice of mutation and nearby predators is one of the most important differences benefiting this non gradient optimization technique.

The formula use for the iterative process is:

$$\mathbf{P}_i^{k+1} = \delta_1 \mathbf{P}_i^k + \delta_2 [\boldsymbol{\alpha} + F(\boldsymbol{\beta} - \boldsymbol{\gamma})]$$

Where \mathbf{P} = the number of individual vector of parameters

K = number of generation.

δ_1, δ_2 = functions that define the mutation.

F = constant that define the mutation between .5 and 1

$\boldsymbol{\alpha}, \boldsymbol{\beta}, \boldsymbol{\gamma}$ = 3 random individuals in the population

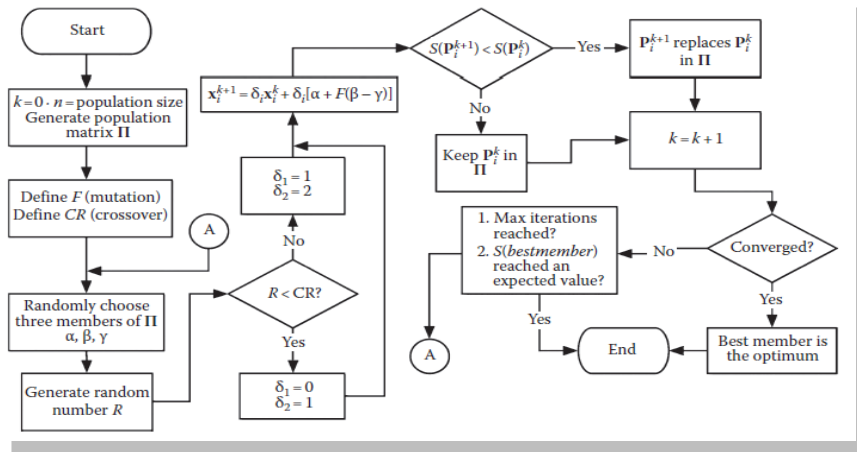


Figure 28 - Example of Differential Evolution Structure and Sequence

- **Particle swarm**

Here there is another non-based method which was created by an electrical engineer and social psychologist called James Kennedy. This method is an alternative to the generic algorithm and works by using social behavior and tries to find the balance between individuality and sociability of the individual of the population in order to find an ideal interest. It is important to find a balance because if the sociability is too high then all individual will converge to the first place they find, and if individuality is too high then individuals may never find an ideal spot. Here the formula used was:

$$\mathbf{v}_i^{k+1} = \alpha \mathbf{v}_i^k + \beta \mathbf{r}_{1i} (\pi_i - \mathbf{P}_i^k) + \beta \mathbf{r}_{2i} (\pi_g - \mathbf{P}_i^k)$$

$$\mathbf{P}_i^{k+1} = \mathbf{P}_i^k + \mathbf{v}_i^{k+1}$$

Here the values for α and β are between 0 to 1 and 1 to 2 respectively also:

\mathbf{P} = the number of individual vector of parameters

$\mathbf{r}_{1i}, \mathbf{r}_{2i}$ = random number with uniform distribution between 1 and 0

$\mathbf{v} = 0$ when $k = 0$

π_i, π_g = best value found by the number of individual \mathbf{P} , and best value of entire population

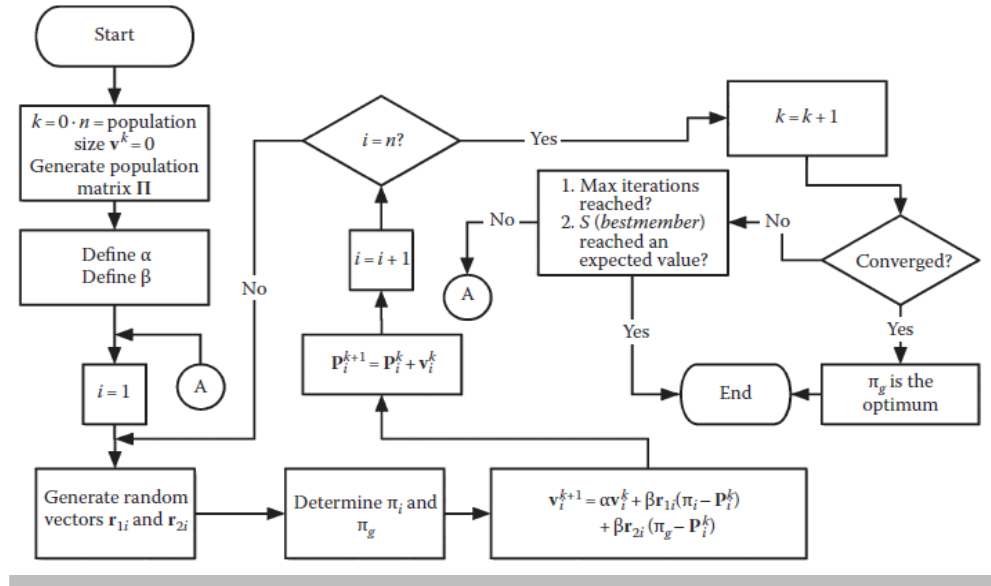


Figure 29 Particle Swarm Sequence and Structure

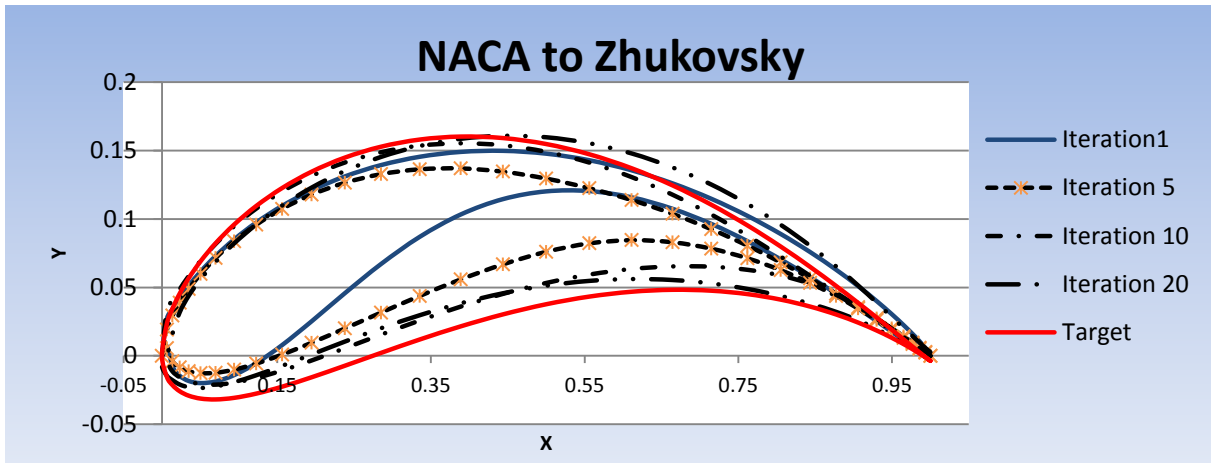
4.2.3. Hybrid Methods

Deterministic algorithms used for optimization, also known as gradient based methods, contain the ability to converge to an extreme point or global minimum in any case as long as the function is of the unimodal variety. In some cases these deterministic methods could reach a global extreme in a multimodal function, this situation however a product of the selection of initial points is as long as the initial parameters allow the gradient based method to search towards a region subject to negative gradient boundaries. These methods have the attribute of achieving this local convergence extremely fast. For such reasons, deterministic approach becomes the obvious choice as

a final extreme finding tool, for systems that can employ two or more algorithms in optimization purposes.

Stochastic methods differ completely from gradient based algorithms, where one falls short the other excels. Differential Evolution and Particle Swarm work as a cloud of some sort. These methods evolve or hover around the area being analyzed showing a numerical preference towards a global minimum. This numerical preference does not impede the algorithm from exploring areas or points nowhere near the global extreme. After a number of iterations the preference begins to form a path of convergence. The great feature of such methods is the fact that they don't rely in local topology to create new path or populations as in the case of evolution. This is of great importance since it allows the system to climb out a local minimum in the search of a global one. These methods are constructed with certain values or coefficients in some cases that guide the magnitude in which the system prefers or selects convergence. If such parameters are left for the user's opinion there is the possibility that the algorithm will unfortunately converge to a local extreme, in the same way, it may be the case that other values will create a very low global convergence preference making finding a minimum point lengthy or impossible. Due to those concerns we find that with changing topologies different stochastic methods will behave very differently.

Hybrid Optimization Algorithms are a mixture of the two types of methods discussed above, that take turns at attempting extreme global convergence with a numerical system that decides when each different method might become beneficial.



Below is a diagram of a common Hybrid Structure using Genetic Algorithms (GA), Simulated Annealing (SA), Nelder-Mead (NM), and finally DFP Gradient search.

Figure 30 - Evolution of Airfoil

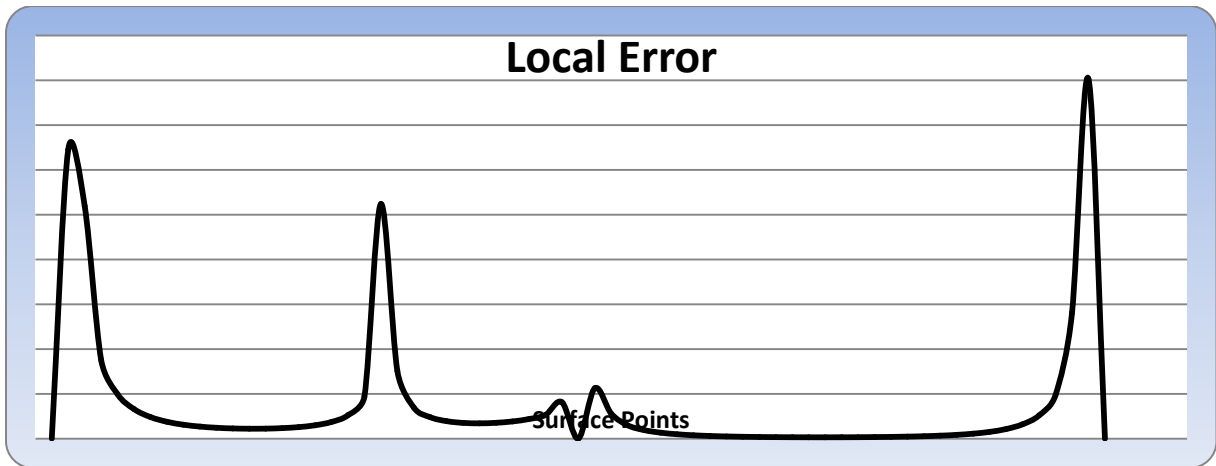


Figure 31 - Case 1 Local Error

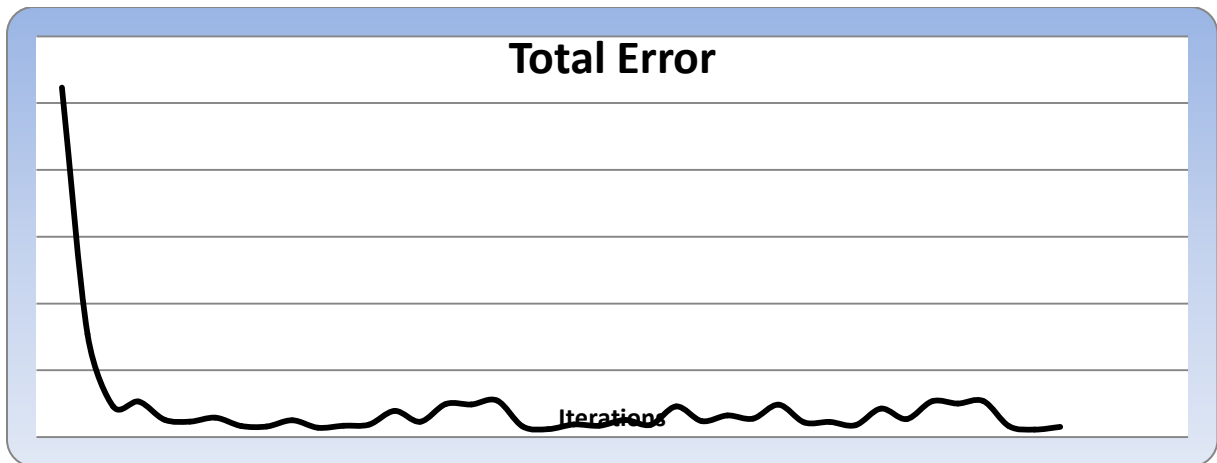


Figure 32 - Case 1 Total Error

4.2.4. Zhukovsky to NACA

Case 2 studies the evolution of a Zhukovsky airfoil into the target NACA8636 Airfoil. Table 3 shows the parameters for these two airfoils.

Table 5 - Case 2 Parameters

Target Airfoil		
NACA	Camber	8%
	Position from L.E	60%
	Thickness	36%
Gessed Airfoil		
Zhukovsky	Camber	0%
	Relative thickness	12%

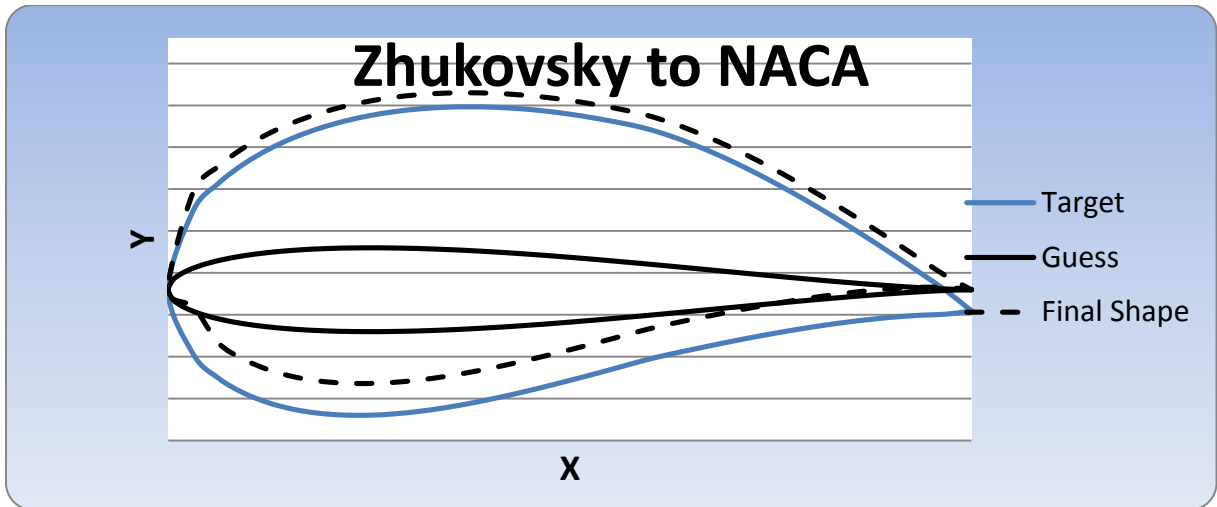


Figure 33 - Case 2 Guess, Target and Final Airfoil

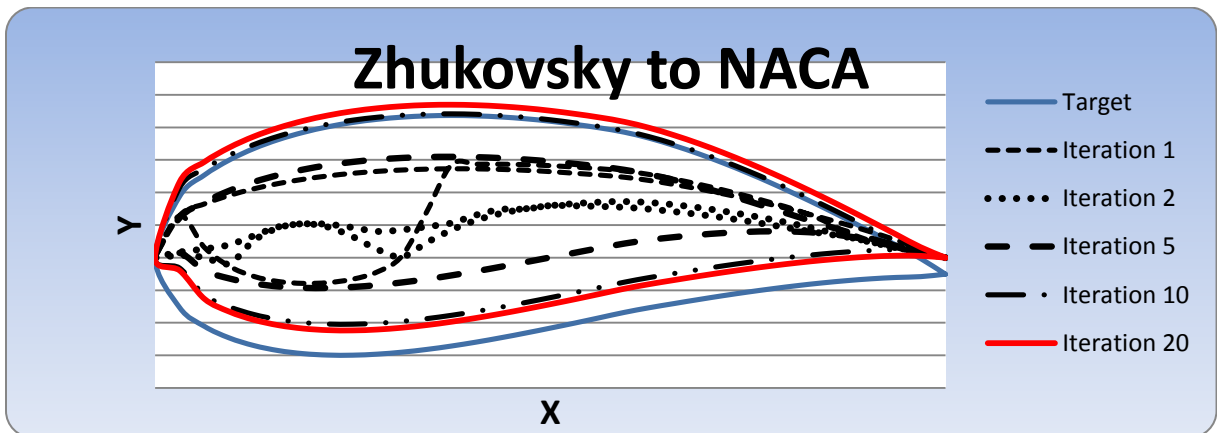


Figure 34 - Case 2 Evolution of Airfoil

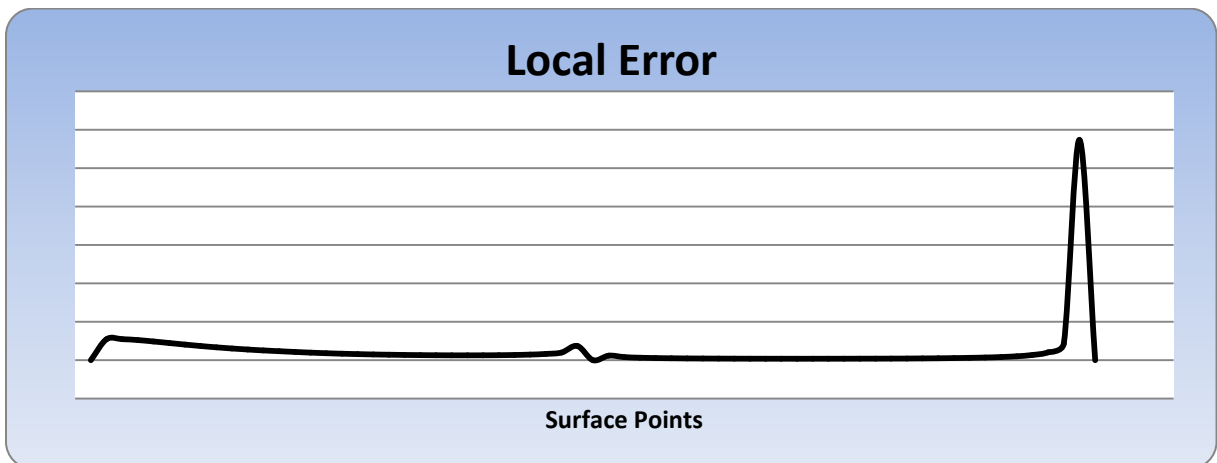


Figure 35 - Case 2 Local Error

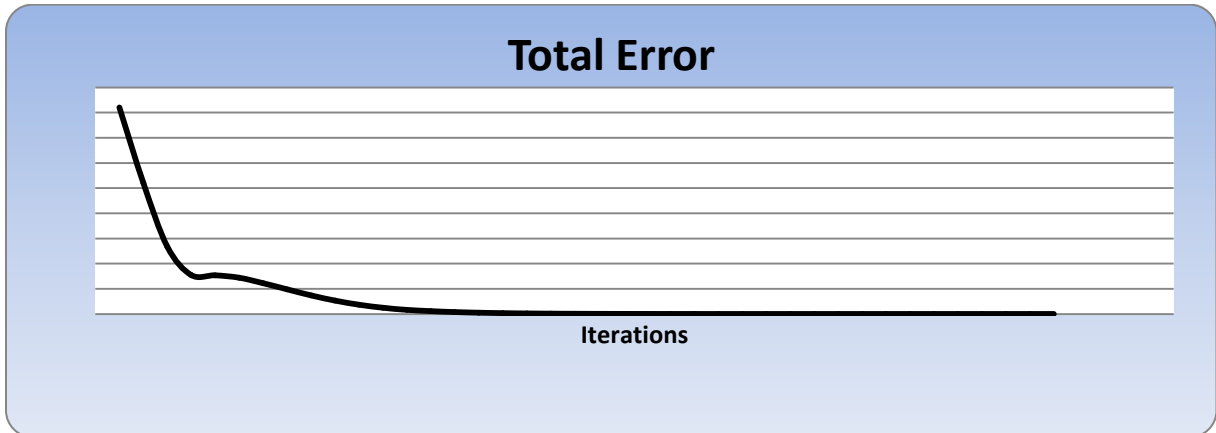


Figure 36 - Case 2 Total Error

4.2.5. Conjugate Gradient

The steepest descent method, in common, converges gradually for non-quadratic functions, since optimum search step sizes produce orthogonal gradients between two consecutive iterations. There is an entire class of variations to the steepest descent method that jointly can be called conjugate gradient methods (CGM). The underlying postulation used by these methods is that, near a minimum, the cost function can be approximated reasonably accurately by a quadratic function. The Conjugate Gradient method improves the convergence rate of the steepest descent method by choosing directions of descent that reach the minimum value of the objective function much more rapidly. The Conjugate Gradient method uses the same iterative procedure for the objective function.

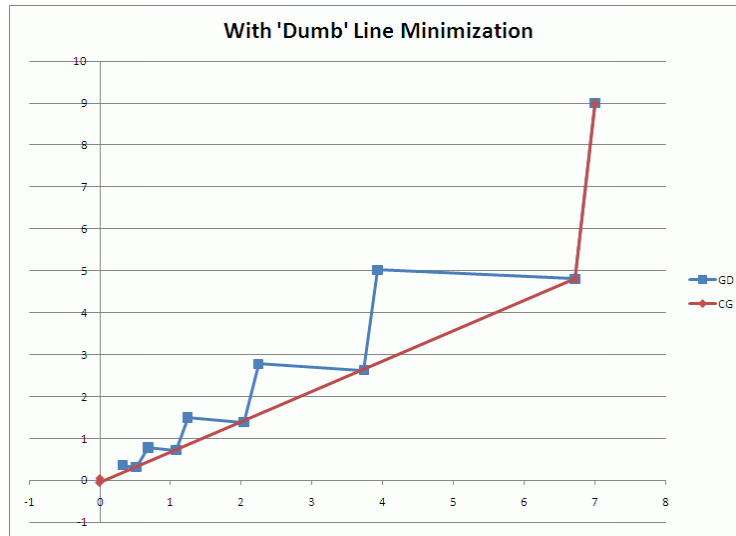


Figure 37 - Convergence path of Conjugate gradient Method

Conjugate gradient method used a conjugation of the gradient to obtain the direction of descent for all iterations, and it can be calculated by using Fletcher-Reeves or Polack-Ribiere method.

$$\gamma^k = \frac{\|\nabla U(\mathbf{X}^k)\|^2}{\|\nabla U(\mathbf{X}^{k-1})\|^2} ; \text{ with } \gamma^0 = 0 \text{ for } k = 0$$

Fletcher-Reeves

Polack-Ribiere

$$\gamma^k = \frac{[\nabla U(\mathbf{X}^k)]^T [\nabla U(\mathbf{X}^k) - \nabla U(\mathbf{X}^{k-1})]}{\|\nabla U(\mathbf{X}^{k-1})\|^2} ; \text{ with } \gamma^0 = 0 \text{ for } k = 0$$

On this case, the optimizer was tested in order to know how it behaved when a random point was selected on the objective function, as explained before, this cases works very good at finding the nearest local minimum to the initial guess, from the following graphs is noticeable how fast this method will converge. Also, it is important to notice that the steps sizes where set to 0.1.

On Figure . the value of X was compared against the number of iterations performed, from this graph is clear that the x value will converge to a point ensuring the convergence of the local minimum.

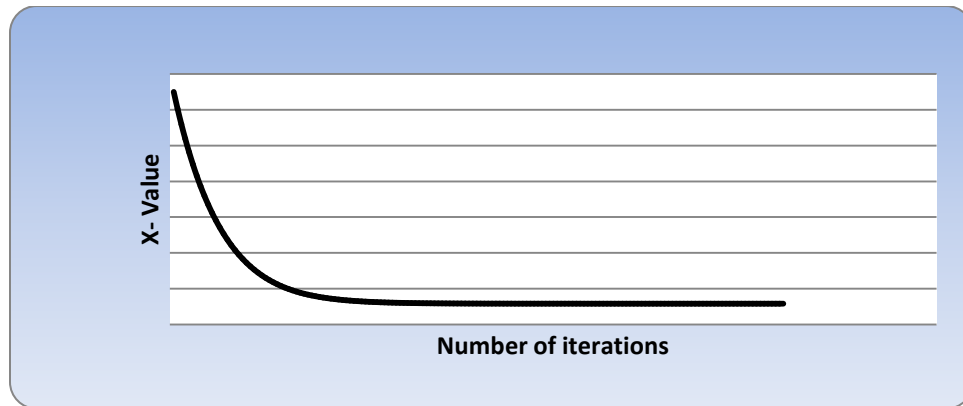


Figure 38 - Value of variable X convergence vs. iterations

On Figure 17 . the value of Y was compared against the number of iterations performed, from this graph is clear that the y value will converge to a point ensuring the convergence of the local minimum but before converging the y value will have a jump or a discontinuity letting the user know that the initial guess for the Y portion is not of good quality.

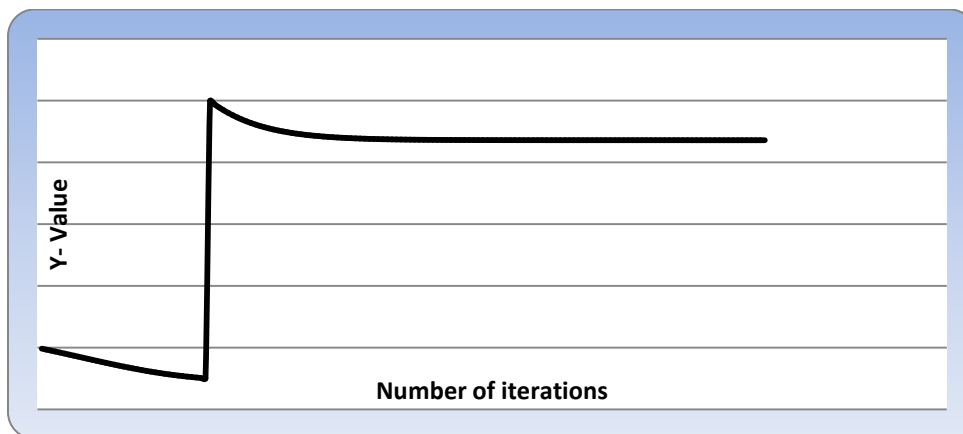


Figure 39 - Value of Y variable vs. iterations

The next figure depicts the plotting of the maximum error against the number of iteration, as the number of iteration increases the maximum error make the opposite path and start decreases until it reaches the desirable value and converges.

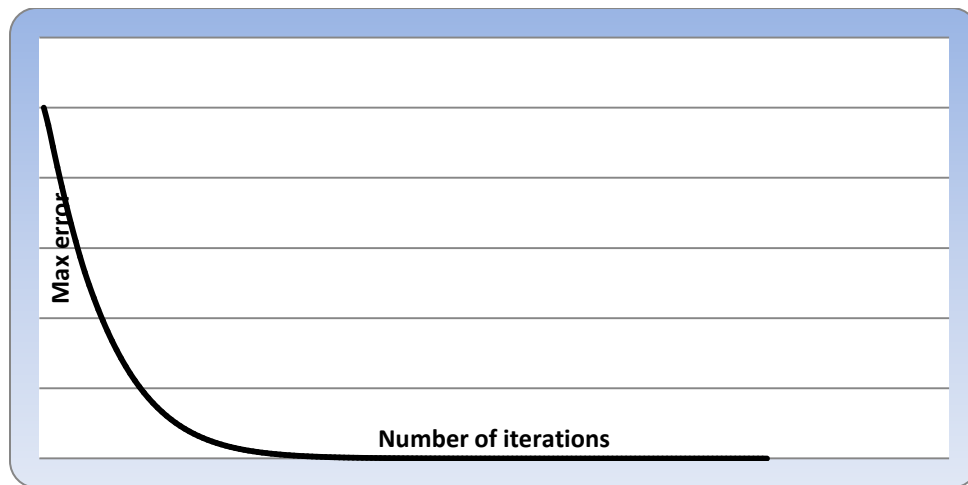


Figure 40 - Max error vs. iterations

The most telling analysis can be appreciated below on Fig 19. The main goal of the operation is shown when it could be seen that the objective function was able to be minimized to reach an asymptote region.

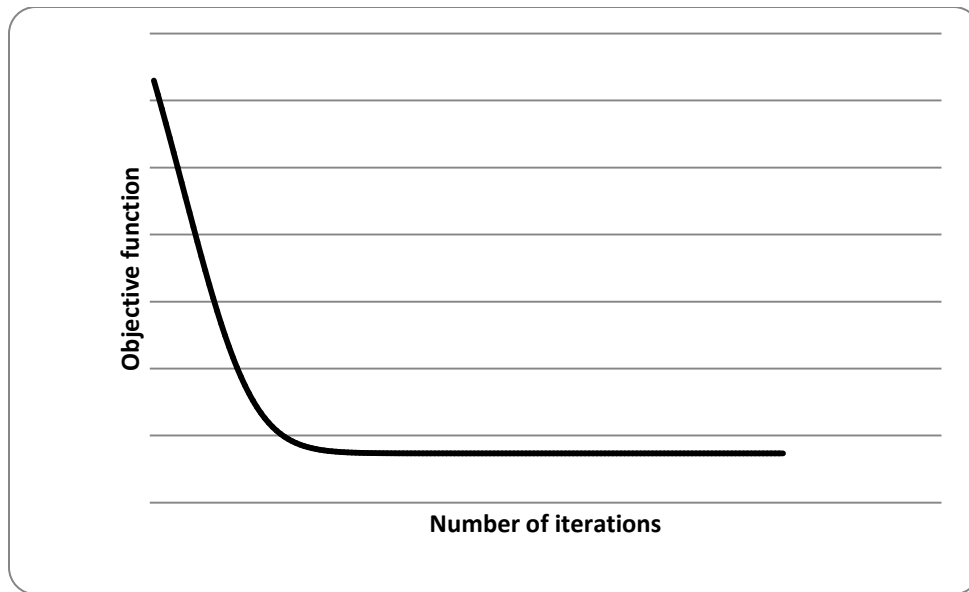


Figure 41 - Objective function convergence vs. iterations

4.2.6. Hybrid Method

Case 1 – Rosenbrock Function

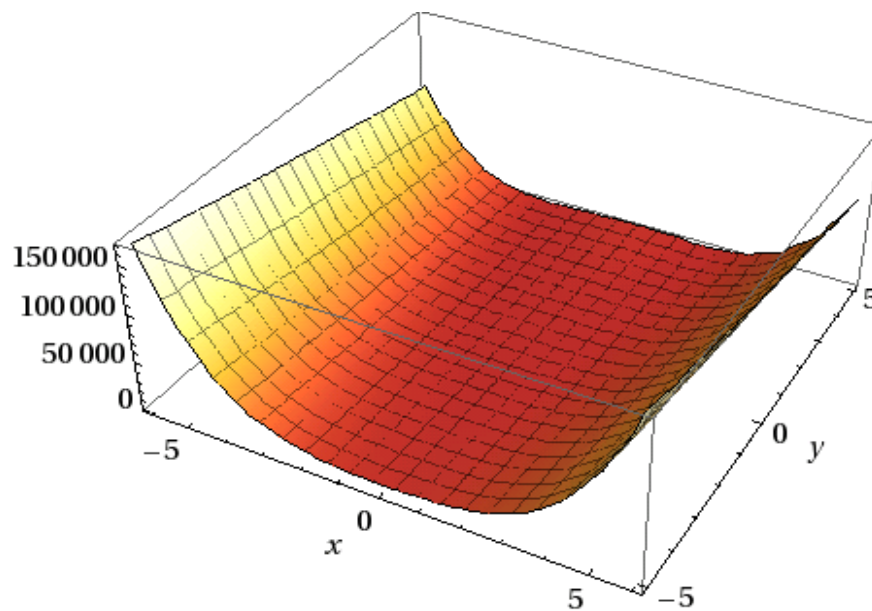


Figure 42 - Screenshot of Case 1

Table 6 - Case 1 Parameters

Function	$z(x, y) = 100(y - x^2)^2 + (1 - x)^2$
Range	$x \in [-6, 6]$ and $y \in [-5, 5]$
Known Optimum	$z_{min}(x_{opt}, y_{opt}) = z(1, 1) = 0$

Table 7 - Case 1 Results

x (guess)	3
y (guess)	2
x (converged)	0.61013085
y (converged)	0.37277063
z (minimum/converged)	0.15202406
Total iterations	205

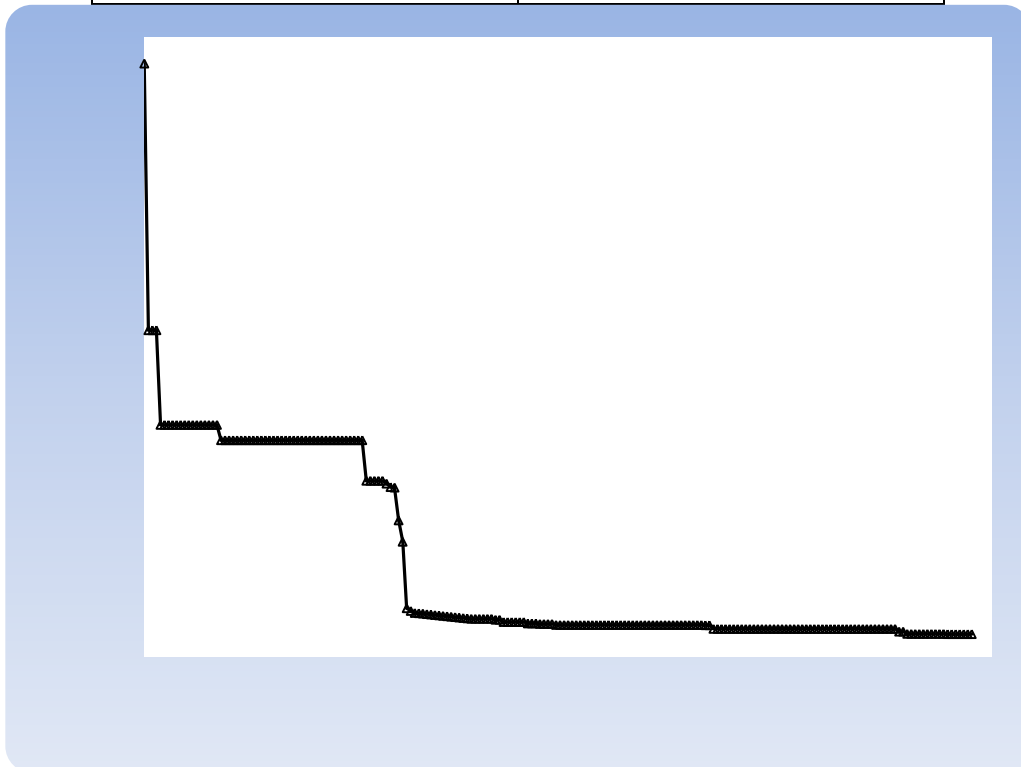


Figure 43 - Case 1 Convergence History

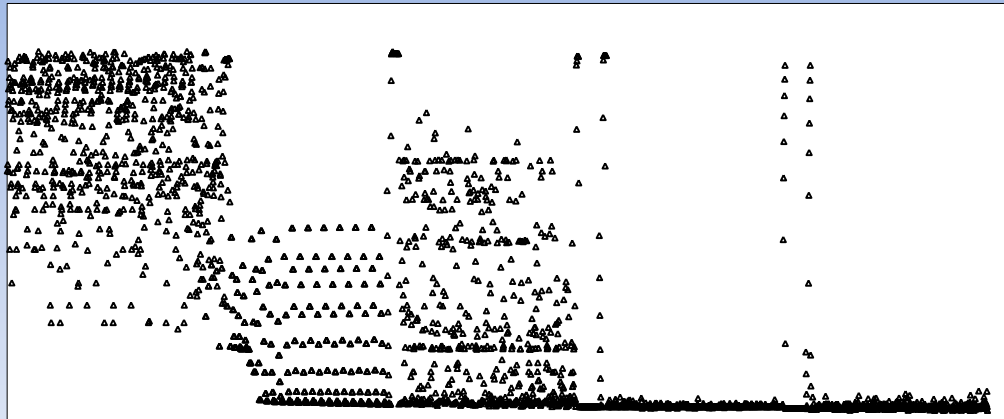


Figure 44 - Case 1 Overall Function Evaluation Convergence

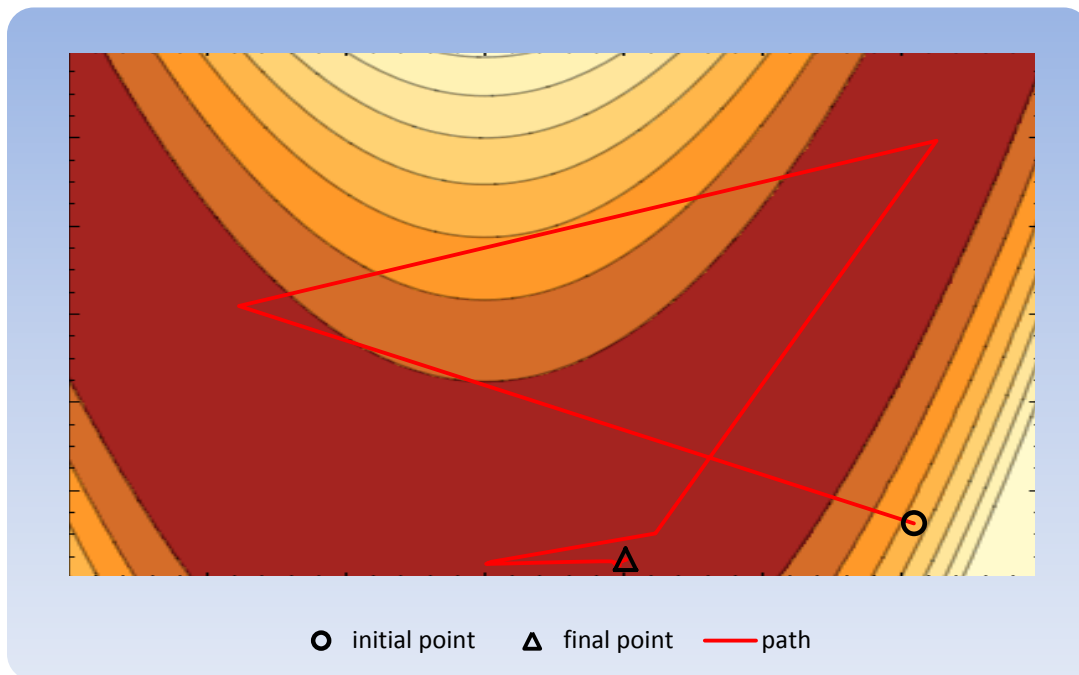


Figure 45 - Path Convergence

Table 8 - Case 1 algorithm sequence

Method	Iterations
Differential Evolution	22
Davidson-Fletcher-Powell	26

Nelder-Mead	10
Sequential Quadratic Programming	21
Linearization Method	2
Davidson-Fletcher-Powell	1
Differential Evolution	20
Genetic Algorithm	5
Nelder-Mead	1
Sequential Quadratic Programming	21
Linearization Method	2
Davidson-Fletcher-Powell	1
Differential Evolution	20
Genetic Algorithm	1
Nelder-Mead	1
Sequential Quadratic Programming	21
Linearization Method	2
Davidson-Fletcher-Powell	1
Differential Evolution	20

Case 2 – Rastrigin Function

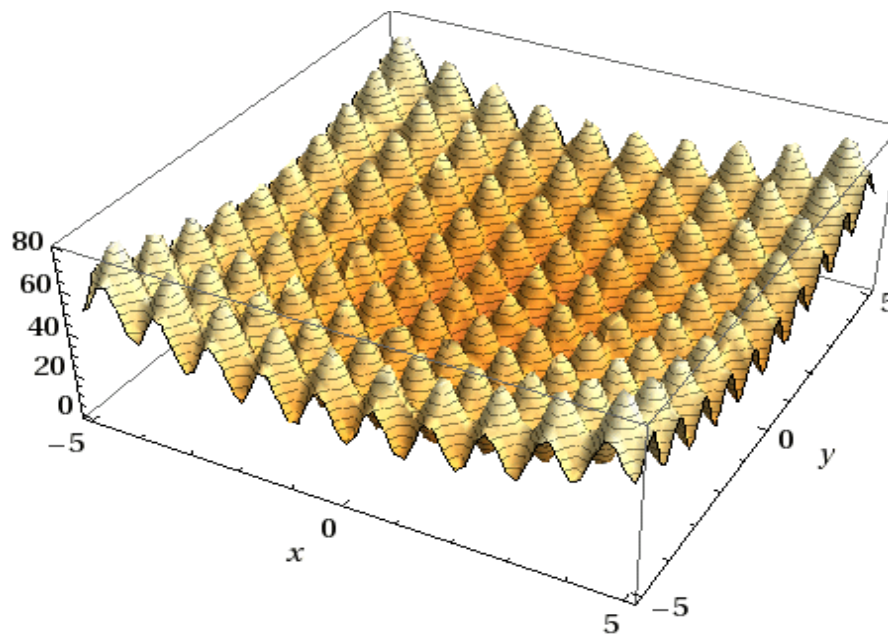


Figure 46 - Screenshot of

Table 9 - Case 2 Parameters

Function	$z(x, y) = x^2 - 10 \cos(2\pi x) + y^2 - 10 \cos(2\pi y) + 20$
Range	$x \in [-10, 10]$ and $y \in [-10, 10]$
Known Optimum	$z_{min}(x_{opt}, y_{opt}) = z(0, 0) = 0$

Table 10 - Case 2 Results

x (guess)	5
y (guess)	5
x (converged)	$-4.9999892 \times 10^{-5}$
y (converged)	$-4.9999892 \times 10^{-5}$
z (minimum/converged)	$4.99997909 \times 10^{-9}$
Total iterations	207

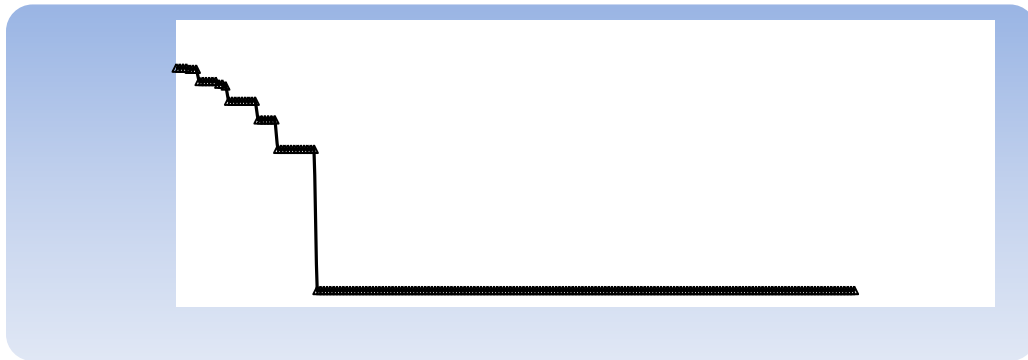


Figure 47 - Case 2 Convergence History

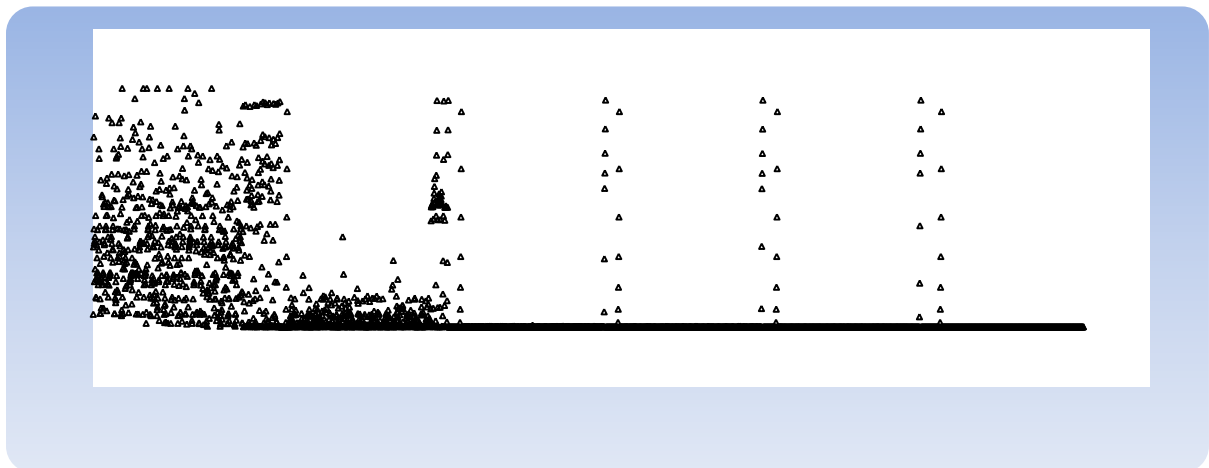


Figure 48 - Case 2 Overall Function Evaluation Convergence

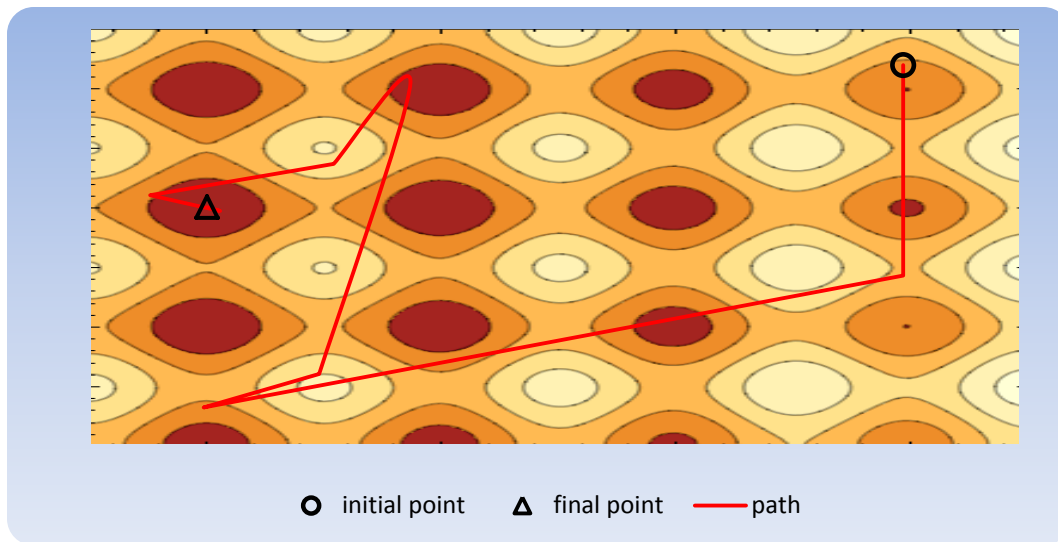


Figure 49 - Path Convergence

Table 11 - Case 2 Algorithm Sequence

Method	Iterations
Differential Evolution	22
Genetic Algorithm	3
Nelder-Mead	17
Sequential Quadratic Programming	2
Linearization Method	2
Davidson-Fletcher-Powell	1
Differential Evolution	20
Genetic Algorithm	7
Nelder-Mead	7
Sequential Quadratic Programming	3
Linearization Method	2
Davidson-Fletcher-Powell	1
Differential Evolution	20
Genetic Algorithm	4
Nelder-Mead	1
Sequential Quadratic Programming	4
Linearization Method	2
Davidson-Fletcher-Powell	1
Differential Evolution	20

Genetic Algorithm	1
Nelder-Mead	1
Sequential Quadratic Programming	5
Linearization Method	2
Davidson-Fletcher-Powell	1
Differential Evolution	20
Genetic Algorithm	1
Nelder-Mead	1
Sequential Quadratic Programming	6
Linearization Method	2
Davidson-Fletcher-Powell	1
Differential Evolution	20

4.2.7. Conclusion of Optimization

Unfortunately after all the methods were studied in depth it was not possible to implement them in the creation or design of an airfoil. It will require some more expertise in the area of programming to be able to write a code that would create the data necessary while also being able to compute behavior models. This could be done manually, but it would take a very long time, considering that the main advantage of the optimization methods is particularly this condition. In order to obtain workable data a smaller amount of data was gathered manually.

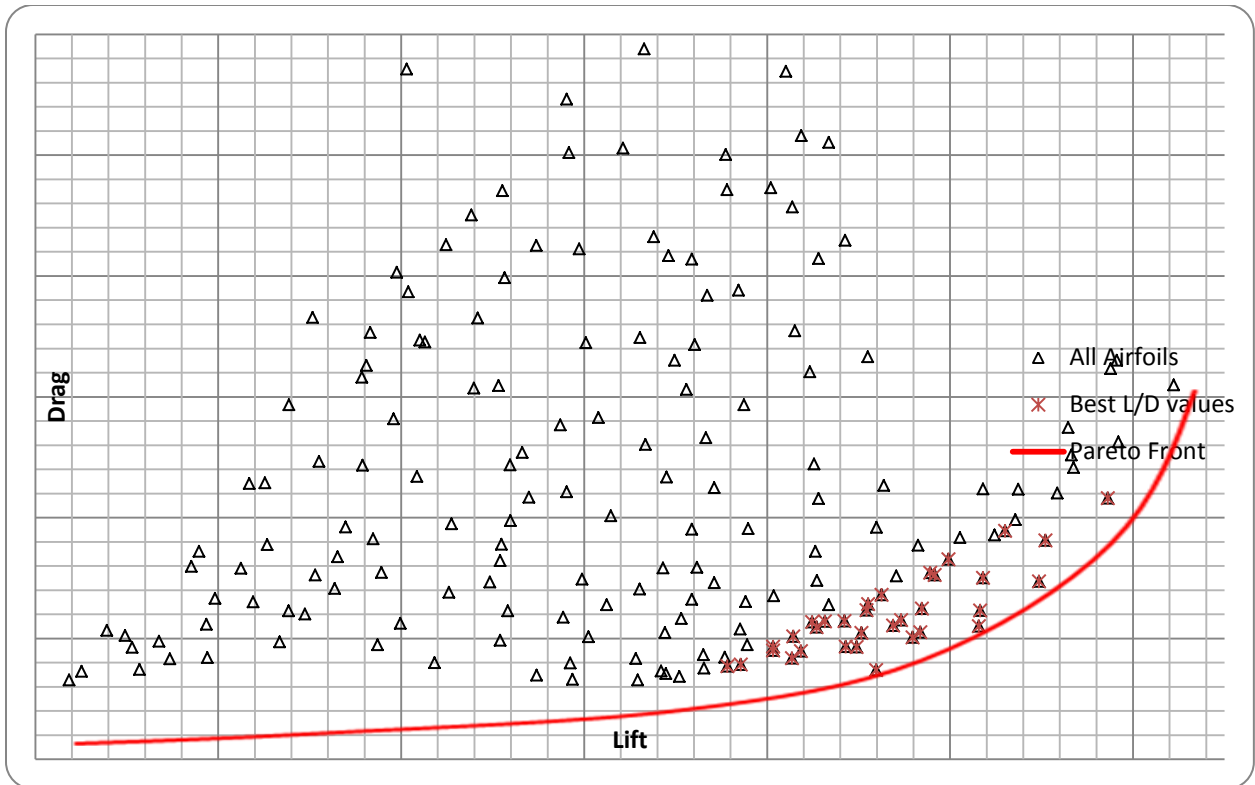


Figure 50 - Pareto Front Analysis

The result of the work researched during the summer served to gain the knowledge necessary to achieve the preceding graphical representation. Each point represents the specific signature in the condition of $(5.5e05)$ Reynolds value. The Pareto front shown in red demonstrates a limit where an infinite amount of solutions arrive at ideal conditions. This is the greatest contribution in optimization, the realization that the ideal condition is not a particular solution, but an ideal relationship between objectives.

5. Airfoil Selection

5.1 Wing Theory

Before selections or design are made for the wing, it was necessary to understand the basics of what can be affected and changed. The rules for the competition require a plane to take off in a particular runway's distance. Do to this rule, it was decided to design characteristics to work ideally at the moment where the aircraft reached a lift equal to the total weight of the aircraft. This happens when the plane is at level flight, but it also occurs at the beginning of the takeoff action. In commercial aviation a pilot must wait past this point in order to ensure safety but also to create a lift force that is significantly larger than total weight. In the competition scenario we could assume this point to be the same, and in this way, use it for convergence of the optimization.

- Chord – a straight line from the leading edge to the trailing edge
- Camber – curvature characteristic
- Mean camber line – set of points equidistant from upper and lower surfaces
- Thickness distribution – the distance from the upper surface to the lower surface measured perpendicular to the mean camber line
- Airfoil thickness ratio (t/c) = max thickness/chord

In order to properly select the wing that would ideally aid the design

$$W = L = qSC_L = \frac{1}{2}C_L V^2 A \quad (\text{In level flight and in our takeoff scenario.})$$

5.2 Wing Loading

This parameter is usually seen as one from which to determine the stress that is experienced on the wing. In our case the aircraft to be design and subsequently tested is only to be ideal at taking off. Therefore turning performance was neglected. We have an approximate value of wing loading of 14.5. The wings could resist higher loads with a few modifications; however our thrust would have not been able to handle such situations.

5.3 Stall Considerations

In order to base the assumptions in theory as well as in historical trends, the design or selection of airfoil takes into account the expected computed behavior as well as common traits that certain airfoils experience.

Thickness of the airfoil as a percentage of chords could determine three types of common outcomes.

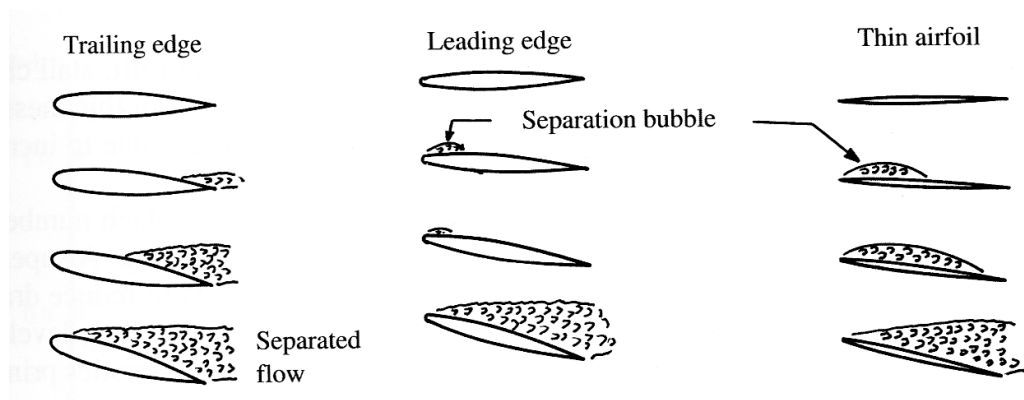


Figure 51 - Airfoil Thickness List

Thick Airfoil ($\frac{t}{c} > 14\%$)

Airfoils with round leading edges display a layer separation occurring from the trailing edge to a point on the upper surface. This type of airfoils show a gradual lost of lift which is

dependent on the amount of layer separation, this usually occurs after the angle of attack goes beyond 10 degrees.

Moderate Airfoil ($6\% < \frac{t}{c} < 14\%$)

Airfoils from this range of thickness display layer separation occurring at the leading edge with potential for reattachment. This condition is possible at very low angles of attack, getting progressively worse to the point where the layer separation totally fails to reattach, this creates an abrupt change in lift.

Thin Airfoil ($\frac{t}{c} < 6\%$)

Thin airfoils do not display the type of problems from the previous two categories, however they do create large changes in pitching moment. Once this condition was understood it was decided that the airfoil should fall in the range depicted by the moderate category. It is understood that moderate thickness airfoils tend to display a particular set of problems which our design is trying to avoid, however it is also necessary to evaluate if selecting thin or thick airfoils would have severe drawbacks in weight and structural fragility.

Taper Ratio

$$TR = \frac{\text{chord at tip}}{\text{chord at center line}} = \frac{0.3 \text{ m}}{0.9 \text{ m}}$$

$$\text{Taper ratio} = 0.33$$

The taper ratio is simply a number that describes the lift across the length of the wing, in the following chart it is illustrated how different ratios divide the lift across the wingspan. In many aircraft this graph is of severe importance, since some aircraft display a twist in the airfoil geometry, this variation or twist is created in order to create a wing that never experiences total stall conditions.

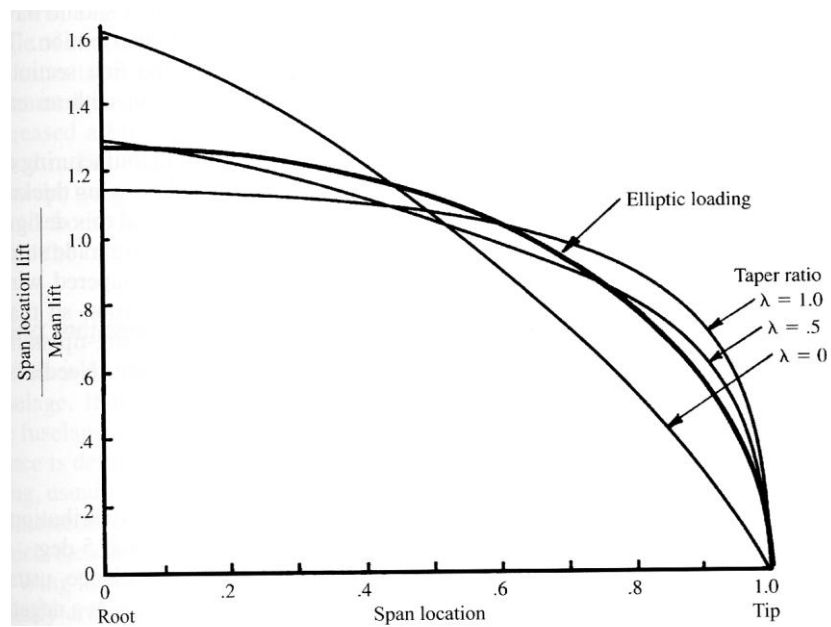


Figure 52 – Span/Mesh vs. Span location plot

The model built for the senior project does not exhibit such twist in airfoil geometry, therefore the taper ratio works only to project structure loads, and to predict conditions with

historical perspective. Based on recommended values for taper ratios we tried to stay away from values smaller than 0.2.

5.4 Wing Incidence and Dihedral angles.

The wing incidence of the design is a factor that was optimized as a part the wing and airfoil parameters. The angle of incidence found a particular ideal value of 7 degrees.

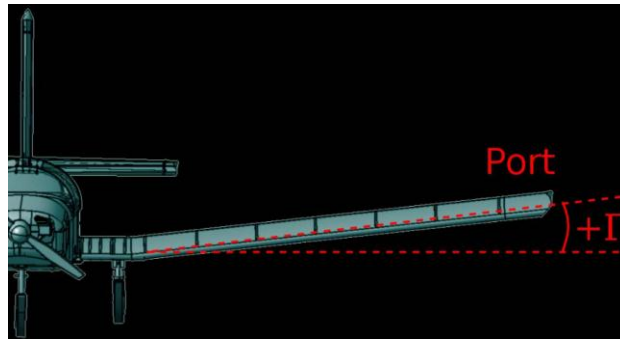


Figure 53 - Incidence Angle Picture

The dihedral angle is sometimes required on aircrafts with high wing location. Again, due to time considerations, we selected a conservative dihedral value of negative 4%. The use of a negative dihedral value in a plane similar to our in concept is shown below in the Antonov 225.



Figure 54 - Antonov 225

5.5 Take-Off Properties Calculations

In order to reach equations that will serve to understand what happens during takeoff it is important to break down the forces behind this action.

L = Lift force

a = Constant used to calculate T using T_0

R = Ground Normal force

t =

W = Aircraft's weight

T = Thrust

T_0 = Static Thrust

D = Drag force

μ = Coefficient of rolling friction

m = mass

g = Gravity constant

ρ = Air density

S = Wing area

V = Aircraft's velocity

C_{Dg} = Coefficient of drag during ground run

S = Distance

C_{lg} = Coefficient of lift during ground run

The team calculated a summation of forces in the vertical and horizontal directions.

$$L + R - W = 0 \quad \Rightarrow \quad R = W - L$$

Since after the thrust is applied the aircraft begins to accelerate, we end up with an equation that will give horizontal acceleration.

$$T - D - \mu R = m \frac{dV}{dt}$$

Rearrange using W and L

$$T - D - \mu(W - L) = \frac{W}{g} \frac{dV}{dt}$$

Rearrange again leaving acceleration by itself and substituting Lift and Drag equations we obtain the following formula.

$$g \left(\frac{T}{W} - \mu \right) - \frac{g}{W} \frac{1}{2} \rho S V^2 (C_{D_g} - \mu C_{L_g}) = \frac{dV}{dt}$$

In some applications or situations we can assume thrust to be constant during takeoff. In propeller aircraft this is not the case, but if we want to arrive at precise values we must account for this change.

$$T = T_0 - a V^2$$

Following some changes we obtain a new formula that accounts for changing thrust.

$$\frac{dV}{dt} = g \left(\frac{T_0}{W} - \mu \right) - \frac{g}{W} \left[\frac{1}{2} \rho S (C_{D_g} - \mu C_{L_g}) + a \right] V^2$$

In order to better visualize the factors that influence the system it is important to separate the values into two secondary equations. In A there will be conditions not depending on velocity, and B will consist of factors that change with speed.

$$A = g \left(\frac{T_0}{W} - \mu \right) \qquad B = \frac{g}{W} \left[\frac{1}{2} \rho S (C_{D_g} - \mu C_{L_g}) + a \right]$$

At this point we can clearly construct a formula that will give us the time it takes for the aircraft to be able to become airborne.

$$dt = \frac{dV}{A - B V^2}$$

Since factor B could possibly fall in the negative range, we must create a different result for such occasion.

Time for Ground Run Between any Two Speeds, Constant α_g , A, B > 0

$$t_2 - t_1 = \int_{V_1}^{V_2} \frac{dV}{A - B V^2} = \frac{1}{2\sqrt{AB}} \left\{ \ln \left[\frac{\sqrt{A} + V_2 \sqrt{B}}{\sqrt{A} - V_2 \sqrt{B}} \right] - \ln \left[\frac{\sqrt{A} + V_1 \sqrt{B}}{\sqrt{A} - V_1 \sqrt{B}} \right] \right\} \quad (7b)$$

Time for Ground Run Between any Two Speeds, Constant α_x , $A > 0$, $B < 0$

$$t_2 - t_1 = \int_{V_1}^{V_2} \frac{dV}{A + |B| V^2} = \frac{1}{\sqrt{A|B|}} \left[\tan^{-1} \left(\sqrt{\frac{|B|}{A}} V_2 \right) - \tan^{-1} \left(\sqrt{\frac{|B|}{A}} V_1 \right) \right] \quad (8)$$

The team established that the formulas previously discussed will predict the moment and aircraft could become airborne. This does not mean that in real life situation pilots should use these values. A commonly used ratio is displayed below that ensures that the aircraft is safely above minimum lift conditions or as is called stall.

$$V_{TO} = 1.2 V_{stall}$$

Assuming that the aircraft takes off from complete rest, we can further simplify the formula to the following:

$$t_{TO} = \frac{1}{\sqrt{A|B|}} \tanh^{-1} \left(\sqrt{\frac{|B|}{A}} V_{TO} \right) = \frac{1}{2\sqrt{A|B|}} \left[\ln \frac{\sqrt{A} + V_{TO} \sqrt{|B|}}{\sqrt{A} - V_{TO} \sqrt{|B|}} \right]$$

Now that take off time is known we could arrive at equations that will predict the distance required to achieve take off.

$$\frac{\frac{dV}{dt}}{\frac{dS}{dt}} = \frac{dV}{dS} = \frac{A - BV^2}{V} \qquad dS = \frac{V dV}{A - BV^2}$$

After integration the following is obtained.

$$S_2 - S_1 = -\frac{1}{2B} \ln(A - BV^2) \Big|_{V_1}^{V_2} = \frac{1}{2B} \ln \frac{A - BV_1^2}{A - BV_2^2}$$

Finally we arrive at a point where, assuming total rest at the beginning, the two factors previously described could be seen in how they affect the task of reducing take off distance.

$$S = \frac{1}{2B} \ln \frac{A}{A - BV_{TO}^2}$$

This theoretical calculations were used to double check the approximations done by the optimization of the wing parameters. At the end a certain convergence was found in the lift generated at the end of the run way length and the runway needed for takeoff as described above.

5.6 Selection Process

The Airfoil selection for this design is being analyzed by using MIT software called Xfoil version 6.96, which let the team analyze the shape and the coefficient of lift and drag of different shapes of NACA airfoils. In total, the team analyzed a total of 84 airfoil profiles.

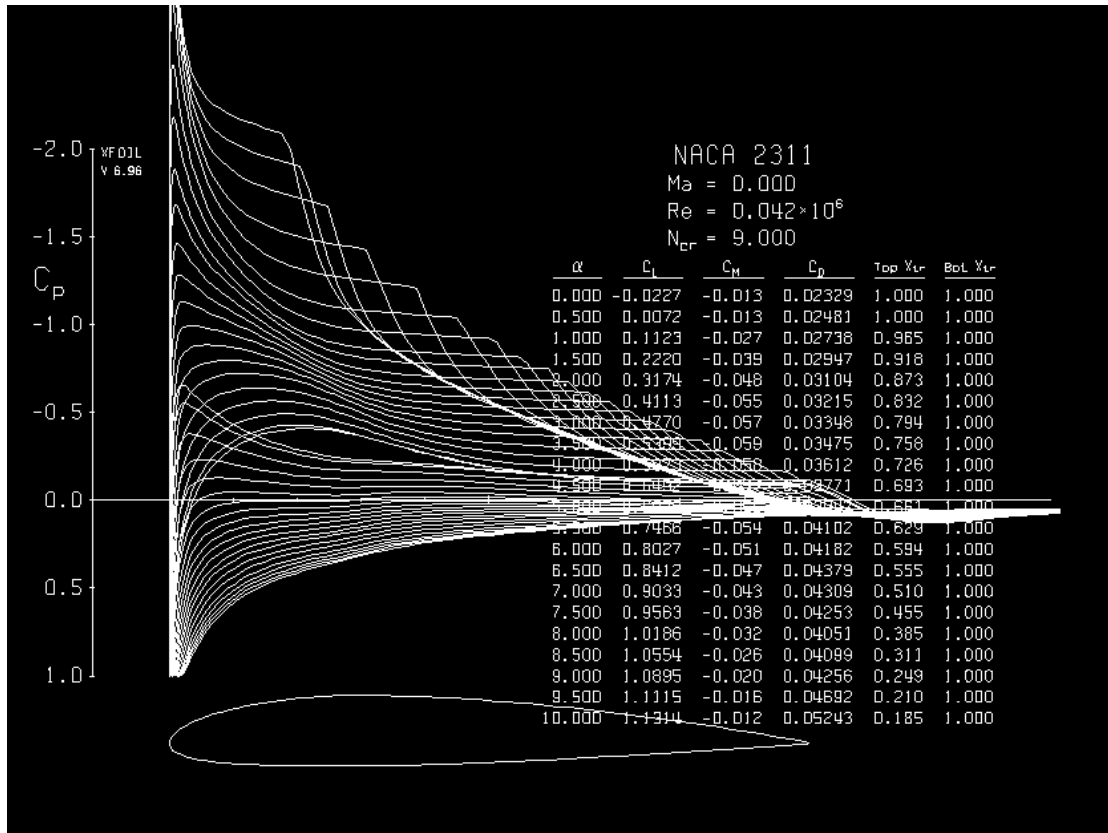


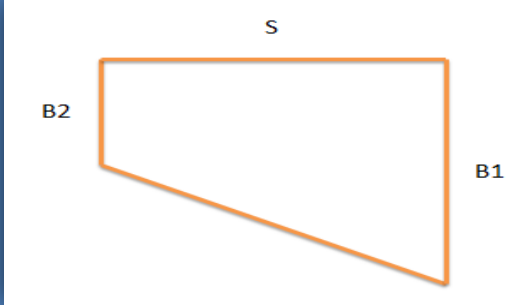
Figure 55 - XFOIL 6.96 Interface

The team selected the airfoil based on the optimum trade off situation that allowed for the best lift situation at takeoff. The following steps explain how the team was able to obtain the results in Microsoft Excel.

Using total lift as a constant, computing some common airfoils and after arriving at the approximate velocity that the plane would reach at the end of the runway specified by the regulations the team was able to concur on a fixed wing geometry. This geometry was then used as a constant from which the optimization could be generated. The first step of the process was to establish the shape of the wing. In this case, the shape was a tapered at the end,

for wing loading considerations, as one can see in the following table; also, it shows the dimensions of the wing and the value of the area for a total wing span.

Table 12 - Wing Area



The diagram shows a trapezoidal shape representing a wing area. The top horizontal edge is labeled 's'. The right vertical edge is labeled 'B1'. The left vertical edge is labeled 'B2'. The bottom edge is a diagonal line labeled 'Bx'.

Wing Area	
s (m)	1.4
B1 (m)	0.6
B2 (m)	0.3
A (m ²)	1.26
Bx (m)	0.45

Then, the team set up the conditions such as the air properties, and the desired cargo weight of the aircraft.

Table 13 - Air Properties

Air Properties	
μ (kg/s*m)	1.80E-04
ρ (kg/m ³)	1.204

Table 14 - Desired Weight of Aircraft

Plane mass and weight	
Weight (N)	147.15
Mass (Kg)	15.00

From the previous section and the results of the thrust experiment, the team was able to calculate the take-off properties required for the plane to fly.

Table 15 - Take-off Calculations results

Take-off Analysis	
So (m)	60
T (N)	30
Vto (m/s)	12
Re	3.61E+04

Once the take-off results were obtained the team used XFOIL software to analyze a total of 84 airfoil profiles. The goal of this step is to feed data to our objective function, which at this point, was able to calculate total lift at the moment the aircraft reached the end of the run way. It is important to note that contrary to intuition, the best scenario did not occurred at the iteration with the highest lift coefficient, but instead, it happened when the combination of drag and lift coefficient where optimal to our specific situation. The lift and drag coefficient helped the team to calculate the lift and drag forces of the airfoil. As mentioned before the team studied 84 profiles further separated in angles of attack, this methodology gave us about 1200 design scenarios. Performing an optimization process through the best 20 profiles, and finally selecting the best airfoil-alpha combination that guaranteed the best possible lift maintaining the design considerations.

In the following table, one can see a small portion used to create the parameters of study and the results obtained. The color red shows the best results of each profile.

Table 16 - Calculations of the airfoil

NACA #	α	C_L	C_D	k	Do (N)	vTo (m/s)	Re n	Lo (N)	L	Lo (lbf)	L/D
2110	0.50	0.0591	0.02299	0.0174384	3.906	14.967	4.51E+04	10.042	6.455309	2.257554	2.570683
	1.00	0.0901	0.0244	0.0185079	4.129	14.936	4.50E+04	15.246	9.841342	3.427378	3.692623
	1.50	0.1194	0.02626	0.0199187	4.419	14.895	4.48E+04	20.093	13.04169	4.517034	4.546839
	2.50	0.285	0.02933	0.0222474	4.891	14.828	4.46E+04	47.528	31.12966	10.6847	9.717013
	3.00	0.4713	0.02746	0.020829	4.605	14.868	4.48E+04	79.030	51.47863	17.76676	17.16315
	3.50	0.5508	0.02569	0.0194864	4.330	14.907	4.49E+04	92.845	60.16217	20.87249	21.44025
	4.00	0.5974	0.02657	0.0201539	4.467	14.888	4.48E+04	100.439	65.25214	22.57962	22.484
	4.50	0.6451	0.02854	0.0216482	4.771	14.845	4.47E+04	107.830	70.46226	24.24125	22.60336
	5.00	0.6925	0.03132	0.0237568	5.193	14.784	4.45E+04	114.811	75.63961	25.81044	22.11047
	5.50	0.7403	0.03435	0.0260552	5.645	14.719	4.43E+04	121.649	80.86066	27.34785	21.55167
	6.00	0.7805	0.03811	0.0289072	6.194	14.638	4.41E+04	126.853	85.25158	28.51775	20.48019
	6.50	0.8191	0.04249	0.0322295	6.818	14.545	4.38E+04	131.440	89.46774	29.54901	19.27748
	7.00	0.8386	0.0493	0.037395	7.757	14.402	4.34E+04	131.944	91.59766	29.6622	17.01014
	7.50	0.8628	0.05552	0.042113	8.581	14.274	4.30E+04	133.347	94.24095	29.97756	15.54035
8.00	0.7142	0.09179	0.0696246	12.812	13.565	4.08E+04	99.689	78.00984	22.411	7.780804	
2111	0.50	0.0254	0.02494	0.0189175	4.213	14.924	4.49E+04	4.291	2.774363	0.964666	1.018444
	1.00	0.0537	0.02656	0.0201463	4.466	14.888	4.48E+04	9.029	5.865483	2.029731	2.021837
	1.50	0.1232	0.02926	0.0221943	4.881	14.829	4.46E+04	20.550	13.45675	4.619741	4.210526
	2.00	0.325	0.03132	0.0237568	5.193	14.784	4.45E+04	53.882	35.49874	12.1132	10.37676
	2.50	0.4755	0.02907	0.0220502	4.852	14.833	4.46E+04	79.357	51.93738	17.84023	16.35707
	3.00	0.5529	0.02733	0.0207304	4.585	14.871	4.48E+04	92.749	60.39154	20.85086	20.23052
	3.50	0.6029	0.02766	0.0209807	4.635	14.864	4.47E+04	101.038	65.85289	22.71432	21.79682
	4.00	0.6484	0.02967	0.0225053	4.943	14.820	4.46E+04	108.022	70.82271	24.28431	21.85372
	4.50	0.6957	0.03214	0.0243788	5.316	14.766	4.44E+04	115.064	75.98914	25.86734	21.64592
	5.00	0.7383	0.0351	0.0266241	5.755	14.702	4.43E+04	121.055	80.64221	27.21415	21.03419
	5.50	0.7802	0.03866	0.0293244	6.273	14.626	4.40E+04	126.601	85.21881	28.4611	20.18107
	6.00	0.8081	0.04393	0.0333218	7.020	14.515	4.37E+04	129.135	88.26624	29.03063	18.39517
	6.50	0.831	0.04968	0.0376833	7.808	14.394	4.33E+04	130.605	90.76754	29.3612	16.72705
	7.00	0.8188	0.05933	0.045003	9.070	14.197	4.27E+04	125.176	89.43497	28.14068	13.80078
7.50	0.7879	0.0721	0.0546893	10.631	13.942	4.20E+04	116.172	86.05986	26.11659	10.92788	
2112	0.50	-0.0099	0.02708	0.0205407	4.546	14.877	4.48E+04	-1.662	-1.08135	-0.37362	-0.36558
	1.00	0.0162	0.02887	0.0218985	4.821	14.838	4.47E+04	2.705	1.769475	0.608164	0.561136
	1.50	0.1665	0.03247	0.0246291	5.365	14.759	4.44E+04	27.511	18.18628	6.184767	5.12781
	2.00	0.3432	0.03327	0.025236	5.484	14.742	4.44E+04	56.575	37.48667	12.71854	10.3156
	2.50	0.4748	0.03105	0.023552	5.152	14.790	4.45E+04	78.780	51.86092	17.7105	15.29147
	3.00	0.558	0.02899	0.0219895	4.839	14.835	4.47E+04	93.148	60.9486	20.94047	19.24802
	3.50	0.6065	0.02925	0.0221867	4.879	14.829	4.46E+04	101.167	66.2461	22.74314	20.73504
	4.00	0.6523	0.0308	0.0233624	5.114	14.795	4.45E+04	108.311	71.24869	24.34931	21.17857
	4.50	0.6947	0.03316	0.0251525	5.468	14.744	4.44E+04	114.555	75.87991	25.75297	20.94994
	5.00	0.7379	0.03616	0.0274281	5.911	14.680	4.42E+04	120.614	80.59851	27.11521	20.40653
	5.50	0.772	0.04018	0.0304773	6.491	14.594	4.39E+04	124.717	84.32315	28.03754	19.21354
	6.00	0.8024	0.04456	0.0337997	7.108	14.501	4.36E+04	127.990	87.64365	28.77327	18.00718
	6.50	0.8226	0.05024	0.038108	7.883	14.383	4.33E+04	129.076	89.85003	29.01756	16.37341
	7.00	0.821	0.0587	0.0445251	8.990	14.209	4.28E+04	125.738	89.67527	28.26706	13.98637

The following table shows the final 20 profiles, and the color green shows the airfoil-alpha selected for the aircraft, the color yellow shows the second best option but due to design considerations . It has to be mentioned that a Computational fluid dynamics simulation was performed in order to compare the theoretical and experimental results.

Table 17 - Optimized results and selection of airfoil

NACA #	α	CL	CD	k	Do (N)	L	Lo (lbf)	L/D
2310	7.00	0.93720	0.03691	0.027997	6.020	138.593	31.1570	23.0222
	8.00	1.01840	0.03637	0.027587	5.941	150.601	33.8564	25.3483
2311	7.00	0.90330	0.04309	0.032685	6.903	133.580	30.0300	19.3521
	7.50	0.95630	0.04253	0.03226	6.824	141.418	31.7919	20.7236
3110	6.50	0.91040	0.04982	0.037789	7.827	134.630	30.2660	17.2010
	7.00	0.90160	0.05971	0.045291	9.118	133.329	29.9735	14.6219
3111	6.00	0.88750	0.04359	0.033064	6.973	131.243	29.5047	18.8228
	6.50	0.90210	0.04985	0.037812	7.831	133.402	29.9901	17.0354
3210	6.00	0.88840	0.04399	0.033367	7.028	131.377	29.5346	18.6923
	6.50	0.91400	0.04905	0.037205	7.723	135.162	30.3857	17.5012
4110	6.00	0.92900	0.05183	0.039314	8.096	137.380	30.8844	16.9696
	6.50	0.92940	0.06071	0.04605	9.245	137.440	30.8977	14.8668
4111	6.00	0.93300	0.05107	0.038738	7.994	137.972	31.0173	17.2586
	6.50	0.93270	0.05907	0.044806	9.037	137.928	31.0074	15.2623
4210	5.50	0.89880	0.04649	0.035264	7.374	132.914	29.8804	18.0241
	6.00	0.93370	0.05069	0.038449	7.944	138.075	31.0406	17.3820
5110	5.00	0.93190	0.04782	0.036272	7.556	137.809	30.9808	18.2381
	5.50	0.95040	0.05430	0.041188	8.422	140.545	31.5958	16.6888
5111	5.50	0.95790	0.05297	0.040179	8.247	141.654	31.8451	17.1771
	6.00	0.96210	0.06039	0.045807	9.204	142.275	31.9848	15.4573
5210	4.50	0.90740	0.04181	0.031714	6.722	134.186	30.1663	19.9608
	5.00	0.94300	0.04567	0.034642	7.261	139.451	31.3498	19.2044
6110	4.50	0.95550	0.05078	0.038518	7.956	141.299	31.7653	17.7609
	5.00	0.92910	0.06175	0.046839	9.375	137.395	30.8877	14.6550
6111	4.50	0.95700	0.04968	0.037683	7.808	141.521	31.8152	18.1251
	5.00	0.94350	0.05839	0.04429	8.950	139.525	31.3664	15.5885
6210	4.50	0.94510	0.04928	0.03738	7.754	139.761	31.4196	18.0242
	5.00	0.96080	0.05541	0.04203	8.566	142.083	31.9415	16.5861
7110	3.50	0.94480	0.04863	0.036887	7.666	139.717	31.4096	18.2251
	4.00	0.97150	0.05395	0.040922	8.376	143.665	32.2973	17.1527
7111	4.00	0.93750	0.05579	0.042318	8.616	138.637	31.1669	16.0912
	4.50	0.93240	0.06434	0.048803	9.697	137.883	30.9974	14.2193
7210	3.50	0.97350	0.04301	0.032624	6.891	143.961	32.3638	20.8900
	4.00	0.95560	0.05211	0.039526	8.133	141.314	31.7687	17.3757
8110	2.50	0.92090	0.05048	0.03829	7.915	136.183	30.6151	17.2046

	3.00	0.94890	0.05494	0.041673	8.505	140.323	31.5459	16.4986
8111	3.00	0.95010	0.05350	0.040581	8.317	140.501	31.5858	16.8942
	3.50	0.97370	0.05752	0.04363	8.839	143.991	32.3704	16.2903
8210	3.00	0.97970	0.04890	0.037092	7.703	144.878	32.5699	18.8087
	3.50	1.00710	0.05323	0.040376	8.281	148.930	33.4808	17.9846

5.7 Computational Fluid Dynamics Simulation

5.7.1 Introduction to CFD

Once the team has selected the airfoil to use, it is important to test and compare the flight properties from the theoretical calculations with the results obtained from the simulations, this help the team to avoid any kind of inconvenient at the time of prototyping and testing.

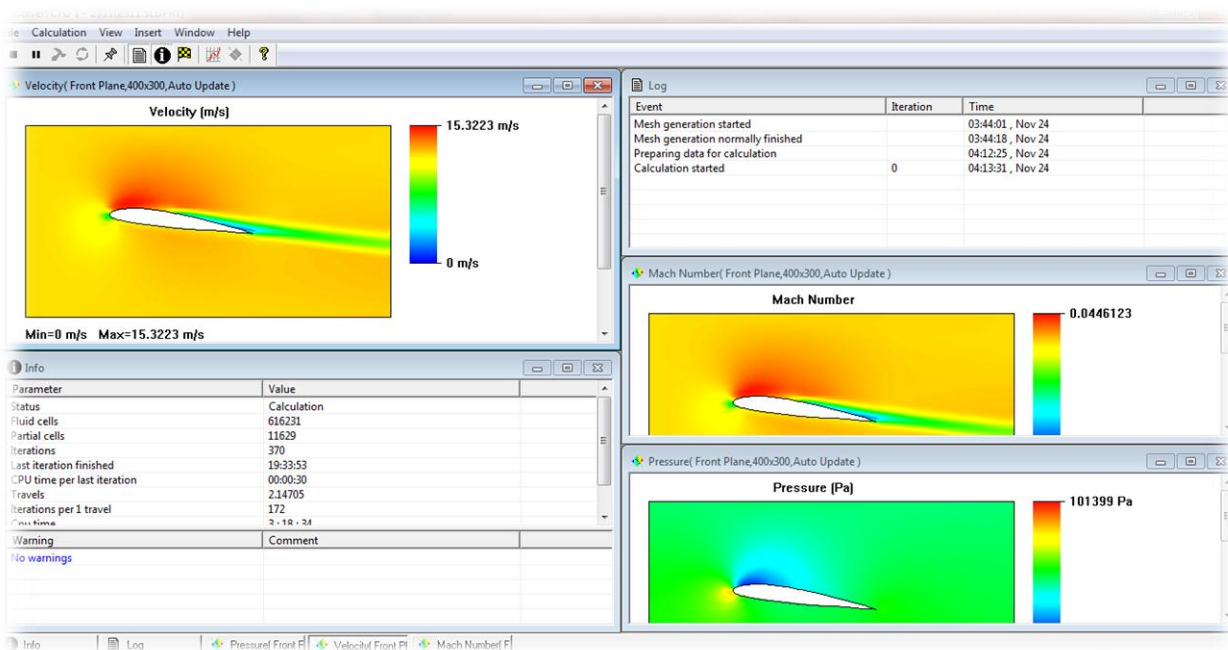


Figure 56 - SolidWorks Calculation screen of the CFD Simulation

Also, It has to be mentioned that different flow speeds will produce different results, so for that reason, computational flow dynamics simulation are extremely important for a total verification of the calculations which were performed through extensive periods of research.

The software used for this task was SolidWorks 2012 and its add-in option of Flow simulation to solve for the amount of lift and drag force. Due to the lack of software the team was limited to use only one kind of software analysis.

5.7.2 Simulation Set up

In order to be able of performing the simulations, the team has to establish some initial parameters to run them and to have the right case of study. From the theoretical calculations the team has obtained the thrust force generated by the engine, the theoretical lift and drag forces, Reynolds number and the take-off velocity. The parameters are shown in the following table and were introduced in the flow simulation analysis performed in SolidWorks.

Table 18- Initial parameters to consider in the flow simulation

Initial Parameters	Value (SI)	Value (Eng)
Thrust Force	30.00 N	6.74 lbf
Take-off Velocity	15.00 m/s	472.44 in/s
Take-off Distance	60.00 m	2362.20 in
Reynolds Number	4.203E+04	4.203E+04
Lift Force (Desired)	141.42 N	31.79 lbf
Drag Force (Desired)	6.82 N	1.53 lbf

In the following figure, one can see the entire wing; which was made using the NACA 2311 airfoil profile; and the computational domain, which is the calculation zone selected by the user.

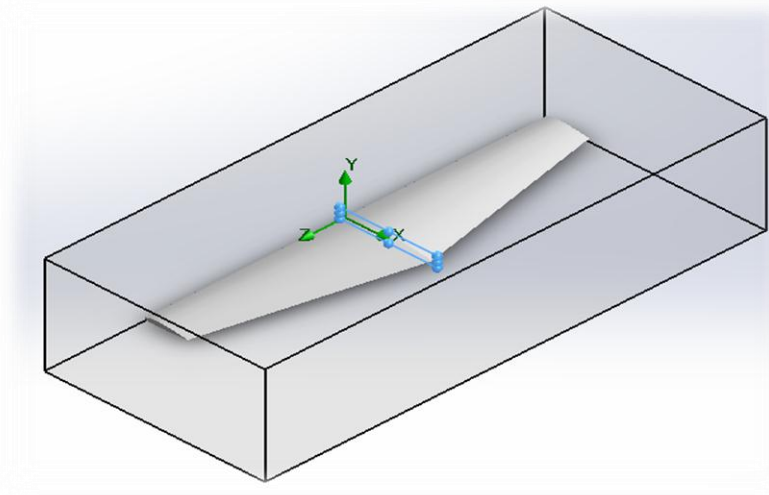


Figure 57 - CAD model of wing and its computational domain

The team input a total of 4 surface goals, which are:

- SG Normal Force (X)
- SG Normal Force (Y)
- SG Force (X)
- SG Force (Y)

5.7.3 Simulation Results

The simulations gave the following results for the surface goals with a little variation between the forces with same axial components because they are expected to be approximately the same.

Table 19 - SCFS Simulation Results

Goal Name	Unit	Value
SG Normal Force (X) 1	[N]	16.84139689
SG Normal Force (Y) 1	[N]	103.3567046
SG Force (X) 1	[N]	17.40393591
SG Force (Y) 1	[N]	103.2563398

In the following figures, one can show the pressure distribution of the airplane in the top and bottom surface and a cut plot viewed from the right plane.

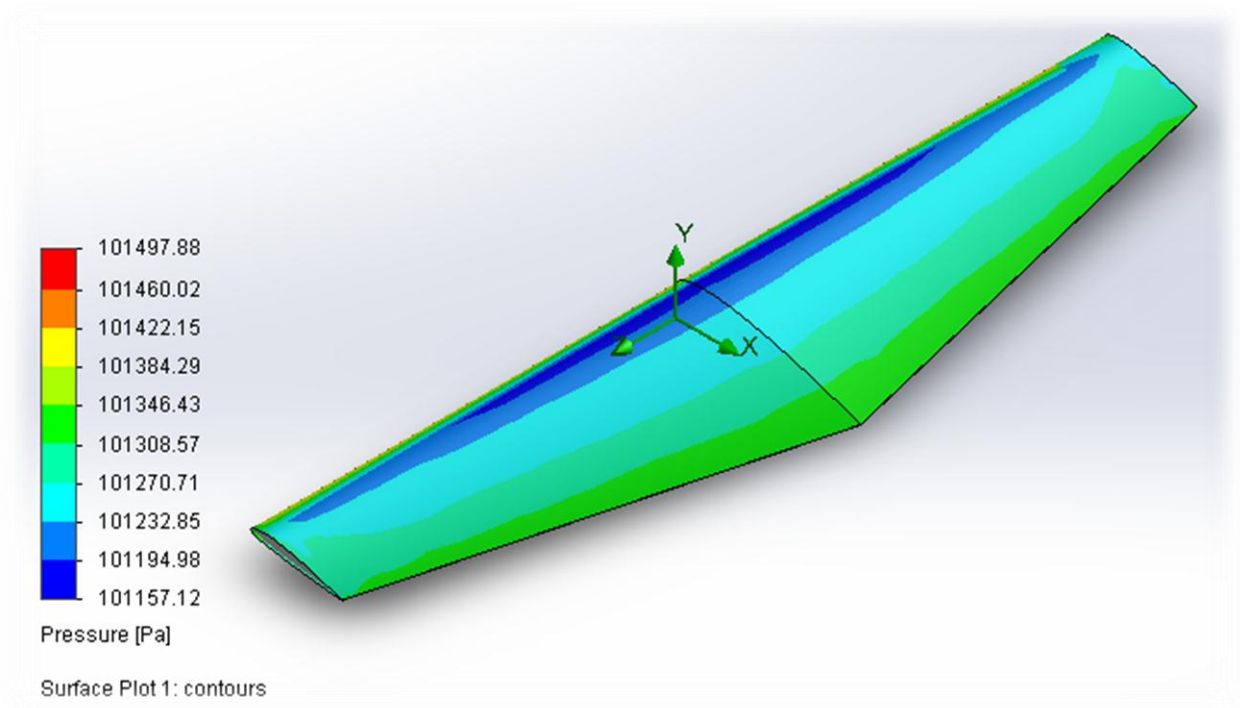


Figure 58 - Pressure distribution on the top surface

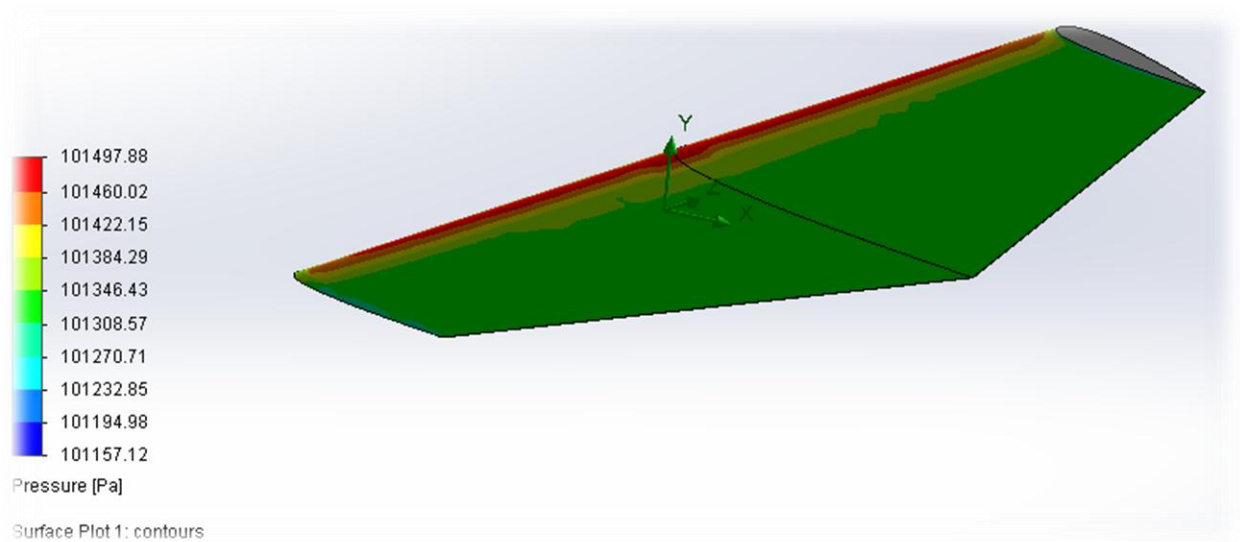


Figure 59 - Pressure distribution on the bottom surface

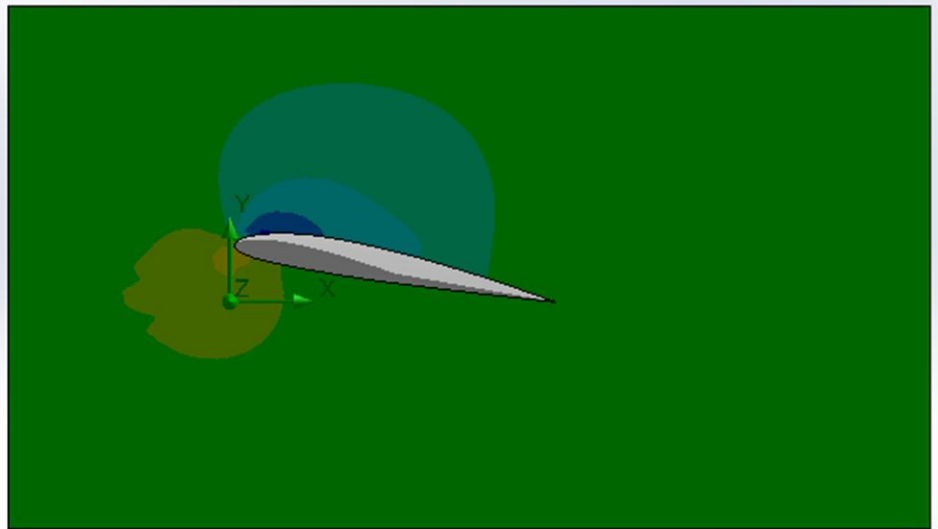


Figure 60 - Cut Plot of Pressure

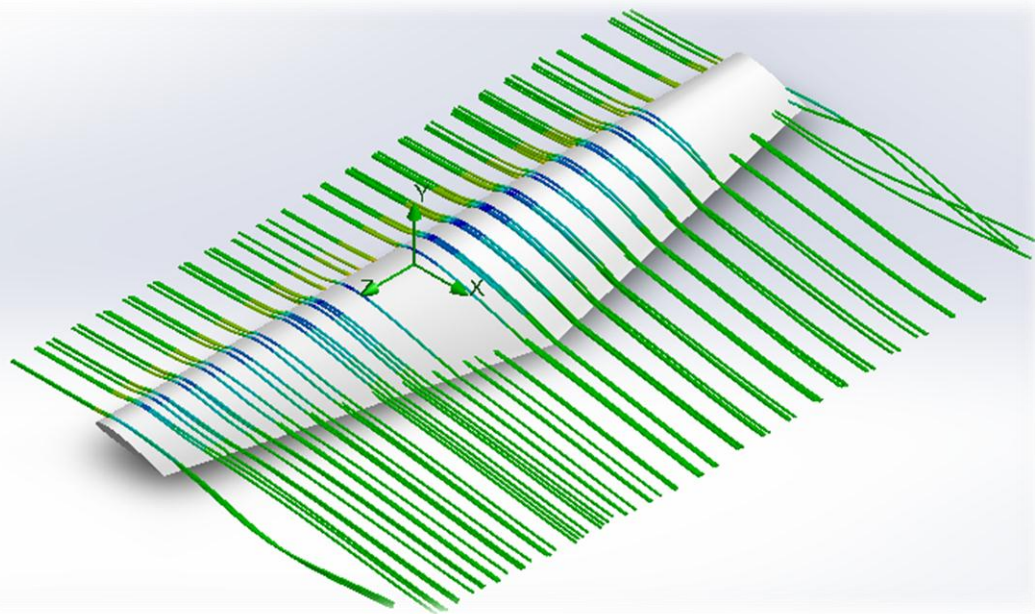


Figure 61 - Flow trajectories of the pressure on the top surface

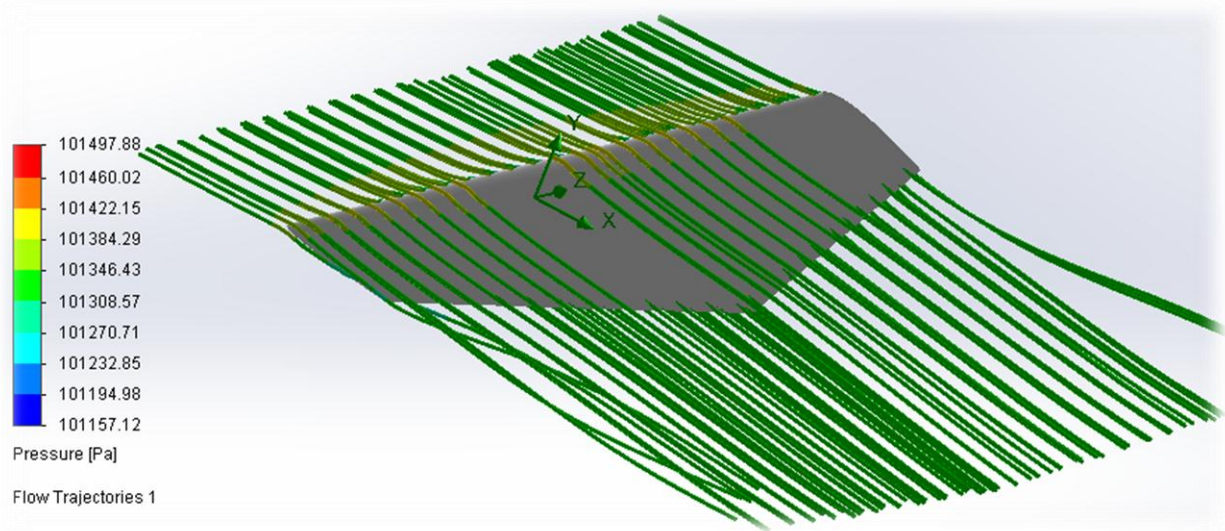


Figure 62 - Flow trajectories of the pressure on the bottom surface

The velocity and the vorticity were other points of consideration in this study, and in the following figures one can see their flow trajectories and cut plots.

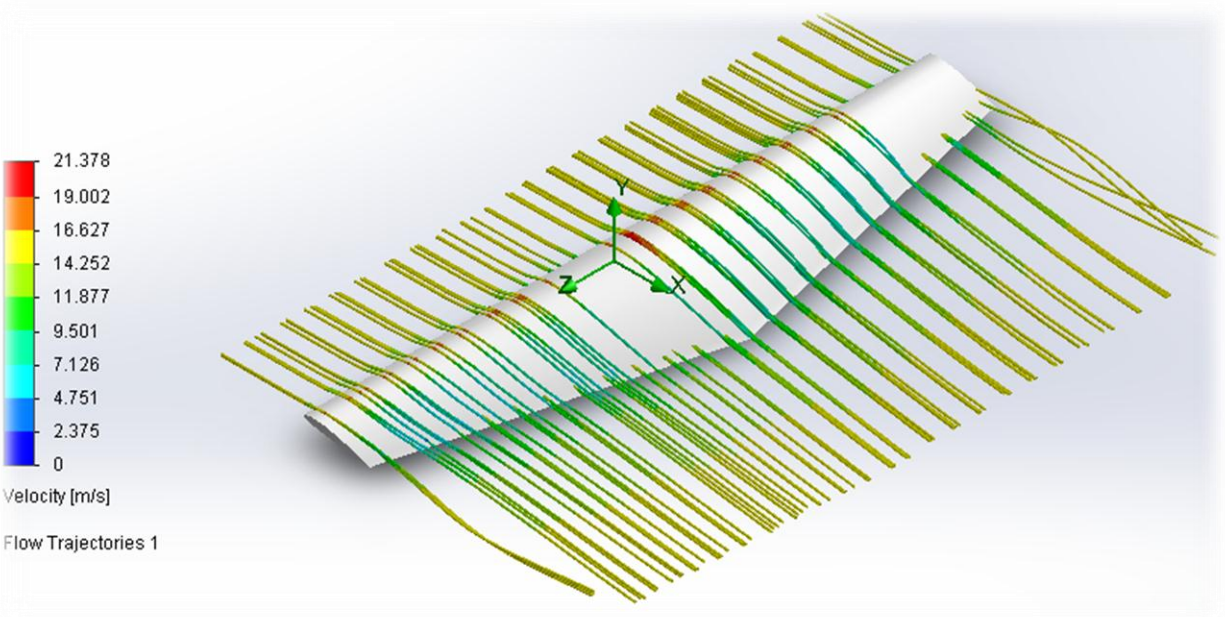


Figure 63 - Flow Trajectories of the Velocity

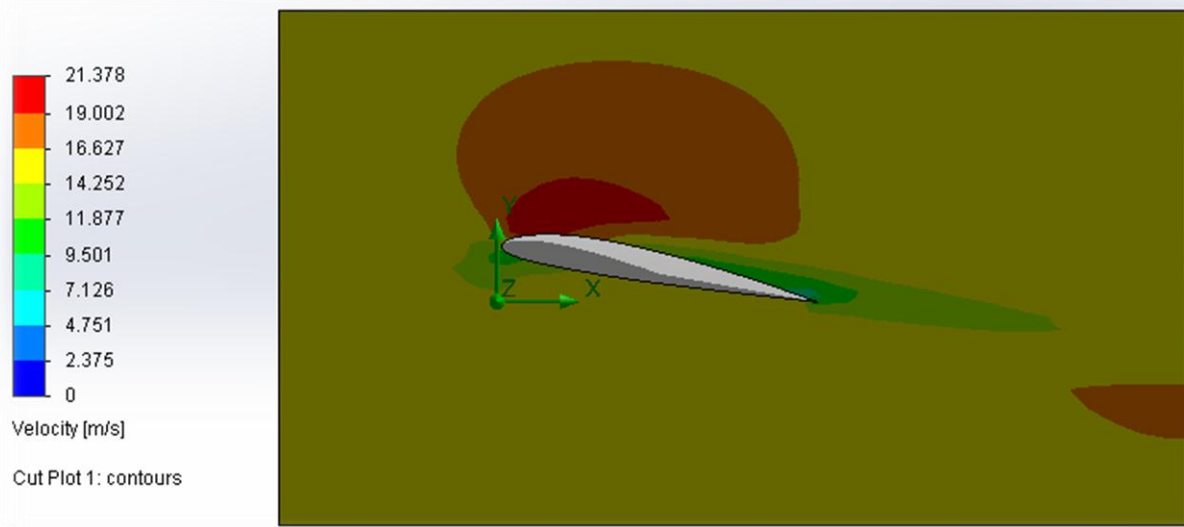


Figure 64 - Cut plot of the velocity

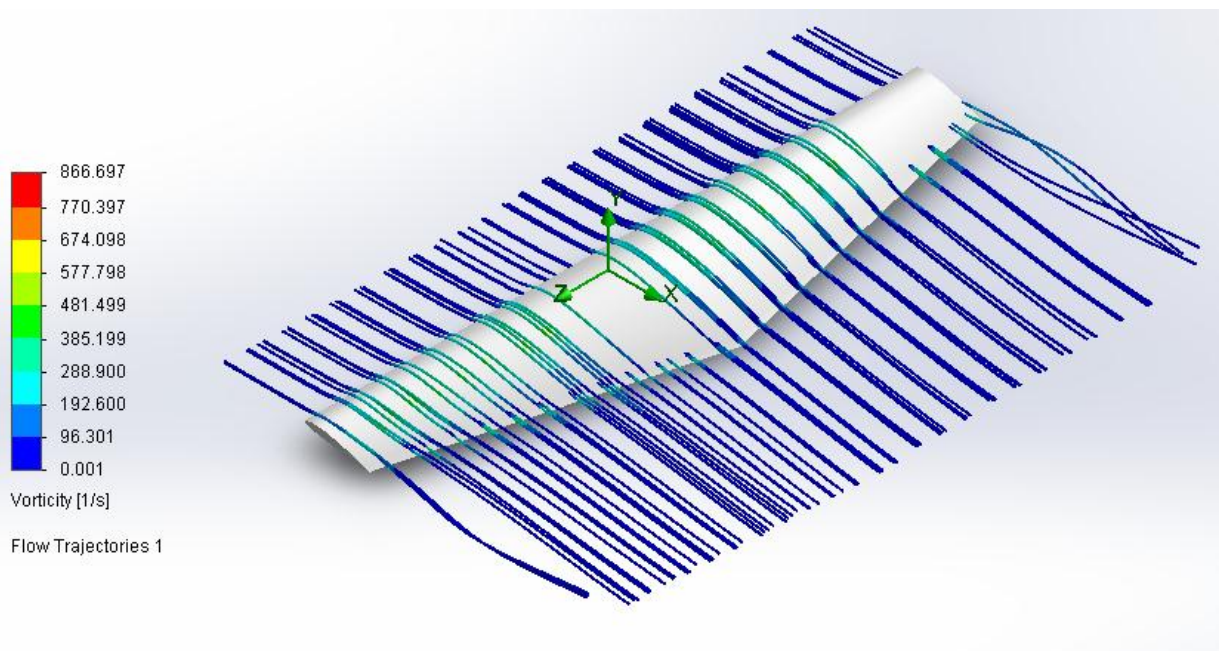


Figure 65 - Flow trajectories of the Vorticity

5.8 Static Thrust Force Calculation

This section of the project was done in order to differentiate the research and theoretical calculations from teams in the past. The team proposed to calculate the static thrust force of the engine in order to develop more accurate theoretical calculations.

The experiment was made by using a test bench where the engine will pull a force gauge. The team had tested the three different types of propeller, 13x4 1st pitch, 13x4 wide pitch, and 14x7.

In the following tables, it can be seen the results obtained from the test for each of the propellers.

Table 20 - 13X4 1st Pitch Propeller results

Propeller 13x4 (1st Pitch)			
Trial #1			
Speed	Force (N)	Force (lbf)	RPM
Idle	5.0	1.124	9300.00
Low	13.0	2.923	14912.00
Mid	23.0	5.171	20400.00
High	28.0	6.295	21400.00
Trial #2			
Speed	Force (N)	Force (lbf)	RPM
Idle	4.0	0.899	9200.00
Low	10.0	2.248	13400.00
Mid	22.0	4.946	19700.00
High	27.0	6.070	21500.00
Trial #3			
Speed	Force (N)	Force (lbf)	RPM
Idle	3.0	0.674	8600.00
Low	9.0	2.023	12720.00
Mid	21.0	4.721	18500.00
High	27.0	6.070	21200.00
Average			
Speed	Force (N)	Force (lbf)	RPM
Idle	4.0	0.899	9033.33
Low	10.7	2.398	13677.33
Mid	22.0	4.946	19533.33
High	27.3	6.145	21366.67

Table 21 - 13X4 Wide Pitch Propeller results

Propeller 13x4 (Wide Pitch)			
Trial #1			
Speed	Force (N)	Force (lbf)	RPM
Idle	6.0	1.349	10700.00
Low	11.0	2.473	12550.00
Mid	20.0	4.496	19700.00
High	29.0	6.519	21800.00
Trial #2			
Speed	Force (N)	Force (lbf)	RPM
Idle	5.8	1.304	10000.00
Low	11.0	2.473	12500.00
Mid	23.0	5.171	20100.00
High	27.0	6.070	21200.00
Trial #2			
Speed	Force (N)	Force (lbf)	RPM
Idle	4.0	0.899	9500.00
Low	10.0	2.248	13500.00
Mid	20.5	4.609	20400.00
High	28.5	6.407	21300.00
Average			
Speed	Force (N)	Force (lbf)	RPM
Idle	5.3	1.184	10066.67
Low	10.7	2.398	12850.00
Mid	21.2	4.758	20066.67
High	28.2	6.332	21433.33

Table 22 - 14X7 Propeller results

Propeller 14x7 (Wide Pitch)			
Trial #1			
Speed	Force (N)	Force (lbf)	RPM
Idle	6.0	1.349	10300.00
Low	11.0	2.473	11200.00
Mid	20.0	4.496	19550.00
High	31.0	6.969	23500.00
Trial #2			
Speed	Force (N)	Force (lbf)	RPM
Idle	5.4	1.214	10050.00
Low	12.0	2.698	13500.00
Mid	26.0	5.845	21050.00
High	29.0	6.519	21200.00
Trial #2			
Speed	Force (N)	Force (lbf)	RPM
Idle	6.5	1.461	9650.00
Low	11.2	2.518	12300.00
Mid	21.0	4.721	19300.00
High	29.5	6.632	21900.00
Average			
Speed	Force (N)	Force (lbf)	RPM
Idle	6.0	1.341	10000.00
Low	11.4	2.563	12333.33
Mid	22.3	5.021	19966.67
High	29.8	6.707	22200.00

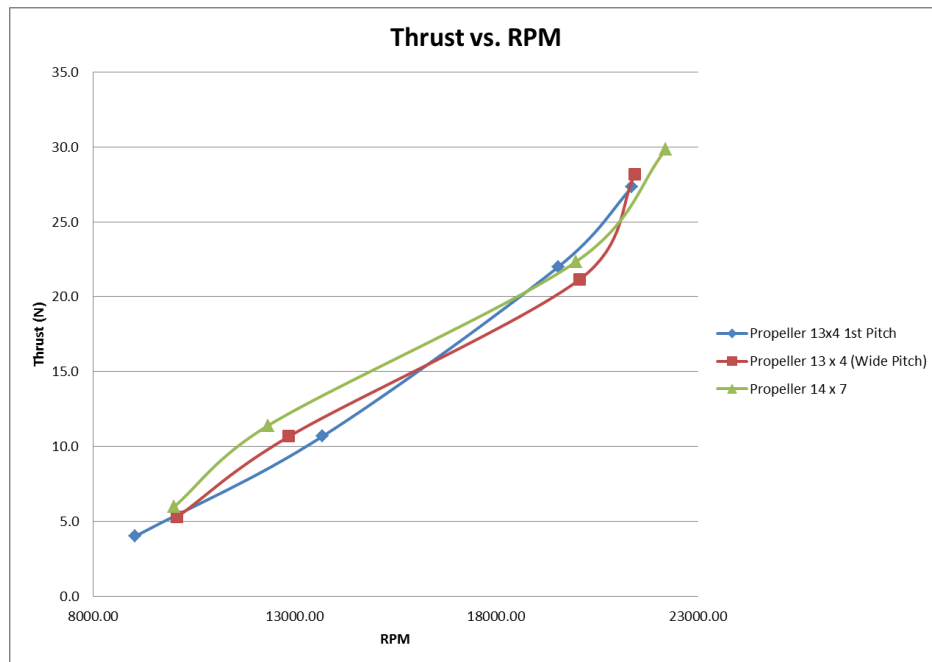


Figure 66 - Thrust Force vs. RPM

From the graph above, the team selected the propeller 14x7 because it gives more static thrust force in a similar RPM scale.

The dynamic thrust force was also important for the team, but a priority was to know the take-off velocity required, and also due to the lack of resources the team could not implemented the dynamic test.

In the following figures, one can see the set-up and the run of the test.

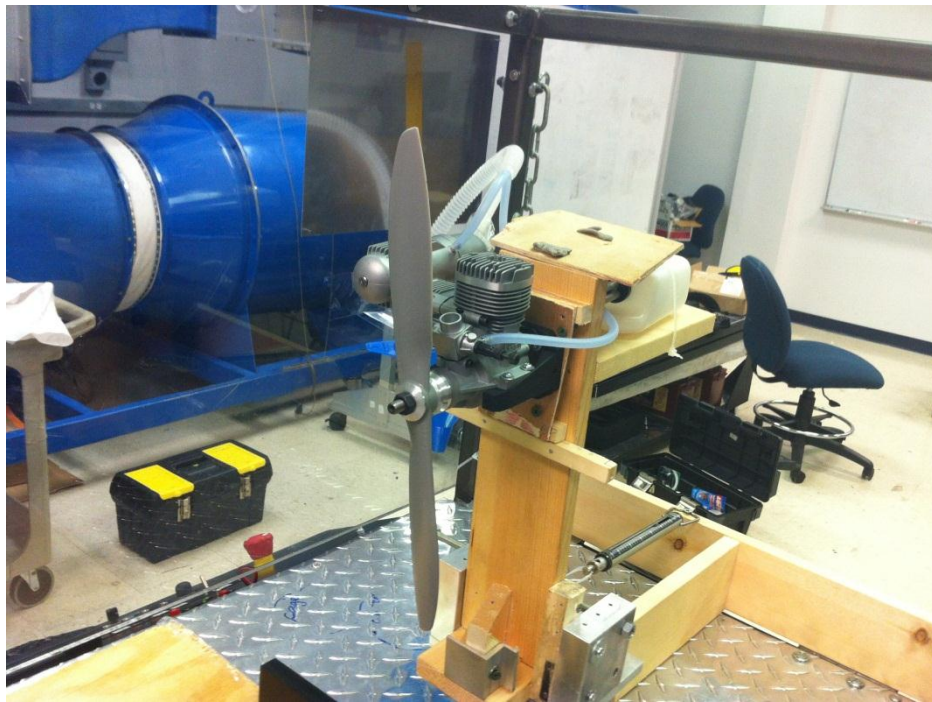


Figure 67 - Test Bench 1

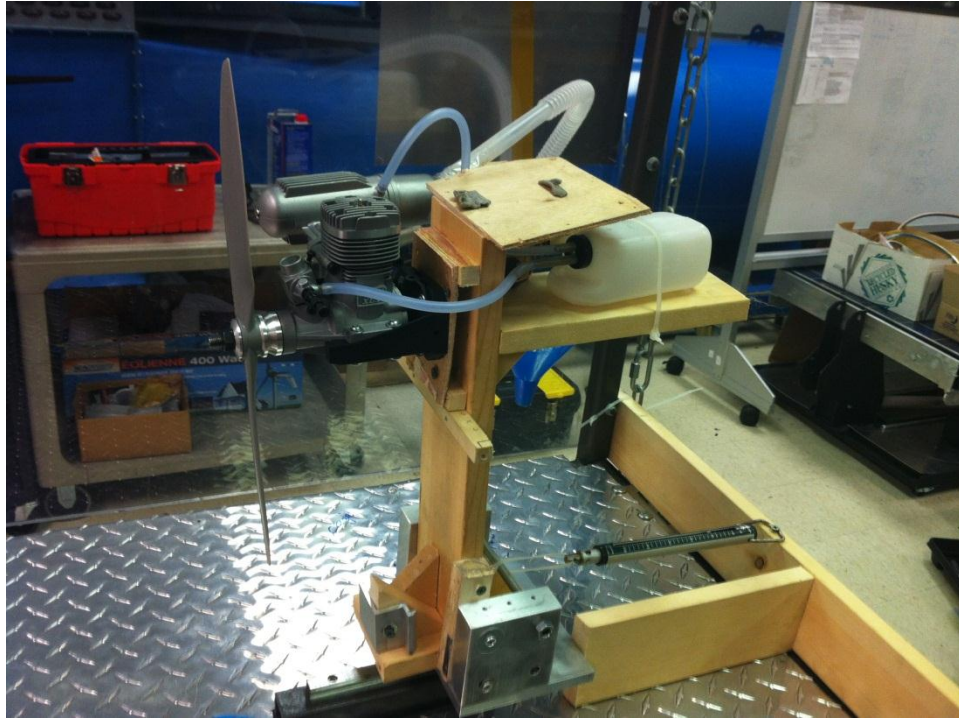


Figure 68 - Test Bench 2

6. Structural Analysis

6.1 Static analysis

The ability of an aircraft to withstand the aerodynamic forces during flight is another important part of the science of structures. The team was focused on the design and build of an aircraft structure having two goals in mind, the first was to minimize the load of every single part to be used in the airplane, and the second one was the structural failure analysis, to prevent the aircraft from disintegrating during the flight. Therefore, the final design of the airplane must have been lightweight, but strong at the same time. The aircraft structure must also have been able to remain intact even through high wind speeds or unsafe flight maneuvers.

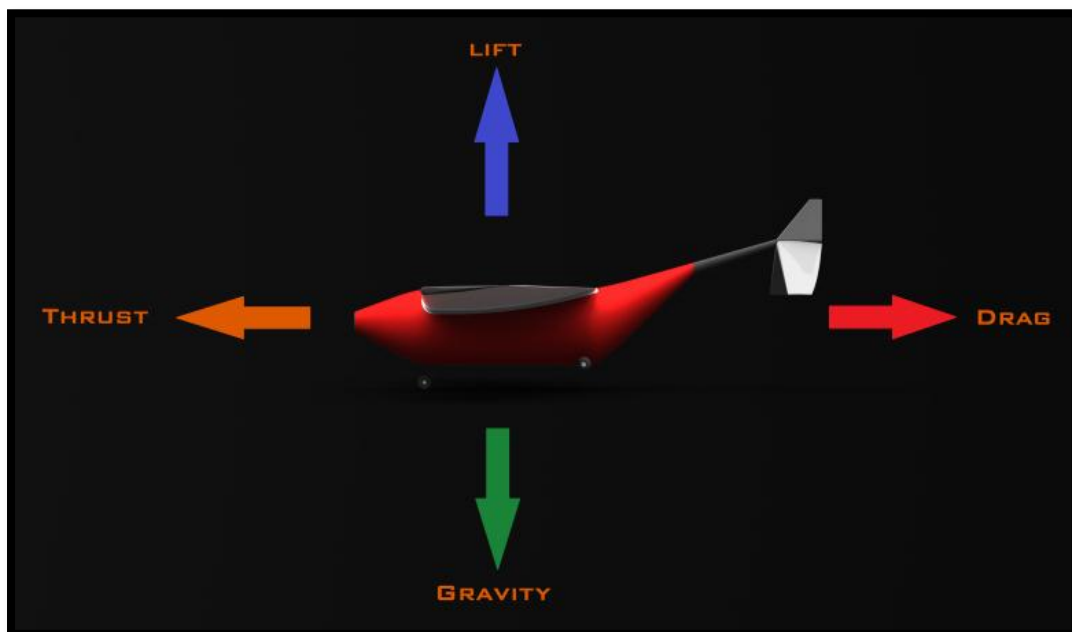


Figure 69 - Flight Mechanics

There are four important forces involved during any flight, these forces are (lift, drag, thrust, and the weight of the airplane itself). The airplane must have sufficient lift force to get the total weight of the aircraft, plus the desired weight to be successful in the competition. Several factors must be considered before a plane is ready for takeoff. The total weight should be raised before the 50 meters track is finished. Having had this restriction in the competition, the takeoff weight became very important since the distance to be covered may have required more fuel, making it necessary to find a balance between all these variables.

The following picture shows a schematic during the simulation process of the structural design.

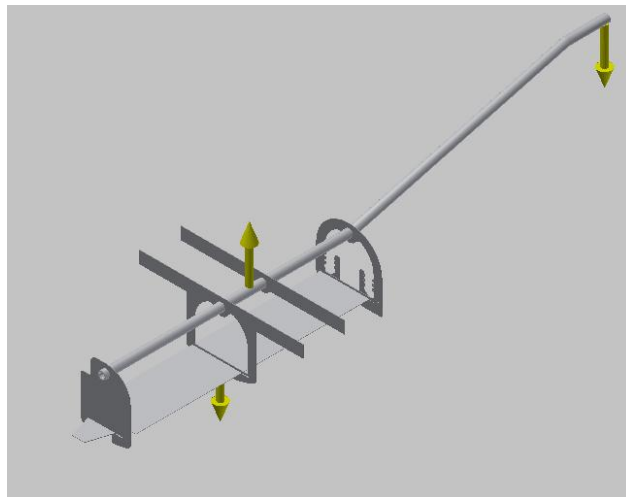


Figure 70 - Conceptual Structural Design with Forces

In the following figure, one can see the displacement in x and z, the Von misses stress of the structure of the airplane. The simulations were performed using Autodesk Inventor.

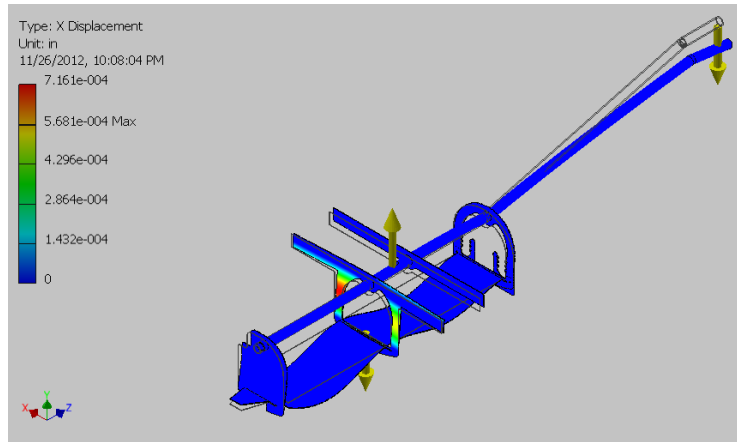


Figure 71 - Displacement in X

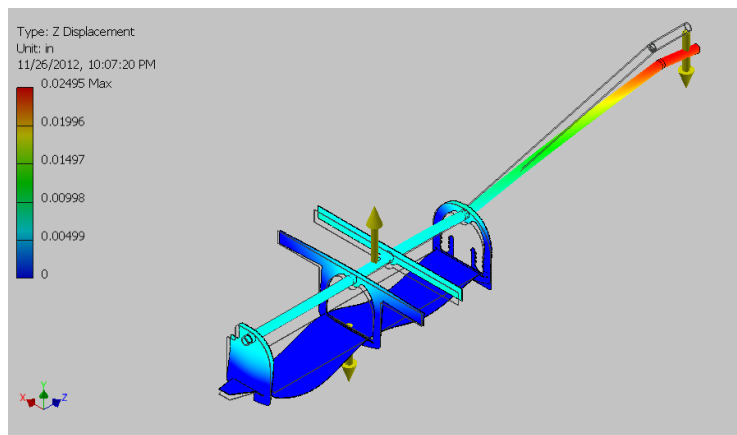


Figure 72 - Displacement in Z

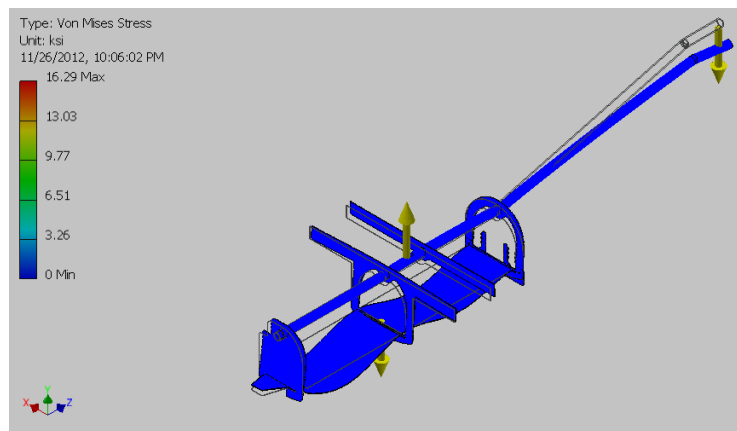


Figure 73 - Von Mises stress

6.2 Wing Loading Test

After having obtained a theoretical solution for wing failure, the team performed an actual failure test on a wing structure comparable to the ones that were designed for the prototype. This was to serve as a last review of possible structural weaknesses. This type of test consisted of literally loading the wings of the aircraft upside down.

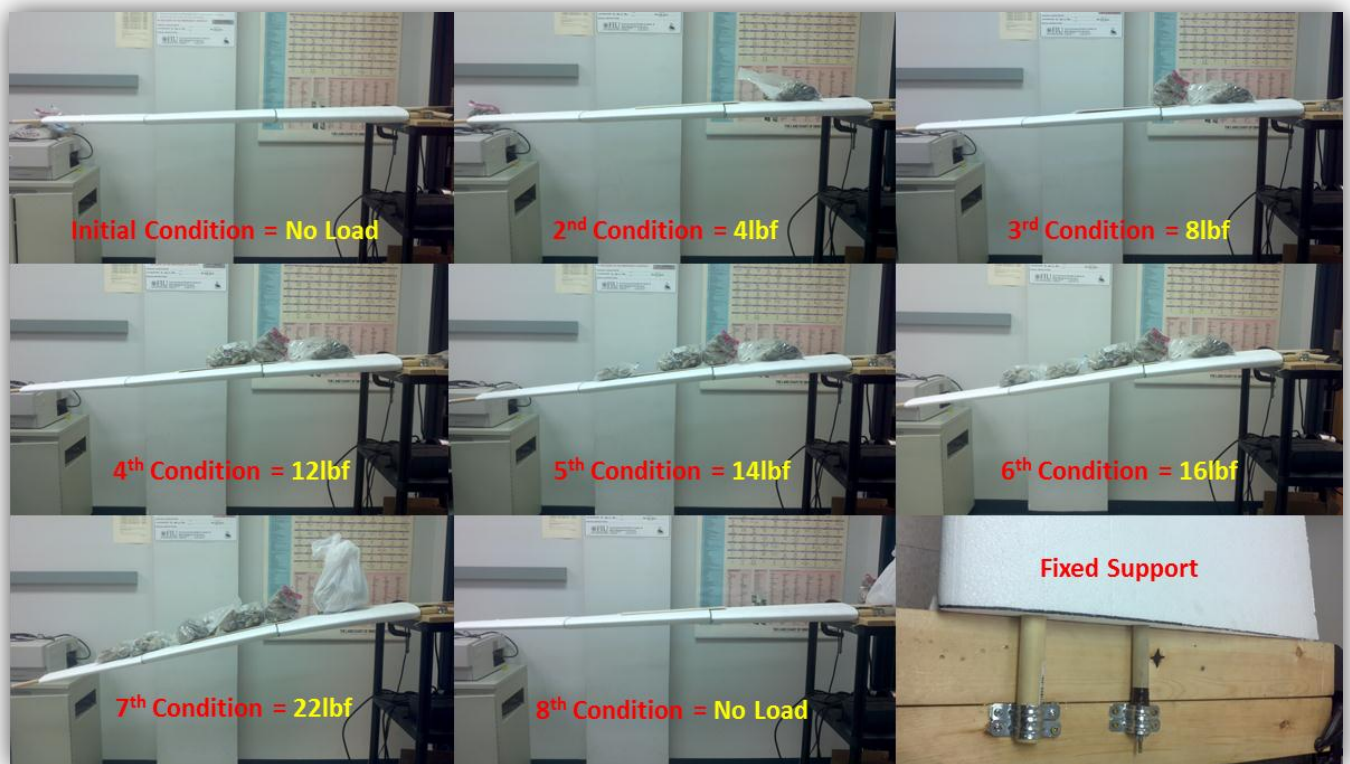


Figure 74 - Wing Load Testing Process

From the experiment, the team has obtained an allowable distributed load of 22lb along the wing which guarantees that the plane plus the load reach 40lb; the wings will remain intact during the flight.

7 Airplane Construction

7.1 Overview

One of the specific goals of this Senior Design Project was to develop an assembly that would closely resemble one of a real life aircraft. It was for this reason that the materials used were not common to airplanes of similar dimensions. All the part that makes up the overall assembly consists of materials commonly used in modern aviation with one exception. The wings were designed and manufactured primarily with foam, resin, and wood. The inclusion of wood in the wing structure came as a substitution to carbon fiber tubes and rods. The carbon fiber would have dramatically increased the stability and strength of the wing structure, however the team decided against it due to price considerations, due to the fact that wood rods were significantly less costly.

At the end of the construction our goal was to create an aircraft that could realistically be disassembled and reassembled depending on need. This anticipation allowed the members of the team to gain valuable experience in Design for Manufacturability techniques (DFM), which are currently very important factors and skills to consider moving forward with our professional endeavors. The easy route would have included the reliance in balsa wood and resin in an overwhelming form throughout the structure. Making the structure more realistically built aided the final design quality and, as mentioned before, benefited the members with valuable experience.

7.2 Body

It is the main airplane structure or chassis. Supporting all airplane components as well as static and dynamic forces generated during the flight. The airplane body must meet a perfect combination of conditions for a successful performance: Strong, to handle all flight stresses and lighter, so the carrying capacity or airplane payload is increased; an important aspect of the competition.

As part of the body creation, our team adopted a body design inspired by a bird skeleton that it is basically composed of ribs located along the backbone. Please refer to figure below for a better understanding.

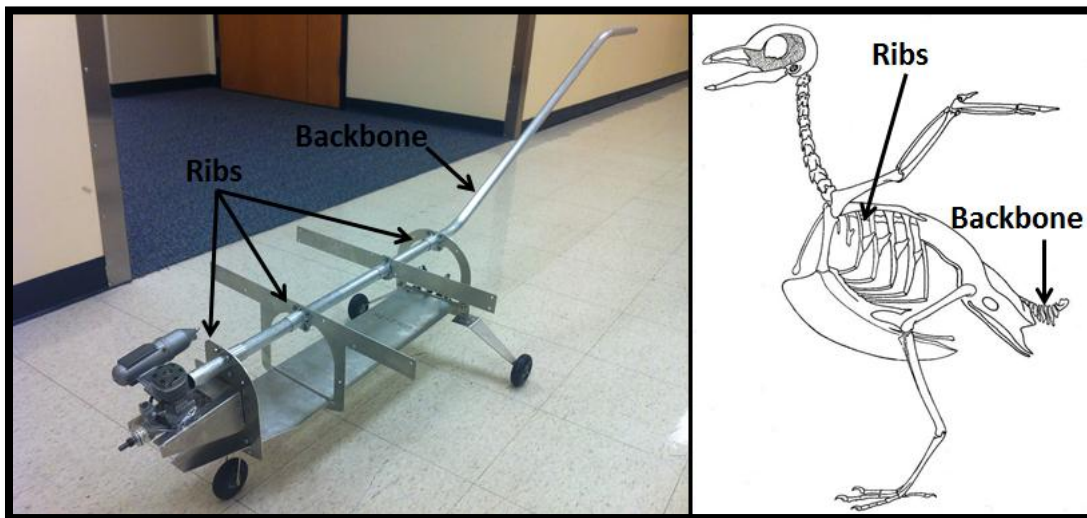


Figure 75 - Body Design Inspiration

After doing some research and gathering professional opinions about the best material to use to create the body of the airplane, as a team we decided to use Aluminum TS-6061 with a thickness of 1/16 of an inch mainly because of its easy handling and cutting by CNC machines cutters; specifically, we used the one at the FIU laboratory under Professor Zicarelli's guidance

(See Appendix A and D for design dimensions of the body). It is also important to mention that screws, washers and nuts were selected instead of considering welding to hold all pieces together.

7.3 Ribs

All ribs were carefully designed to guarantee an easy assembly and disassembly, so serves, wings and accessories could be added later on during the building process. A short description of each rib can be found as follows:

7.3.1 Front Rib

It is located at the front of the airplane or beginning of the aluminum tube or backbone. Main functionalities of this rib include holding the engine mount, front servos, landing gear and the engine cover. For a better understanding please refer to the pictures below

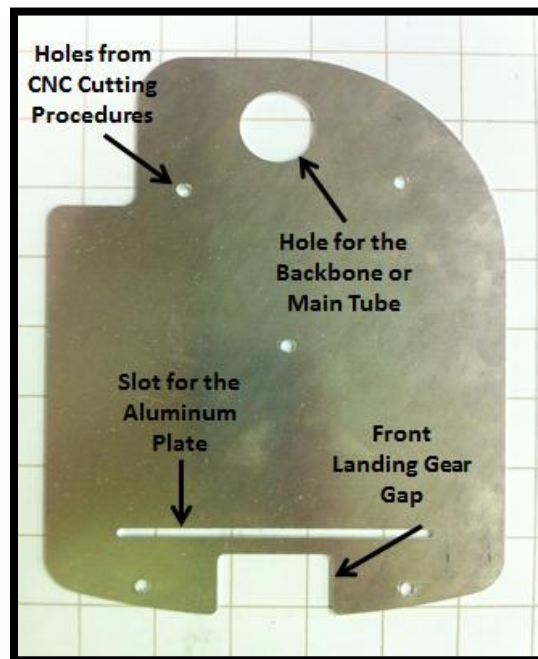


Figure 76 - Front Rib Design and Features

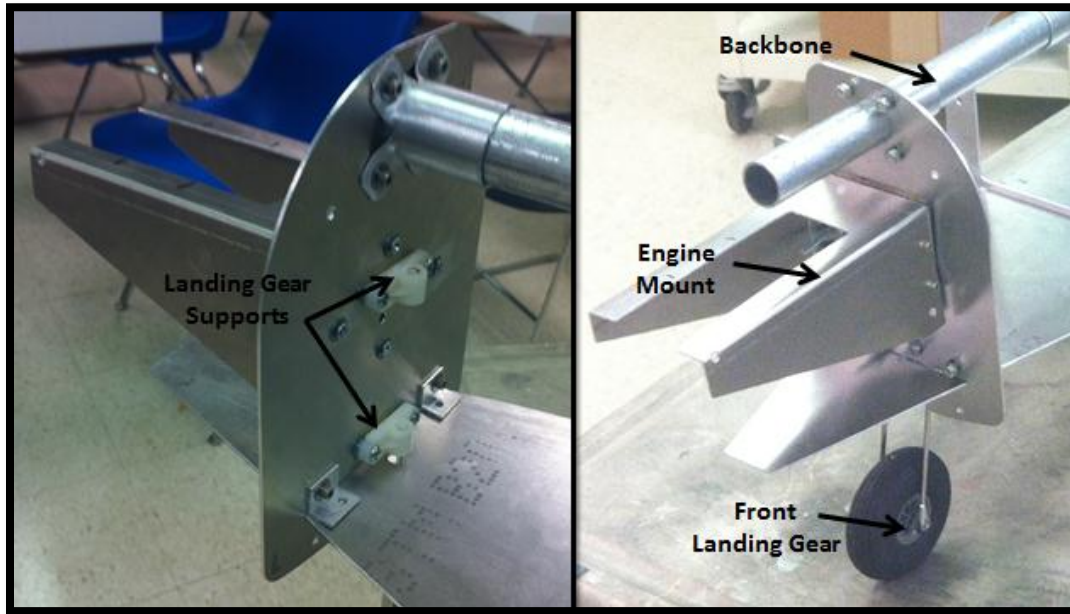


Figure 77 - Parts Attached to the Front Rib

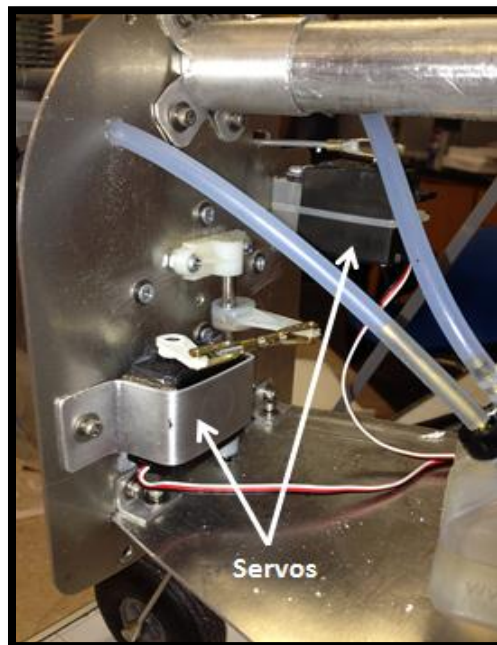


Figure 78 - Front Rib Servos

7.3.2 Middle Rib

It is located at 6 inches behind the front rib. Main functionalities of this rib include wing support attached to the airplane body, as well as stabilizing the plane by avoiding horizontal movement or deflection created by lateral forces during the flight. More details can be found in the following pictures.

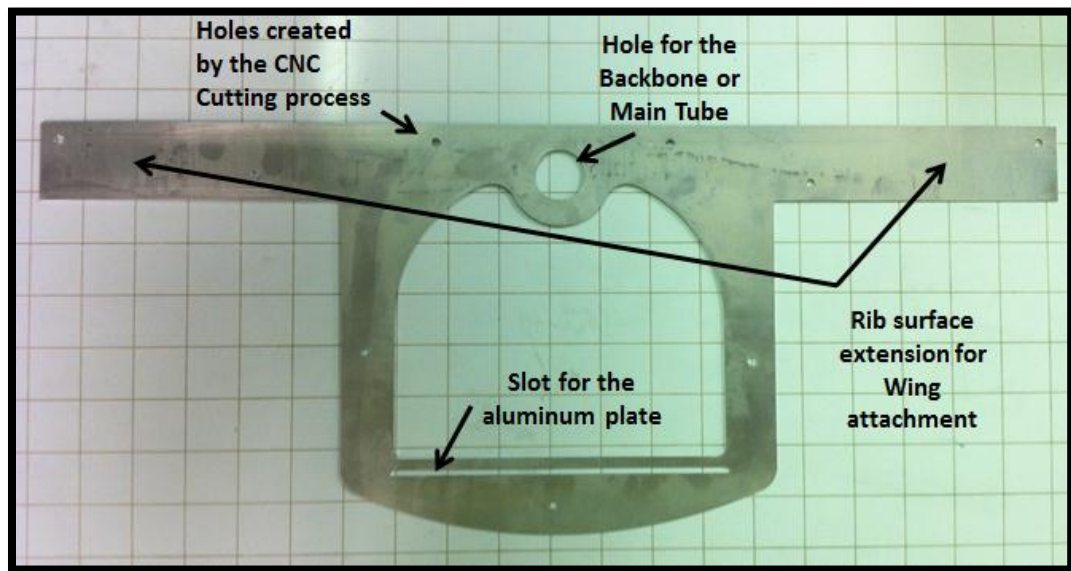


Figure 79 - Middle Rib Design and Features

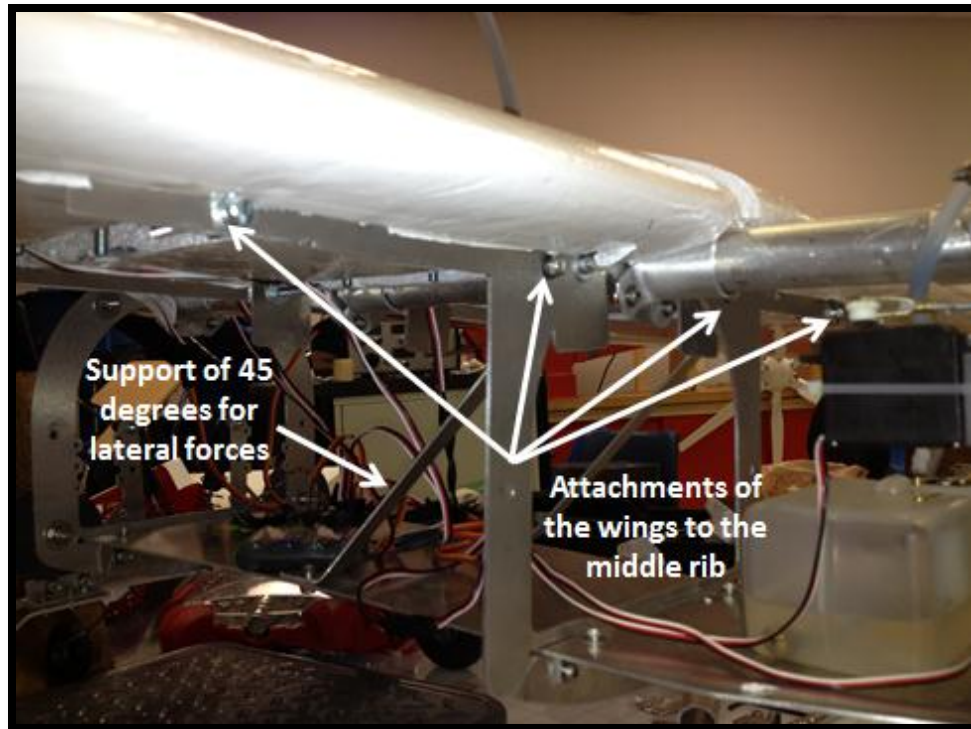


Figure 80 - Wing and Ribs connection

7.3.3 Secondary Middle Rib

With the same function of the middle rib previously described, it performs as a secondary attachment from the wings to the whole structure, and its located 7 inches behind the middle rib.

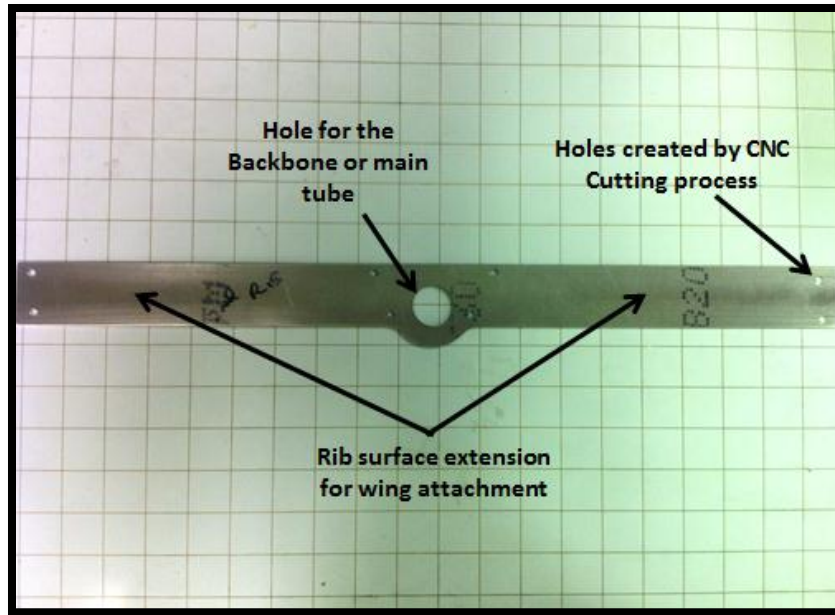


Figure 81 - Secondary Rib Design and Features



Figure 82 - Secondary rib location and configuration

7.3.4 Back Rib

It is located at 13.5 inches behind the middle rib. Main functionalities of this rib include rear landing gear support and shocks absorbers arms support. For a better understanding, please refer to the picture below.

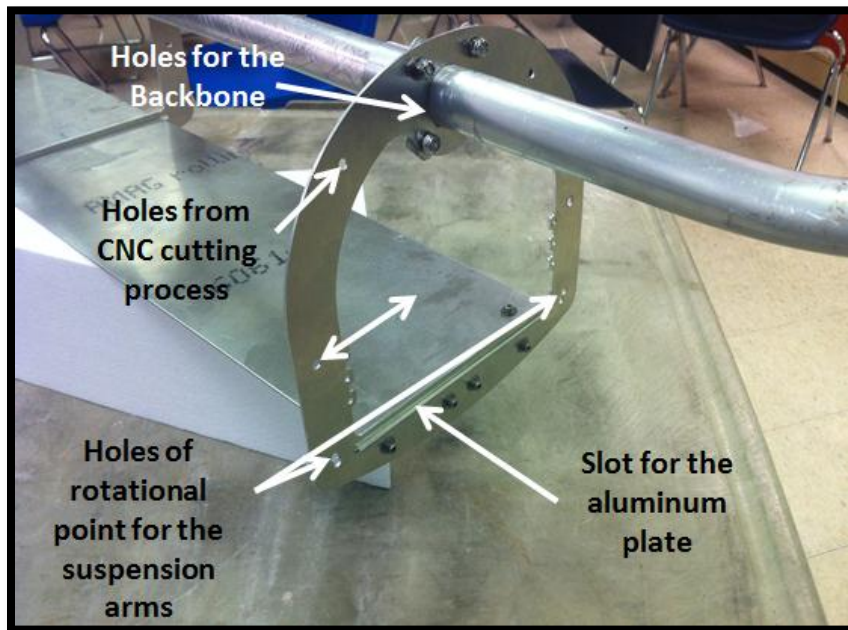


Figure 83 - Back Rib Design and Features

Attached to the back rib, two aluminum TS-6061 arms were also created by the same CNC cutting process. These two arms basically transfer the forces generated by landing or takeoff maneuvers directly to the shock absorbers. Such arms are located as shown in the picture below.

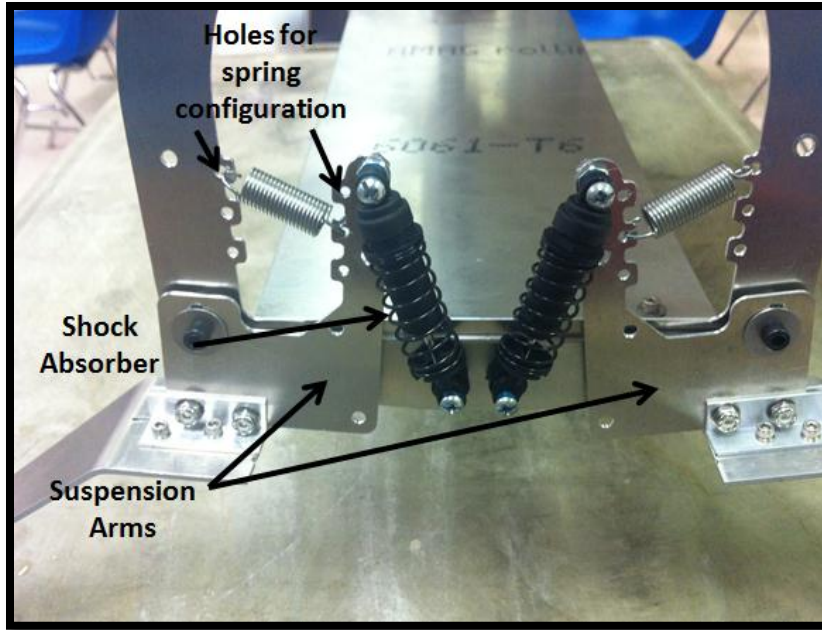


Figure 84 - Back Rib with rear landing gear, arms suspension and shock absorbers

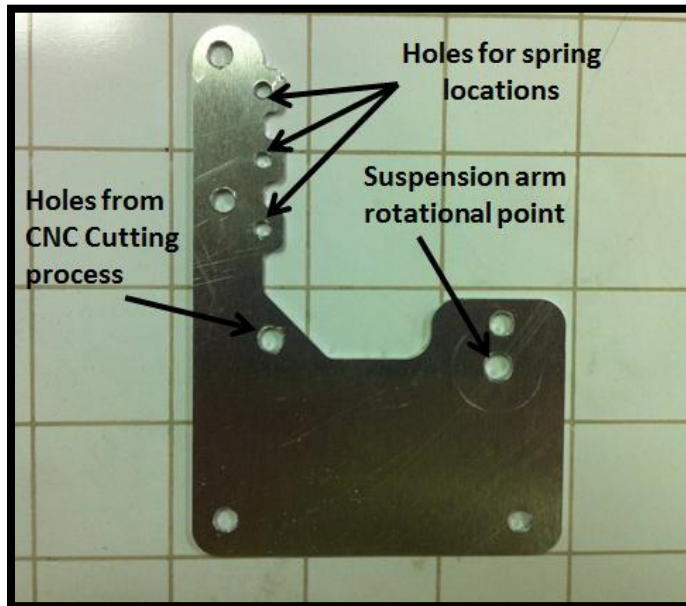


Figure 85 - Suspension Arm design and Features

7.4 Mount

The aluminum mount was designed with the necessity of increasing the possibilities of the engine final location. The first choice for the engine mount was one conventional adjustable plastic mount from the hobby store. Adjustable refers the fact that the mount was compatible to hold engines from .46 up to .71 cc, in our case the engine was .61cc but, the problem of this mount was the fact that only provides one specific location or horizontal distance from the engine to the front rib. This problem can be seen in the following picture.

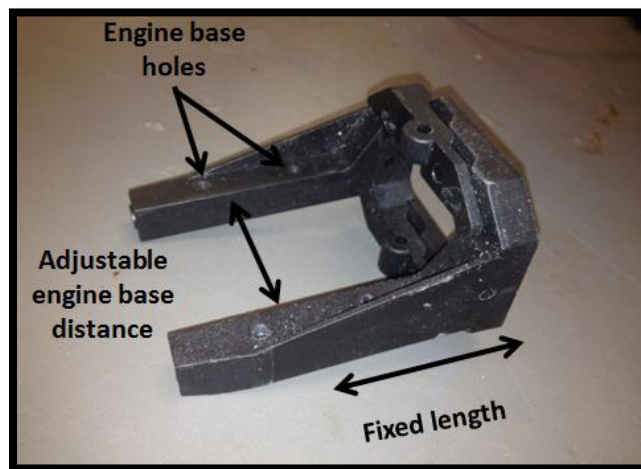


Figure 86 - Plastic Engine Mount

The final mount was made of aluminum TS-6061; we used the same CNC cutting process for the ribs and suspension arms for better results. Three 90 degree bends were performed after the aluminum sheet was cut. A required structure was important to hold the engine without any problem. These bends were performed in 3 different locations and they can be seen with more details in the picture below.

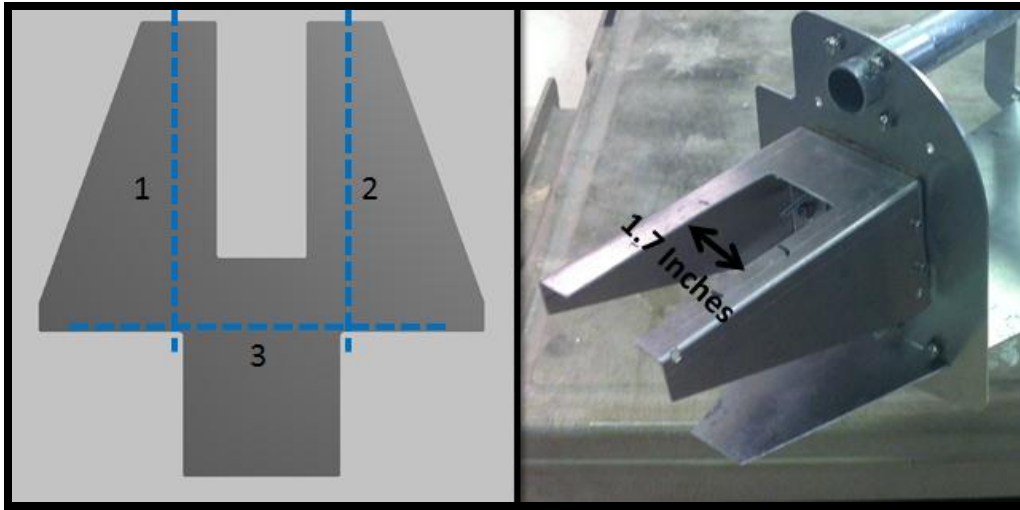


Figure 87 - Aluminum Engine Mount

7.5 Backbone or Aluminum Tube

The Airplane backbone consists of an Aluminum TS-6060 tube. Dimensions of this tube are 1 inch of outer diameter and thickness of approximately 1/16 of an inch. Such tube goes through all three ribs previously mentioned above.



Figure 88 - Backbone or Main Tube Design and Specifications

This tube required two bends of 20 degree angle each. The Bending process was performed by using a tube bending machine located at FIU's machine shop. Each bend required heat application during the bending process to successfully reach the 20 degree angle without generating any crack or material rupture.

Dimensions and specifications can be found in the picture below.



Figure 89 - Bending process of the Aluminum Tube or Backbone

7.6 Plate

This part was created from the same Aluminum TS-6061 sheet mentioned for the ribs and arms. A Hacksaw was used to cut this piece instead of a CNC machine as it didn't require a precise dimension as well as to save money and time. This plate goes through every single rib and its main functionality is to create the airplane floor and structure as well, where the gas tank, receiver, servos are located.

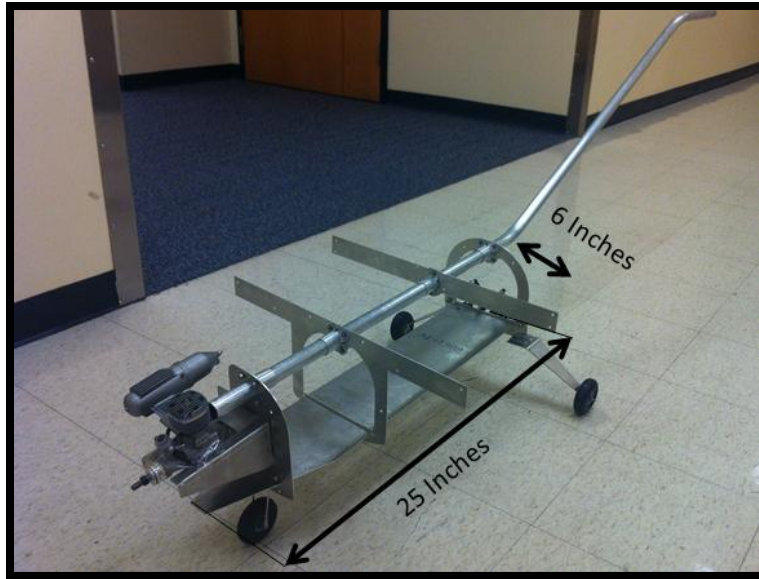


Figure 90 - Plate design and Dimensions

7.7 Connectors

7.7.1 "L" Connector

It is located between the airplane ribs and plate. Its 90 degree angle facilitates the attachment of horizontal and vertical parts. Holes were carefully measured and created in each edge of the connector, and screws were inserted through such wholes to complete the assembly. For more details please refer to the picture below.

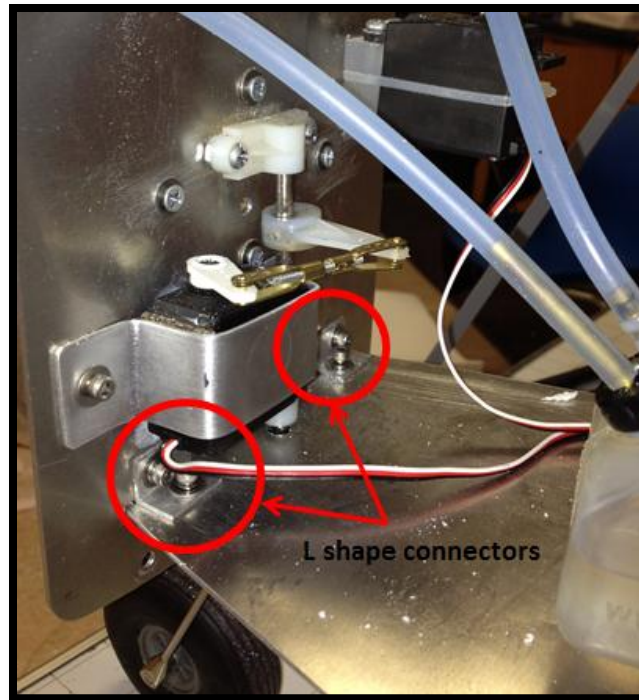


Figure 91 - L shape Aluminum connectors Design

7.7.2 Butterfly Connector

A total of four (4) butterfly connectors were created to successfully hold the airplane backbone to its three ribs and secondary middle rib, preventing the horizontal movement that ribs could cause to the tube. Each piece was created from Aluminum TS-6060 tube with a 1" ID and a thickness of 1/16 of an inch.

The use of heat was required to successfully meet the shape of each connector as can be seen in the image below.

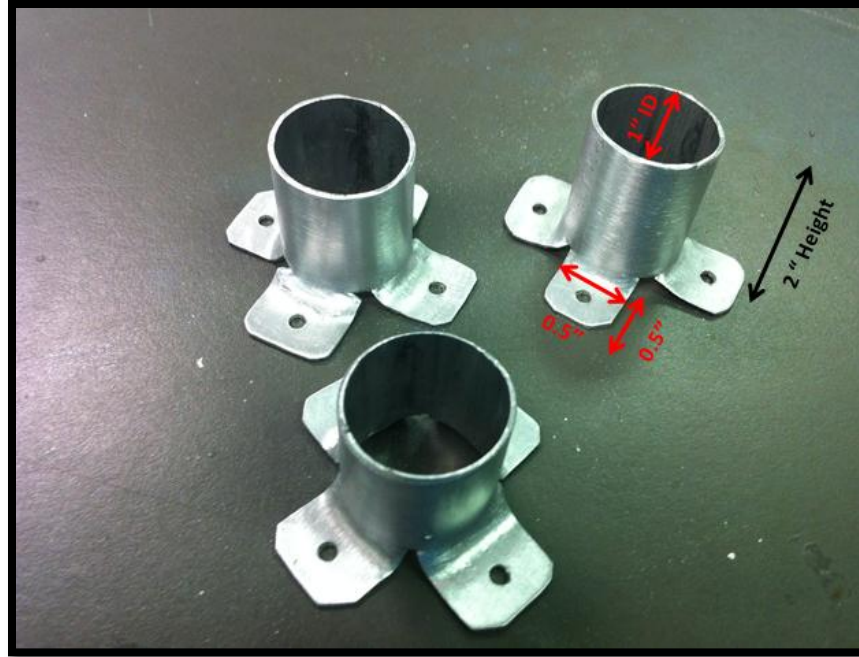


Figure 92 - Butterfly connection

7.8 Fuselage

In contrast to conventional airplane design, the fuselage of this airplane is not part of its main structure; instead, its main function is to cover the aluminum structure or body previously described in an aerodynamic way.

Its main components are as follows:

7.8.1 Cowl

The cowl goes on the front of the airplane covering the engine unit. Taking into consideration a 7 inch distance from the propeller to the front rib, we used floral foam with the help of sandpapers to create the mold and to get the desired final shape. The team was able to

create a unique and aerodynamic engine front cover using Fiber glass composite and resin after the creation of the mold. How this process was performed can be seen in the images below:

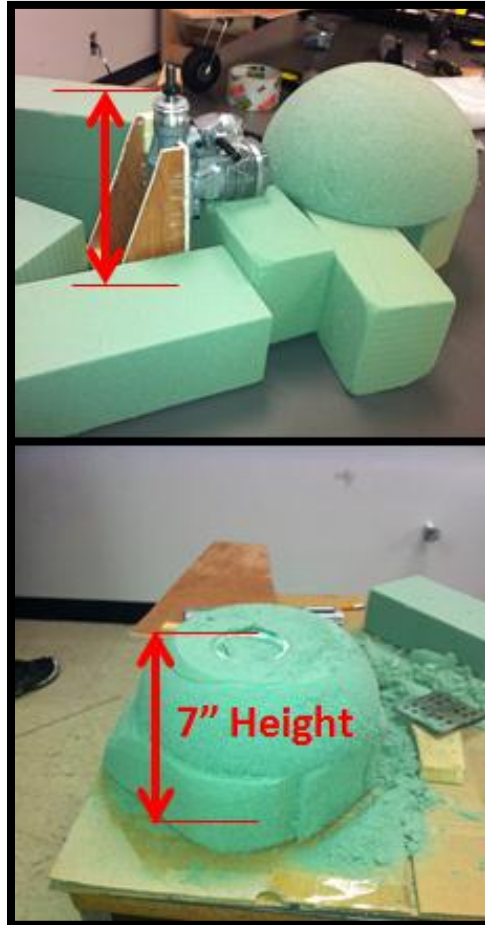


Figure 93 - First Two steps of the manufacturing process of the Cowl

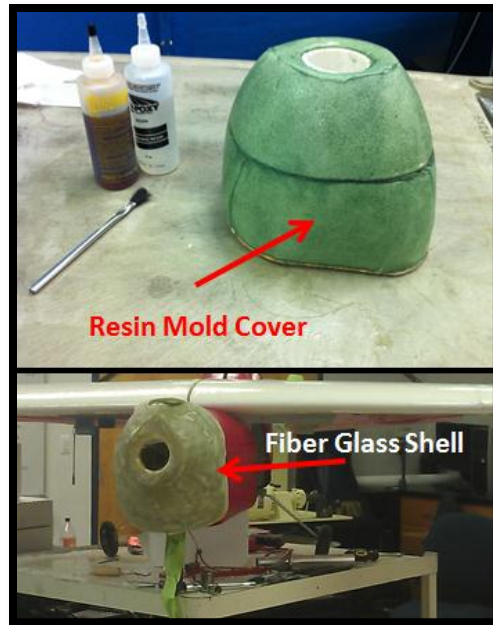


Figure 94 - Steps 3 and 4 of the manufacturing process of the Cowl



Figure 95 - Final steps of the Cowl manufacturing process

7.8.2 Body Fuselage

It was originally designed by using a 3D CAD loft tool between the three rib profiles. Such loft tool consists of generating a single solid part by using a transitional algorithm through many profiles at the same time, this feature was created by using the Autodesk Inventor 2012 software. Due to the distance between ribs, the single 3D part was divided in two. The first part covers between front and middle rib while the second part happens to be between the middle and back rib. For more details please refer to the following picture.

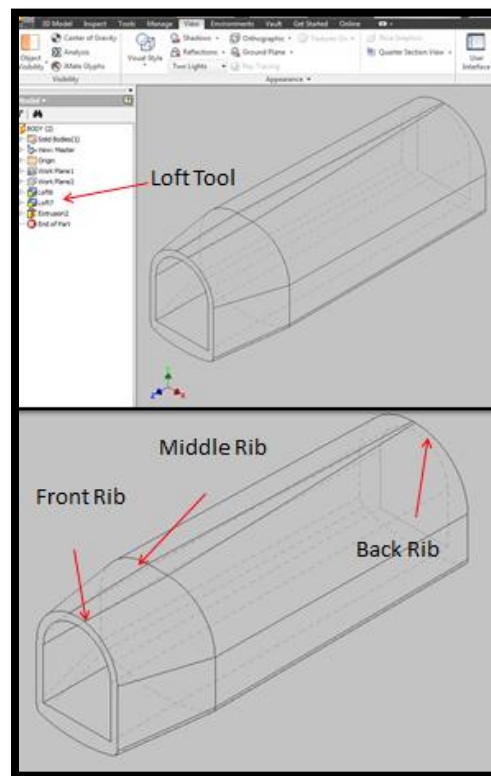


Figure 96 - Fuselage Foam Design

Once the 3D shape was done, a .dxf file containing the top front and side view of the shape was created including its dimensions. Such file was used to create the part physically by using a 3D hotwire CNC foam cutting machine. The company in charge of this foam cutting process was Hotwire Florida Technicians (See Appendix B).



Figure 97 - CNC Foam Cutting of the Body Fuselage

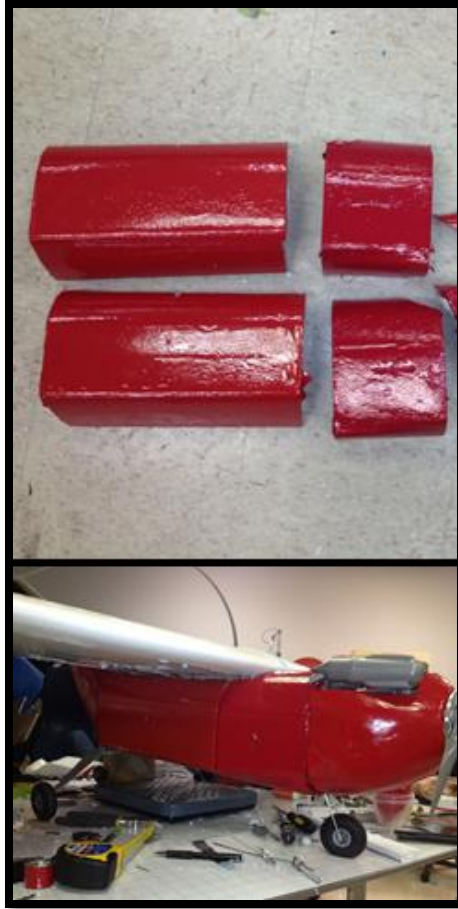


Figure 98 - Fuselage Assembly

7.9 Tail and Wings Construction

Two identical wings were created by using a CNC foam cutting machine; both wings were designed to have the airfoil shape described in the Airfoil selection section. Due to the large wingspan, the cutting process was as follows:

1. The hotwire moved along both profiles at the same time with a distance between them equal to 1.4 meters (55.11 inches) generating the wing.



Figure 99 - CNC Wing manufacturing process

2. Each wing was divided into three sections. First two sections 0.5 meters (19.69 inches) and third part 0.4 meters (15.75 inches). This division was required for an easy handling.

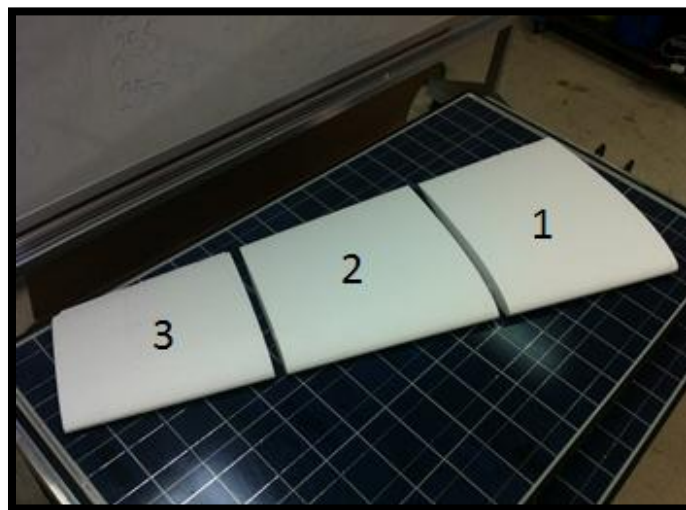


Figure 100 - Main Wing Cutting process

- Holes were created in the middle of the wing among the two first sections in order to place two wood sticks to support the internal wing structure. Holes dimensions equal to 0.9 inches and 0.5 inches respectively.

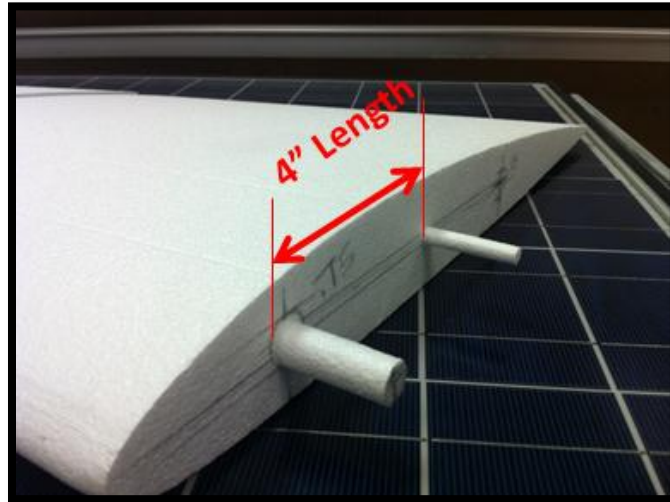


Figure 101 - Holes Diameters and locations in the Main Wing

- Balsa wood was used to reinforce each wing foam section in order to insert the wood sticks.



Figure 102 - Balsa wood reinforcement profiles

5. After the process above was culminated, flaps and ailerons were created by cutting the sections one and three of the wing by using basically the procedure of the following pictures.

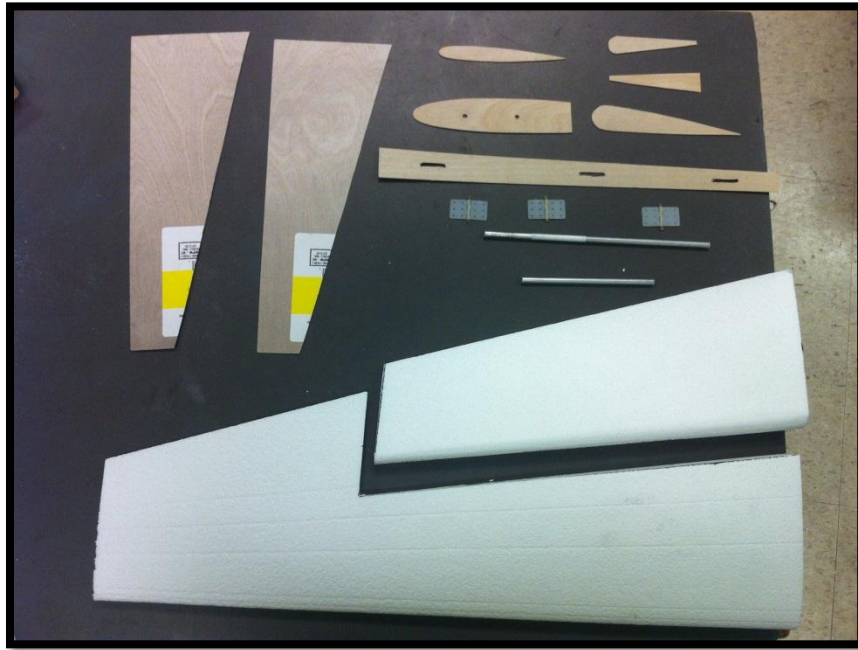


Figure 103 - Tail Wings Elevators construction

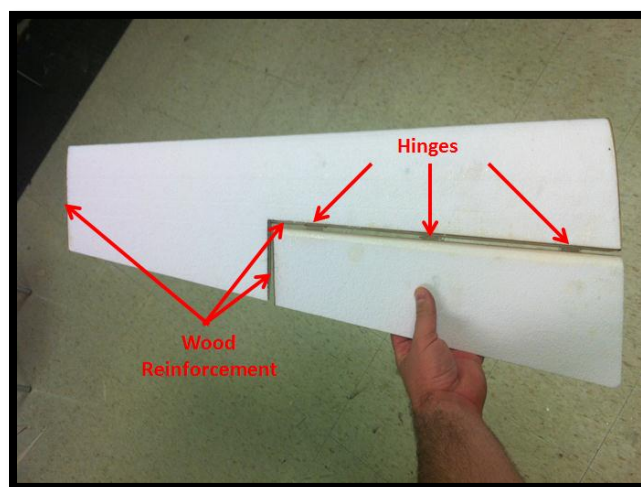


Figure 104 - Tail Wings Assembly



Figure 105 - Ailerons Design



Figure 106 - Flaps Design

7.10 Monokote

Wings, fuselage and empennage structures are covered with Monokote. Monokote is a light plastic utilized to protect and give aerodynamic shape to components. It is available in various colors, as well as transparent tones. White Monokote is utilized on wings and empennage structures. Solid red Monokote is utilized in the fuselage section. Process of adhering Monokote is quite simple, but at the same time it must be performed very carefully in order to obtain the quality results. Material is cut in the required size and one of the sides of Monokote is adhesive. The material adheres to the balsa after heat is applied, with the use of a hot iron.

Once the Monokote is fixed into the structure, a heat gun is utilized in order to firm material and remove wrinkles. It is highly noticeable where heat gun has been applied. By applying heat gun in the complete structure of wings and empennage, aerodynamic performance is increased due to the new wrinkle-free surface.

7.11 Electronic Components



Figure 107 - Futaba Servos

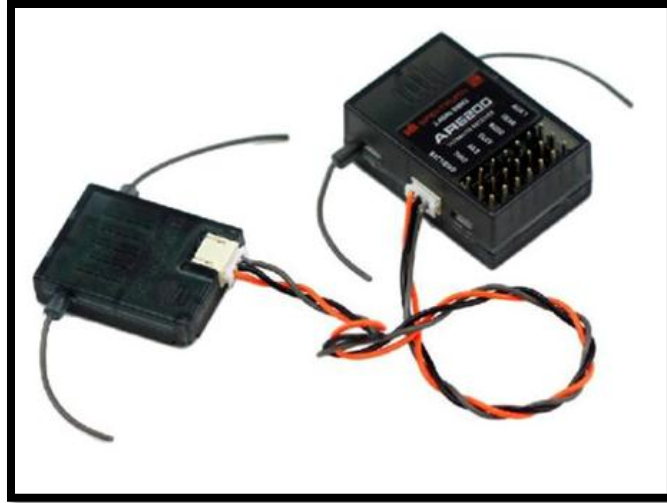


Figure 108 - 6 Channel Receiver



Figure 109 - Splitter Cable



Figure 110 - Transmitter and Battery

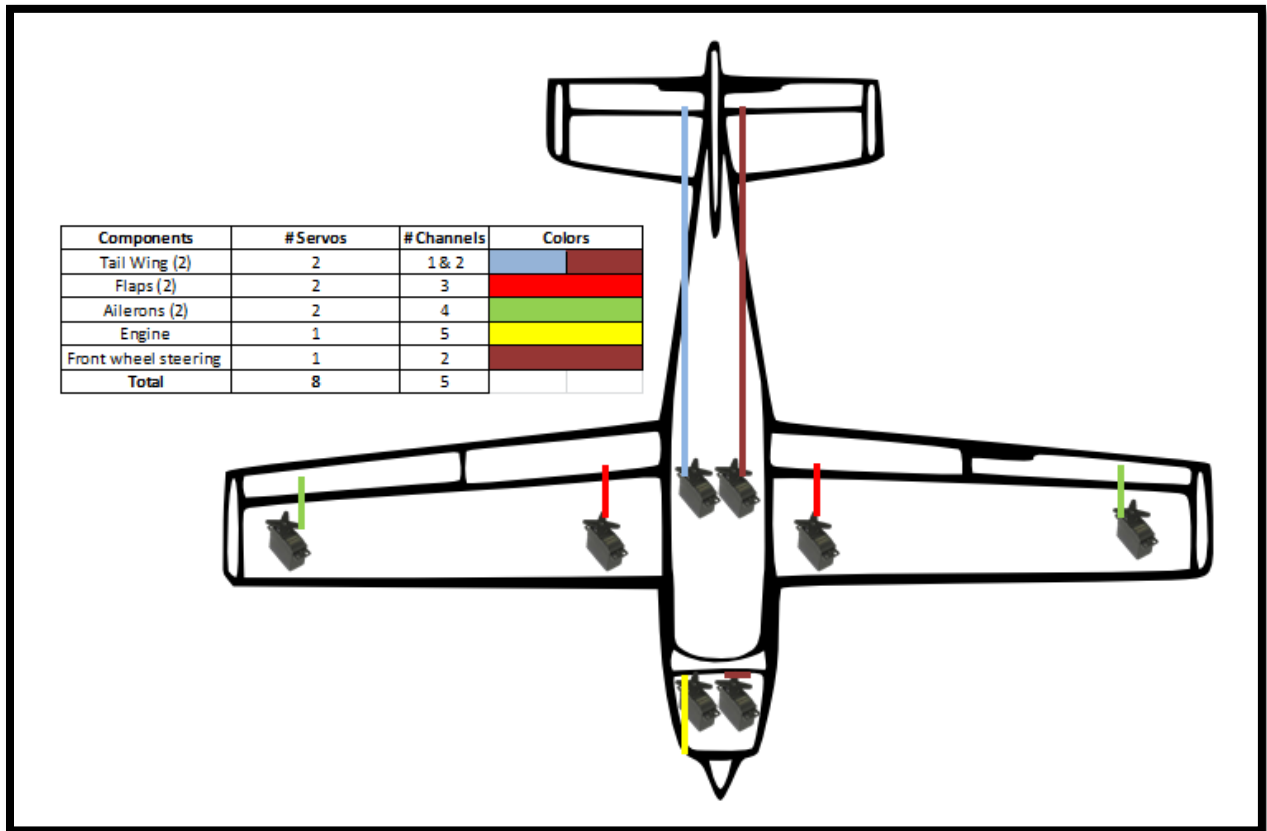


Figure 111 - Servos and Channels Diagram

8 Design Considerations

8.1 Assembly and Disassembly

The process of assembly and disassembly of aircraft is one of the principal considerations of this project. Due to the size of the airplane, the transportation has to be easy and with no possibilities of damaging the airplane. The entire wing span is divided in two pieces which are connected to the fuselage by an aluminum plate and four security screws and lock nuts in each side of the wing. The nose, the fuselage and the tail were constructed and joined together as a single entity connected through the main tube made of aluminum which leads to the tail wings.

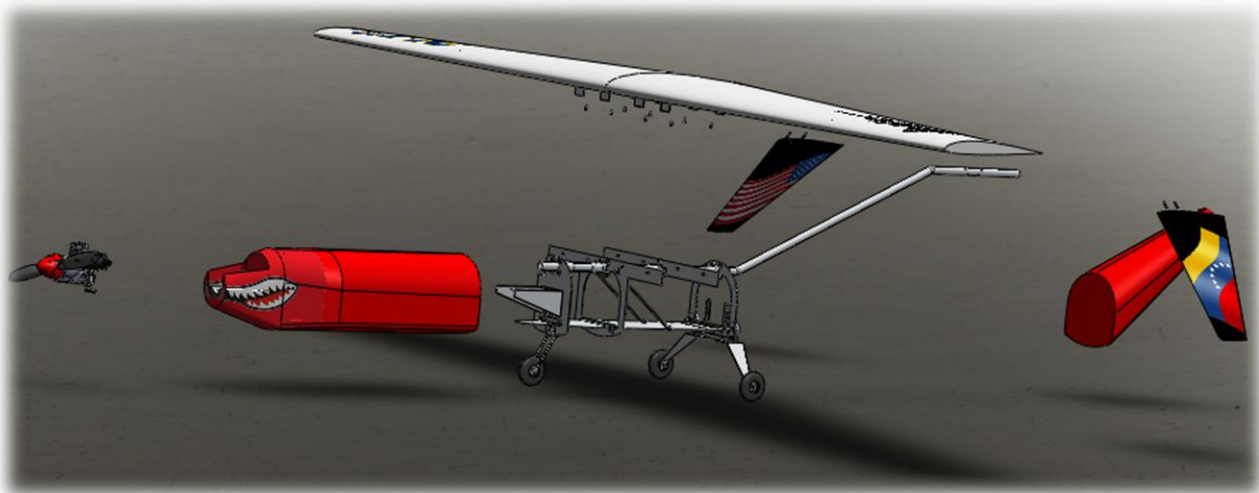


Figure 112 - Screenshot of the exploded view

The process of assembly and disassembly takes about 15 to 20 minutes, and a minimum of two persons to do it. The most of the time consumed is taken by the process of tightening all

the security screws and lock nuts. The fuselage is the main component of the airplane. It is composed by 4 principal ribs connected by the main tube through three tube supports (Butterflies) designed by the team in order to create the stability needed for the body of the plane.

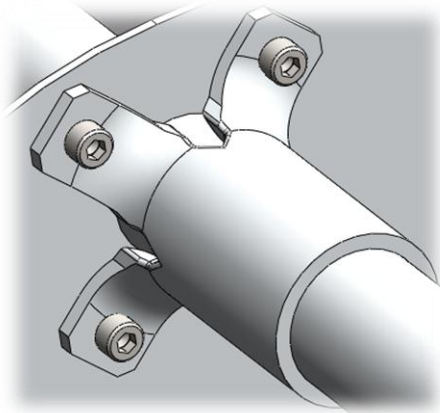


Figure 113 - Tube Support from SolidWorks



Figure 114 - Tube Support Prototype

The plate is another source of stability of the plane; which is connected to the ribs through 2 L-shape supports in each of the ribs and to avoid the parallelogram effect, the team implemented two diagonal supports to maintain the rigidity of the structure.

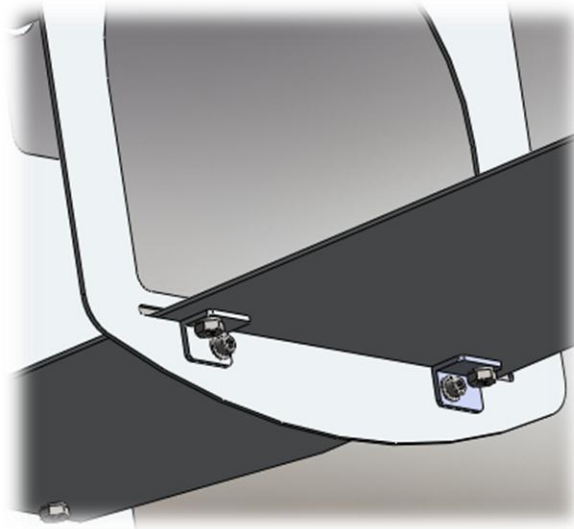


Figure 115 - Connection of the plates to the ribs using L-shape support

Once the wings are assembled to the aircraft, access to the middle section is possible due to disassemble of the fuselage cover which can be done either right or left section.

In the following figure, one can see the entire structure of the airplane and its main components.

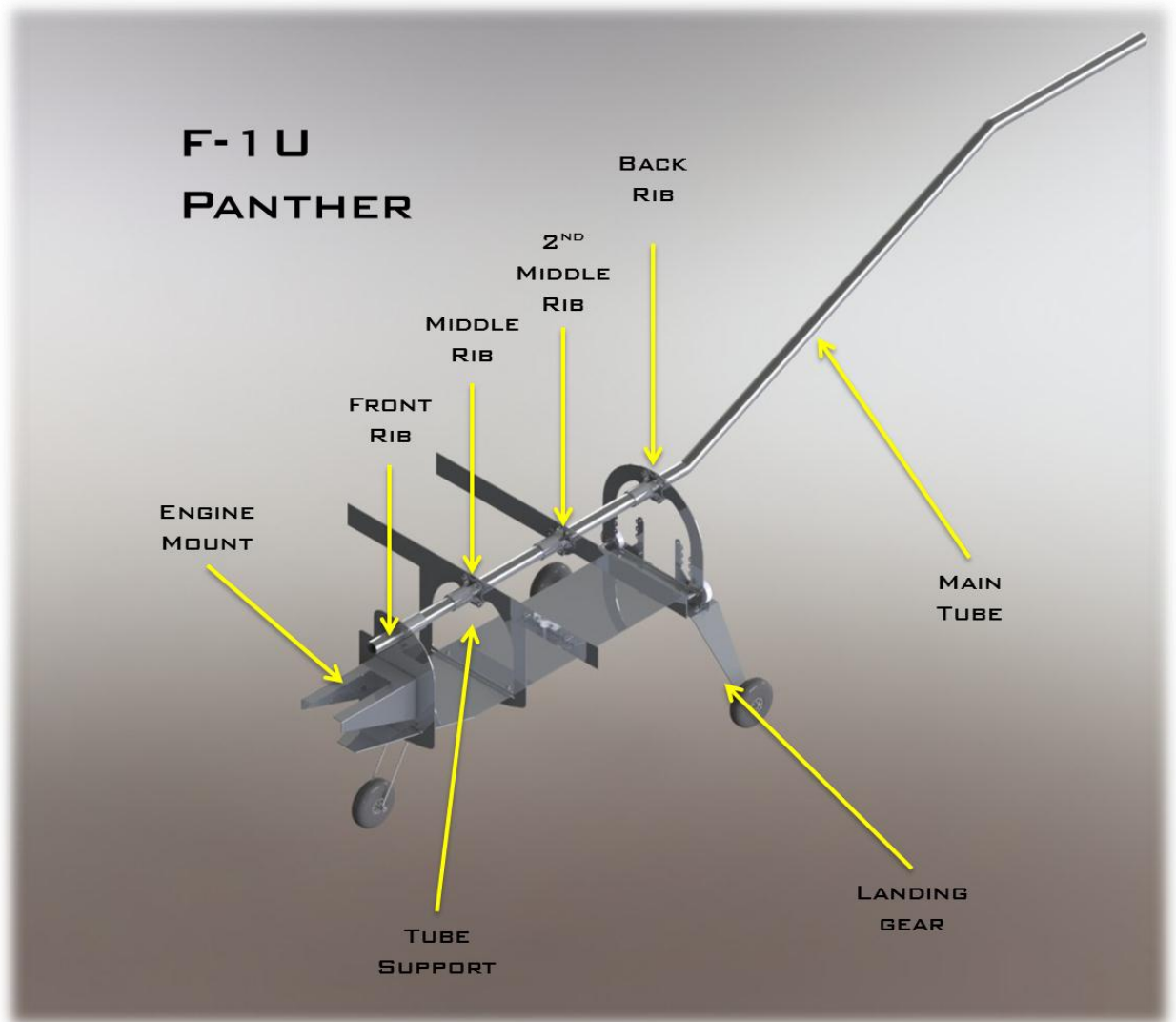


Figure 116 - Structure of the airplane and its main components

8.2 Maintenance of the system

After the airplane is assembled and flight has been performed, maintenance is required upon completion of the tasks.

The gasoline tank must be fueled for further testing, and checking process of the fuel pipes to make sure they are tight enough and gasoline is delivered properly to the engine. Also, the propeller nut and spinner must be re-tightened.

Servos must be checked for proper functioning because they are in charge of the aerodynamic movement capacity of the airplane. Also, they control the thrust of the engine by delivering a secure rotation to the intake valve located in the engine's carburetor.

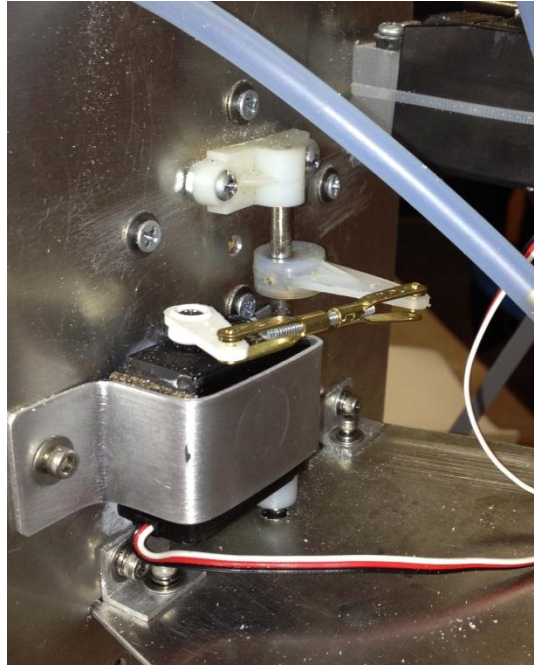


Figure 117 - Servo controller of the front wheel

Finally, the team has to clean any residues of fuel that could be on the fuselage or the wing assembly, in order to prevent any damage to the foam structure of those components.

8.3 Environmental Impact

When constructing the airplane, it is important to maintain the damage to the environment as miniscule as possible. This is an important concept to follow, since new regulations are being targeted at producing less pollution and are more eco-friendly.

The groups that are competing in the Regular Class of the event will use 10% Nitromethane fuel. This type of fuel is hazardous to humans if ingested and if it comes into eye

and skin contact. It causes severe damage to the kidneys, nervous system, and liver. Its vapor and mist is also irritating to the eyes, mucous membrane, and upper respiratory tract. According to studies, long term degradation products may arise from this type of fuel. In order to minimize the exposure of toxic fumes and CO₂, the testing of the engine was done outside in an open field away from flammable objects. Also, it is believed that Nitromethane will not have severe damage to a person's growth and their internal organs.

9 Project Management

9.1 Organization of Work and Timeline

The timeline below represents the actual and future scenario of the work performed by the team, which is subject to change during the whole project.

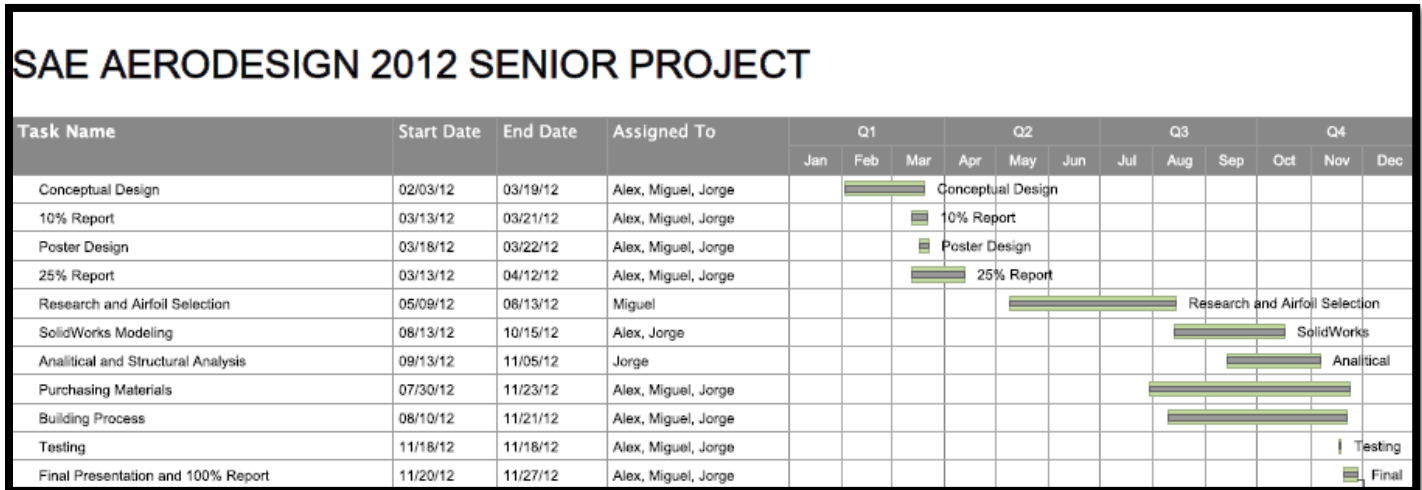


Figure 118 - Timeline Representation

9.2 Project Breakdown

In order to achieve the purpose of design and build the remote aircraft to compete in the SAE aero-design competition in Brazil, the team considered imperative to divide the entire project into the following main tasks:

- Theoretical Research: it describes all the hours spent during investigations and analysis of each of the parts of the remote aircraft.
- Theoretical Analysis: for this part, the team will spend time doing the necessary calculations to achieve an acceptable design, modeling the aircraft in SolidWorks.
- CFD Simulation: Computational Fluid Dynamics simulation will study the dynamics of the aircraft.

- Prototyping: it is the part of the project where the team spends time building the prototype to be used at the competition.
- Testing: It will be the part of the project where all the testing plans designed by the team are going to be performed and it is the final step where the remote aircraft would be capable to meet the goals previously described in this report.

9.3 Research and Development Cost

An estimated summary of the tasks realized by each member of the team is displayed in table 6, specifying the hours inverted and the percentage of each task among the entire project. The man-hour salary value selected for this project was \$30, which is below the average industry salary.

Table 23 - Break Down of Responsibilities by Task and Team Member

Task	Days	Man-Hours	Cost(\$30/hour)	Larrarte		Rosales		Verdia	
				Percentage	Hours	Percentage	Hours	Percentage	Hours
Theoretical Research	67	98.7	\$2,961.00	22.50%	22.2	22.50%	22.2	55.00%	54.3
Theoretical Analysis	39	65.3	\$1,959.00	33.30%	21.7	33.30%	21.7	33.30%	21.7
CFD and Simulation	35	75.0	\$2,250.00	35.00%	26.3	35.00%	26.3	30.00%	22.5
Prototyping	45	103.6	\$3,108.00	33.00%	34.5	33.00%	34.5	33.00%	34.5
Testing	26	35.0	\$1,050.00	33.00%	11.7	33.00%	11.7	33.00%	11.7
Total	212	377.6	\$11,328.00		116.4		116.4		144.7

Figure shows the graphical representation of the task division. It has been mentioned that theoretical research and prototyping are the tasks where the team will spend most of their time because of its importance and also to prevent any possible failures that could arise during this project.

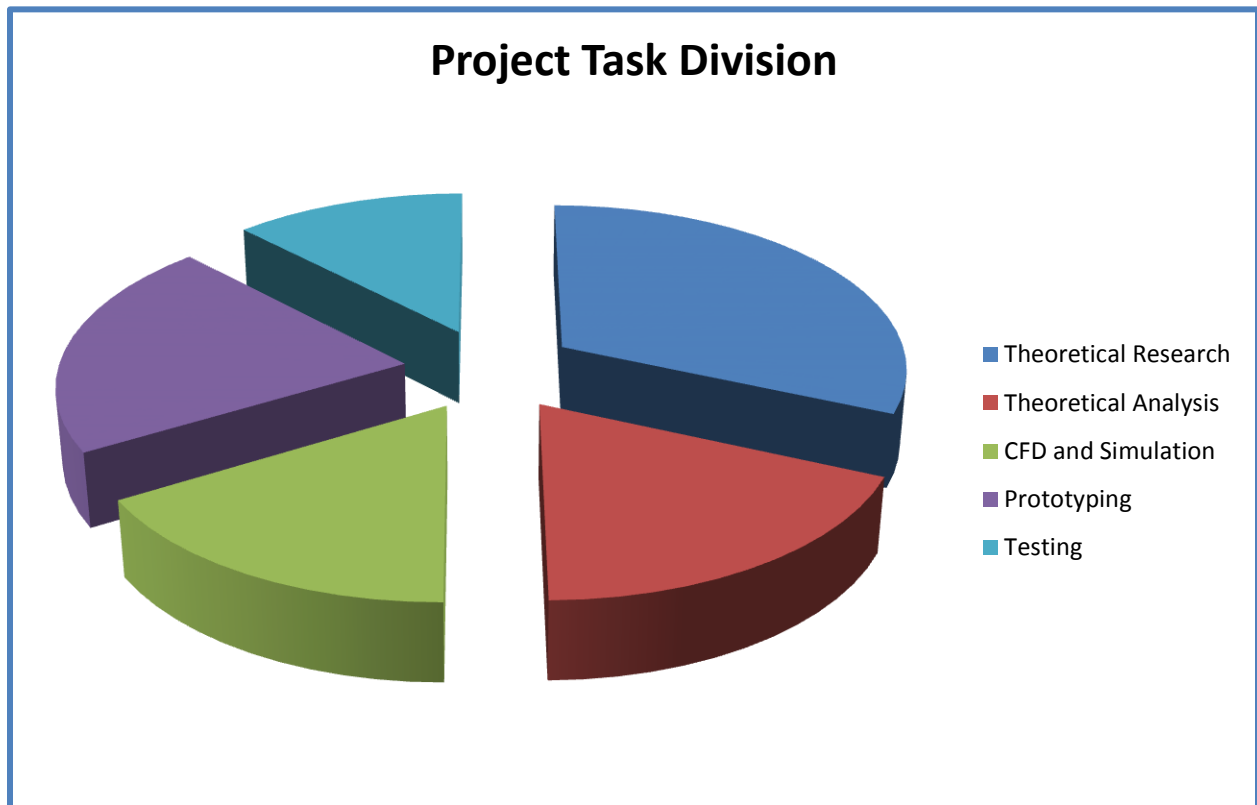


Figure 119 - Project Task Division

9.4 Project Expenses Cost

The team has calculated the total expenses made during the realization of this project. The first table shows the total expenses made in materials and required accessories, and in the second table one can see the two major processes done, the CNC of the aluminum ribs; service provided by Prof. Zicarelli; and the CNC of the foam components for the wings and fuselage assembly, which was provided by Florida Hotwire Technicians.

Table 24 – Material and Accessories Expenses

	Item	Total Price	Purchase Date	Purchase Type	Store
1	Magnum XLS-61A Engine	\$104.99	7/30/2012	Online	Ebay
2	Starter Kit	\$19.57	8/18/2012	Online	Amazon
3	Du-bro Fuel Tank	\$8.25	8/18/2012	Online	Amazon
4	Traxxas Shocks	\$13.56	8/18/2012	Online	Amazon
5	Silicone fuel Tube	\$5.46	8/21/2012	Store Pickup	House of Power at Weston
6	Powermaster Fuel	\$16.99	8/21/2012	Store Pickup	House of Power at Weston
7	OS Glow Plugs	\$13.98	8/21/2012	Store Pickup	House of Power at Weston
8	APC Propeller 11x7	\$2.99	8/21/2012	Store Pickup	House of Power at Weston
9	ADJ Engine Mount	\$4.49	8/21/2012	Store Pickup	House of Power at Weston
10	ToolBox	\$9.58	8/24/2012	Store Pickup	Home Depot
11	6x32 1 in screws & bolts	\$1.18	8/24/2012	Store Pickup	Home Depot
12	2 Props 13x4	\$12.66	8/30/2012	Store Pickup	House of Power at Weston
13	1 Prop 14x4w	\$12.78	9/10/2012	Online	Ebay
14	Rear Landing/wheels & others	\$22.29	9/14/2012	Store Pickup	House of Power at Weston
15	PVC Pipe, Wood, Screws & Nuts	\$12.86	9/14/2012	Store Pickup	House of Power at Weston
16	Radio Control 6 ch, Resin, Battery, Fiber Glass	\$220.95	9/25/2012	Store Pickup	House of Power at Weston
17	Foam (front)	\$13.00	9/26/2012	Store Pickup	Michael's
18	Aluminum 2x4 ft^2 & 7 ft pipe 1" OD	\$70.50	10/16/2012	Store Pickup	Simmons
19	Plywood 2x4 ft and scissors	\$12.50	10/16/2012	Store Pickup	Lowes
20	plate and micellaneous	\$9.84	10/26/2012	Store Pickup	Simmons
21	epoxy, wood stick, bolts nuts and springs	\$39.77	10/27/2012	Store Pickup	Home Depot
22	Bigger OD aluminum pipe, bolts, nuts & washers	\$30.00	10/28/2012	Store Pickup	Simmons
23	Birch wood, sticks	\$46.13	11/2/2012	Store Pickup	Michael's
24	3 servos, wood, cables, arms, hinges etc	\$126.00	11/2/2012	Store Pickup	House of Power at Weston
25	birch and balsa wood, stick	\$30.86	11/3/2012	Store Pickup	Michael's
26	Monokote paper high temperature and Resin	\$34.98	11/3/2012	Store Pickup	House of Power at Weston
27	Iron	\$18.55	11/6/2012	Store Pickup	House of Power at Weston
28	Monokote paper 2 rolls	\$23.30	11/8/2012	Store Pickup	House of Power at Weston
29	wire conectors servos	\$10.39	11/10/2012	Store Pickup	House of Power at Weston
30	balsa wood	\$9.60	11/11/2012	Store Pickup	Michael's
31	screws, sand paper pipe holders etc	\$16.00	11/11/2012	Store Pickup	home depot
32	Replacement of Receiver, paper, battery	\$86.92	11/12/2012	Store Pickup	House of Power at Weston
33	Red Aerosol, 3m tape, screws etc	\$22.57	11/23/2012	Store Pickup	home depot
34	Battery charger, splitters, spinner etc	\$60.37	11/23/2012	Store Pickup	House of Power at Weston
35					
36					
37					
38					
39					
40					
41					
	Total	\$1,143.86			

Table 25 - Engine Specifications and Cost

	TOTAL PRICE	TP/3
FOAM	\$391.62	\$130.54
CNC	\$175.00	\$58.33
Total	\$566.62	

9.5 Commercialization

Even though the remote aircraft used in this project was not as commercial as a hobby store's remote airplane, it could have had other uses such as security, equipment transportation, and also be used in the agricultural industry. The realization of this senior design could also be used for other Florida International University students as a guideline for any SAE aero design competition.

10 Conclusion

This senior design project combined ideas and knowledge acquired during the last three semesters of the team's career. All of the team members were taking classes in the aerospace track. These additional classes gave the team an added motivation as well as an added comfort of the topics and materials needed for this type of competition. Some of the steps of conceptual aircraft design which are being taught in FIU were used in the realization of our models and prototypes. The tools or logic used in the development of aerodynamic shapes can be appreciated in the design and selection behind the tail configuration. This one part of the airplane affects all other parameters and components, which is a situation not unlike from many other components in this type of design. The team must have for these reasons taken a careful approach in the selection of all the components in the aircraft, understanding how each selection would affect the others was also paramount. Because of this reason, a detailed selection of each component is a must in aero shape design.

Some of the design selections were more essential to the overall flight capabilities of the aircraft. These selections are wing cross-sectional shape or airfoil, wing geometry, wing position relative to fuselage, and tail configuration. The team had for these reasons spent the majority of their time fine tuning these crucial components. Relevant to this design topic have been the research that was done during the summer in airfoil and wing geometry optimization. One of the members of the team worked with optimization codes in order to create an original airfoil design that would have benefited the type of mission objective particular to this type of

competition. Without a doubt, working in this project has helped the members of the team learn and appreciate some of the common problems found in the aerospace industry.

11 References

1. **D. Raymer.** *Aircraft Design: A Conceptual Approach, Fourth Edition*, American Institute of Aeronautics, 2006, p. 54-157
2. **J. Anderson.** *Modern Compressible Flow: With Historical Perspective, Third Edition*, McGraw-Hill, 2002, p. 100-125.
3. **George S. Dulikravich, Thomas Martin, Brian Dennis.** *Proceedings of Inverse Problems in Engineering: Theory and Practice*. 3rd International Conference on Inverse Problems in Engineering, June, 1999, [Cited: April 01, 2012]
4. **George S. Dulikravich.** *Aerodynamic Shape Design and Optimization: Status and Trends*. *Journal of Aircraft*, Volume 29, November – December 1992, [Cited: April 01, 2012]
5. **George S. Dulikravich.** *A Criteria for Surface Pressure Specification in Aerodynamic Shape Design*. 28th Aerospace Sciences Meeting. January, 1990, [Cited: April 04, 2012]
6. **George S. Dulikravich.** *Shape inverse Design and Optimization for Three-Dimensional Aerodynamics*. 33rd Aerospace Sciences Meeting and Exhibit, January, 1995, [Cited: April 10, 2012]
7. **Fast Company.** *Fastcompany.com. Inside the Lawsuit That Could Ground Deadly CIA Predator Drones*. [Online] October, 2010. <http://www.fastcompany.com/1695219/cia-predator-drones-facing-ip-lawsuit>
8. **USGC.** *Usgc.mil. The Indispensable Man*. [Online] January, 2012. http://www.uscg.mil/history/articles/indispensable_men.asp

12 Appendix

12.1 Appendix A: FIU CNC METAL CUTTING SERVICES



Richard Zicarelli

Department: Industrial and System Engineering

Phone: (305) 348-6557

Email: zicarell@fiu.edu

12.2 Appendix B: FLORIDA HOTWIRE TECHNICIANS



Southeast USA & Latin America Representatives

Florida Hotwire Technicians
8558 NW 64th Street
Miami, FL 33166

Ernest W. Peeper: 786-281-1959
Silvana Podgaetz: 786-301-7709 (Se Habla Español)
Fax: 786-464-1319
E-mail: sales@floridahotwire.com

12.3 Appendix C: WESTON HOBBY STORE: HOUSE OF POWER



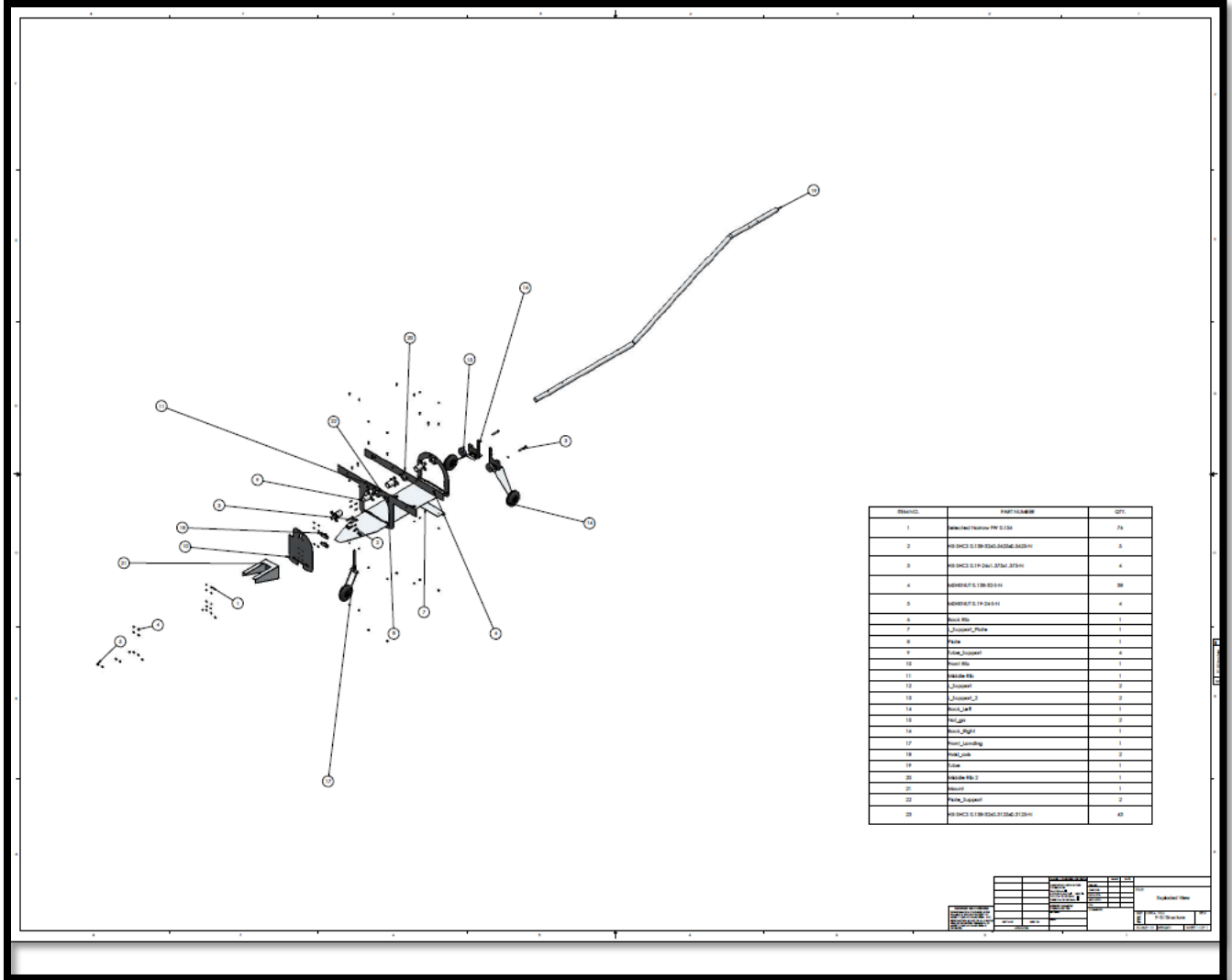
12.4 Appendix D: TECHNICAL DRAWINGS

ITEM NO.	PART NUMBER	QTY.
1	FTU Panther Structure	1
2	Fuselage Body	1
3	Wing Assembly	1
4	Cone	1
5	Magnum Speed 61 Geared Assembly	1
6	TailW_Right	1
7	TailW_Left	1

APPROVALS		DESIGN		CHECK		DATE	

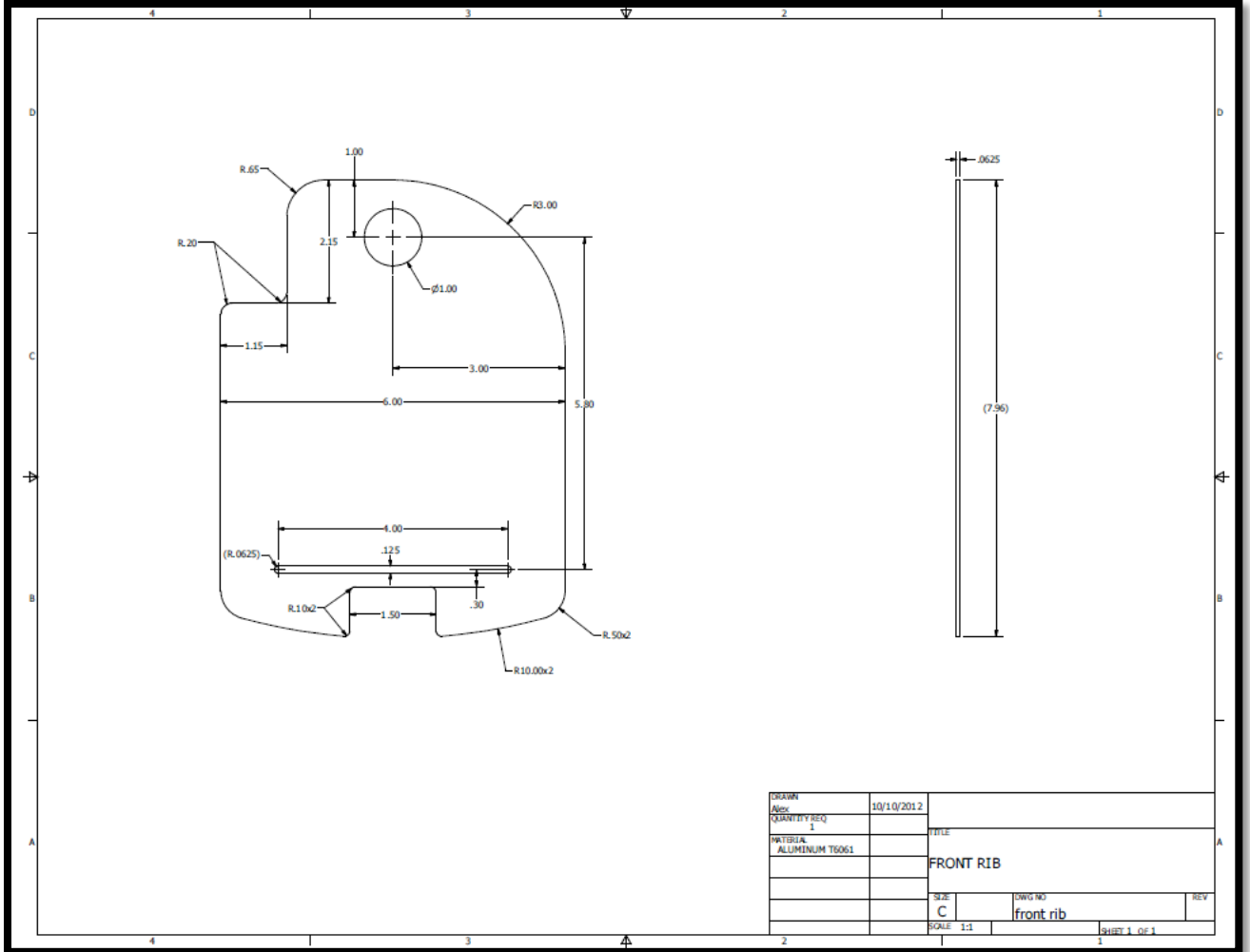
REVISIONS AND COMMENTS:
 ALL DIMENSIONS IN MILLIMETERS UNLESS OTHERWISE SPECIFIED.
 ALL DIMENSIONS ARE TO CENTER UNLESS OTHERWISE SPECIFIED.
 ALL DIMENSIONS ARE TO CENTER UNLESS OTHERWISE SPECIFIED.
 ALL DIMENSIONS ARE TO CENTER UNLESS OTHERWISE SPECIFIED.
 ALL DIMENSIONS ARE TO CENTER UNLESS OTHERWISE SPECIFIED.

Exploded view
 DWG. NO. FTU_Panther
 SCALE: 1:1 X/BGHE SHEET 1 OF 1

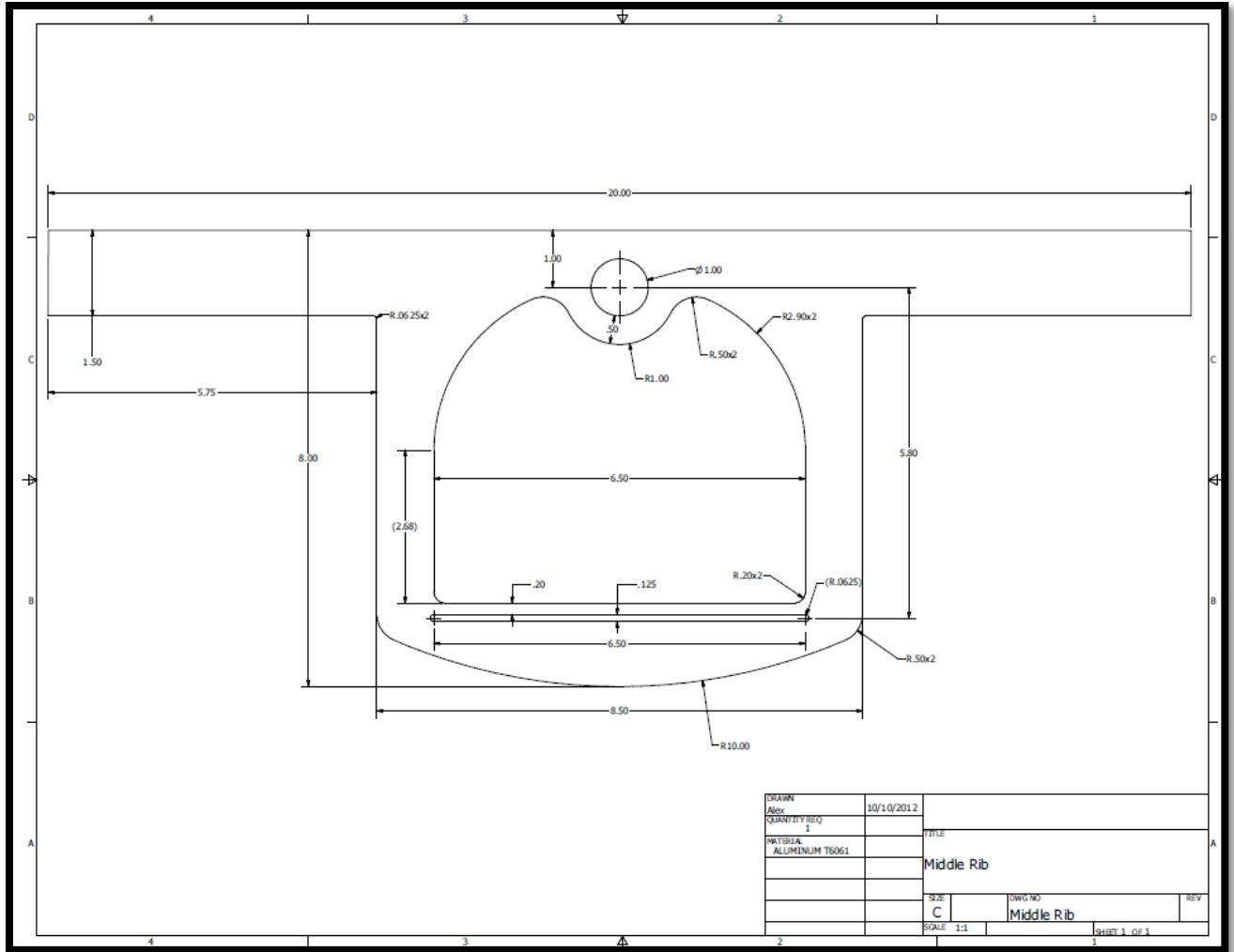


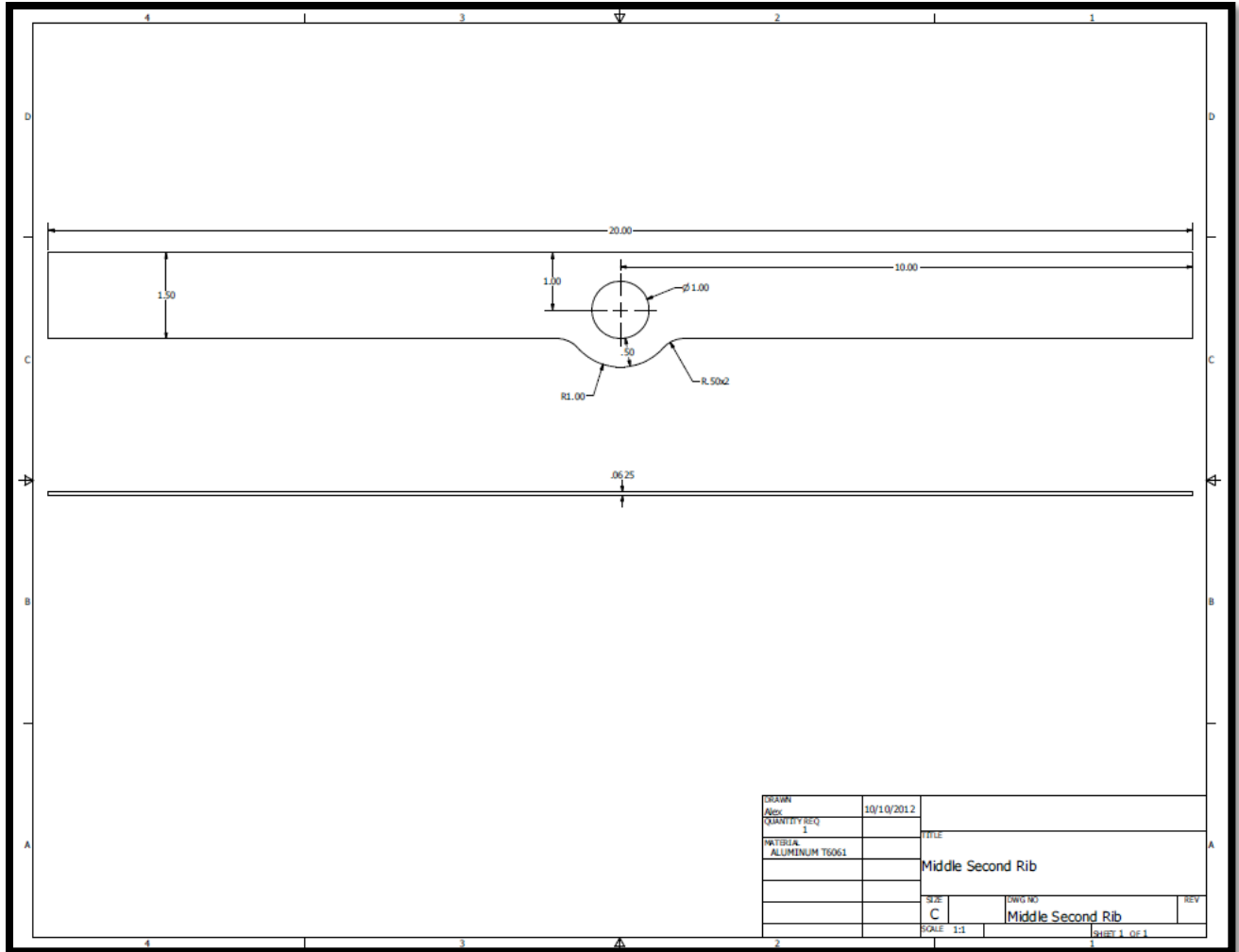
ITEM NO.	ITEM NAME	QTY
1	BRASS PLATE 1/2" X 1/2" X 1/8"	75
2	BRASS ROD 1/8" DIA. X 1/2" L	5
3	BRASS ROD 1/8" DIA. X 1/2" L	5
4	BRASS ROD 1/8" DIA. X 1/2" L	50
5	BRASS ROD 1/8" DIA. X 1/2" L	5
6	BRASS ROD	1
7	BRASS PLATE	1
8	BRASS	1
9	BRASS	5
10	BRASS	1
11	BRASS	1
12	BRASS	2
13	BRASS	2
14	BRASS	1
15	BRASS	2
16	BRASS	1
17	BRASS	1
18	BRASS	2
19	BRASS	1
20	BRASS	1
21	BRASS	1
22	BRASS	1
23	BRASS	5
24	BRASS	50

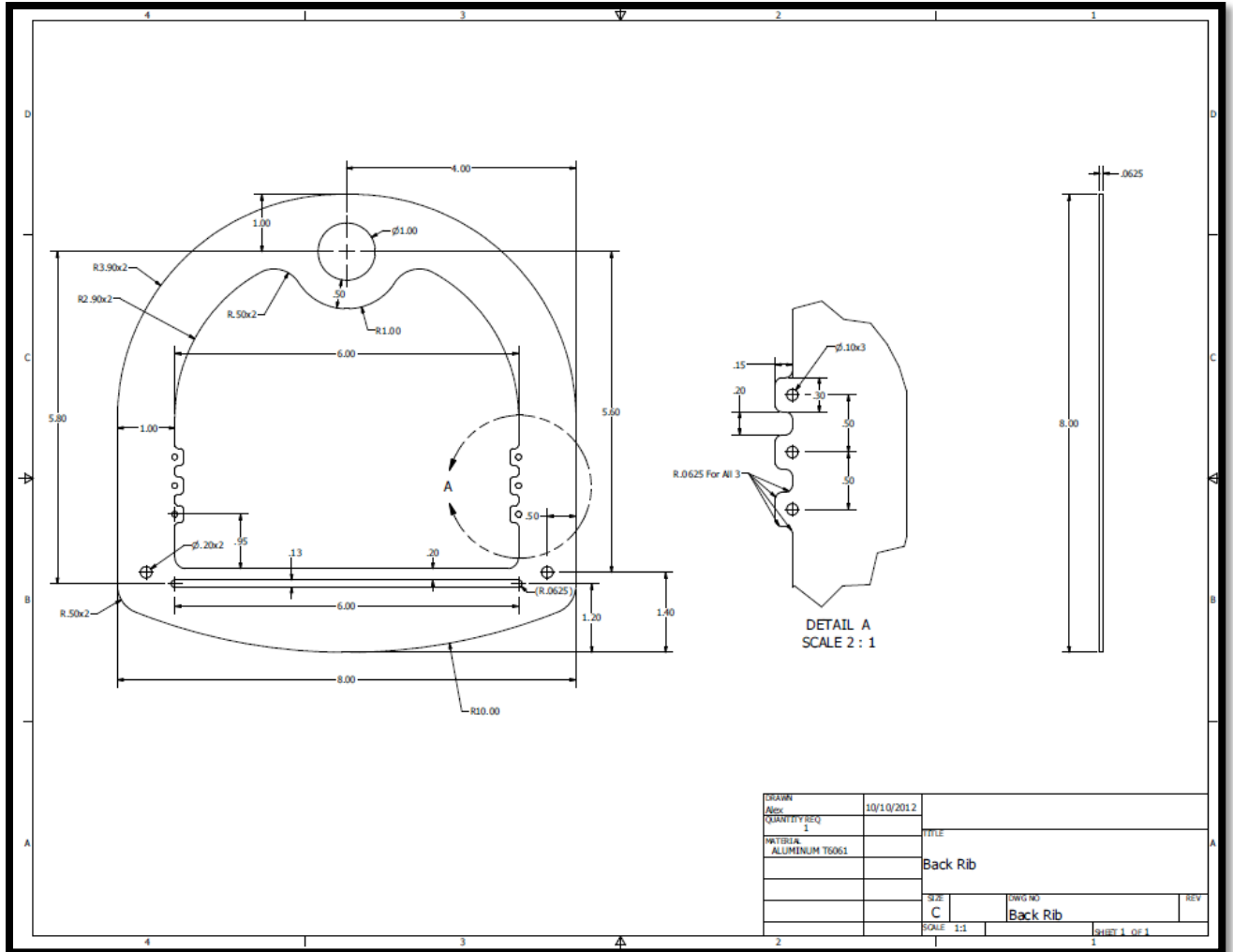
DATE	BY	CHECKED	APPROVED

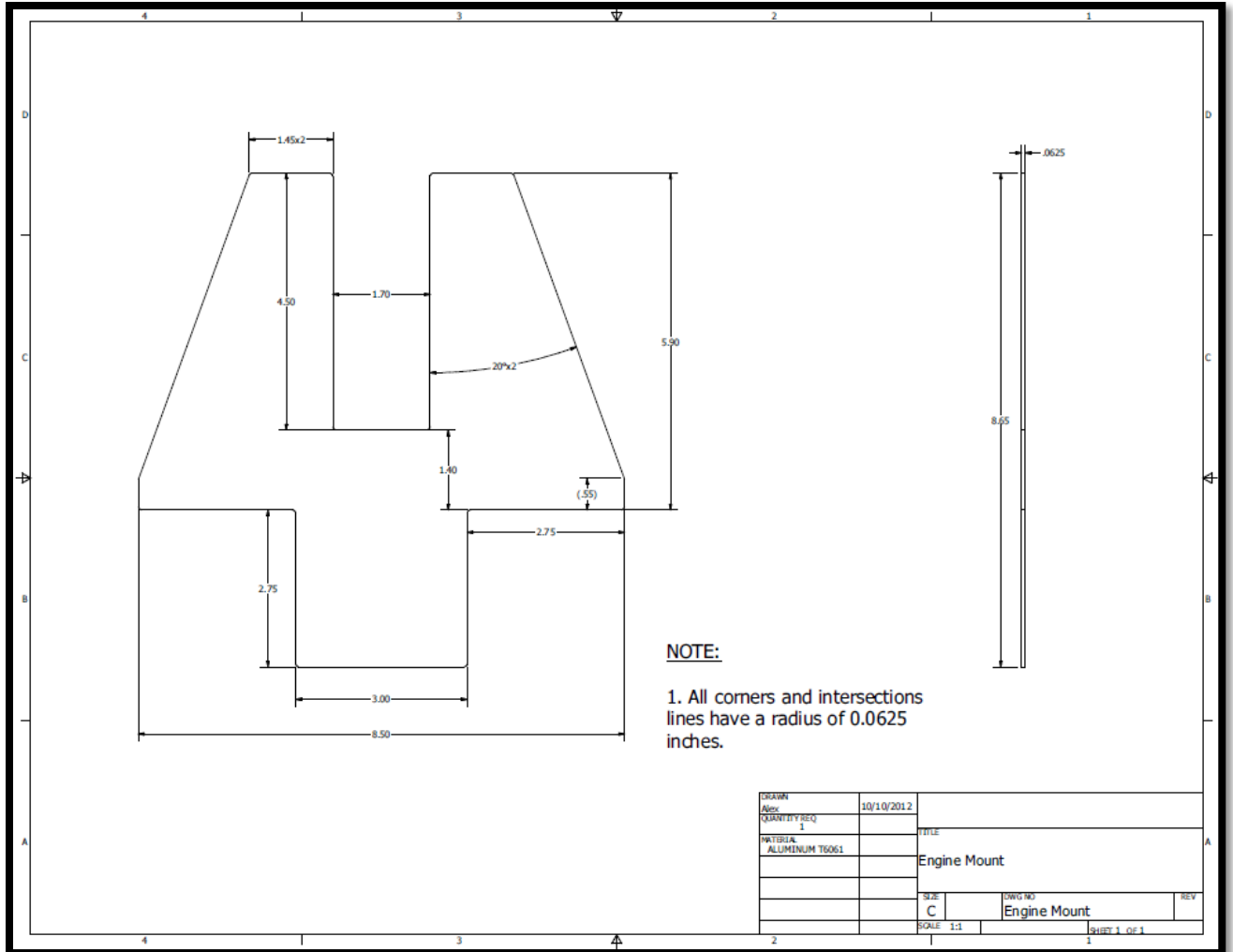


DESIGN	Alex	10/10/2012	
QUANTITY REQ	1		
MATERIAL	ALUMINUM T6061		TITLE
			FRONT RIB
			SIZE
			C
			DWG NO
			front rib
			REV
			SCALE 1:1
			SHEET 1 OF 1









NOTE:

1. All corners and intersections lines have a radius of 0.0625 inches.

DRAWN	10/10/2012		
Qty			
QUANTITY REQ	1	TITLE	
MATERIAL		Engine Mount	
ALUMINUM T6061		SIZE	DWG NO
		C	Engine Mount
		SCALE	REV
		1:1	
			1
			1